APPLICATION OF PHAGE DISPLAY ANTIBODY

TECHNOLOGY FOR THE STUDY OF HUMAN

ANTI-DENGUE MONOCLONAL ANTIBODIES

Sararat Hattakam

A Thesis Submitted in Partial Fulfillment of the Requirement for the

Degree of Doctor of Philosophy in Biotechnology

Suranaree University of Technology

Academic Year 2019

การประยุกต์ใช้เทคโนโลยีการแสดงแอนติบอดีบนผิวเฟจในการศึกษา
แอนติบอดีมนุษย์ต่อเชื้อไวรัสไข้เลือดออก

นางสาวสรารัตน์ หัตถกรรม

วิทยานิพนธ์นี้เป็นส่วนหนึ่งของการศึกษาตามหลักสูตรปริญญาวิทยาศาสตรดุษฎีบัณฑิต
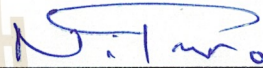สาขาวิชาเทคโนโลยีชีวภาพ
มหาวิทยาลัยเทคโนโลยีสุรนารี
ปีการศึกษา 2562

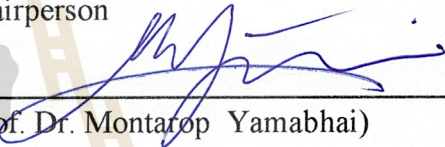# APPLICATION OF PHAGE DISPLAY ANTIBODY TECHNOLOGY FOR THE STUDY OF HUMAN ANTI-DENGUE MONOCLONAL ANTIBODIES

Suranaree University of Technology has approved this thesis submitted in partial fulfillment of the requirements for the Degree of Doctor of Philosophy.

Thesis Examining Committee

_____
(Prof. Dr. Neung Teaumroong)

Chairperson

_____
(Prof. Dr. Montarop Yamabhai)

Member (Thesis Advisor)

_____
(Prof. Dr. Yong Poovorawan, MD)

Member

_____
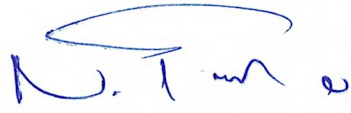(Assoc. Prof. Dr. Sujan Shresta)

Member

_____
(Dr. Annie Elong Ngono)

Member

_____
(Prof. Dr. Santi Meansiri)

Vice Rector for Academic Affairs

and Internationalization

_____
(Prof. Dr. Neung Teaumroong)

Dean of Institute of Agricultural Technology

สรารัตน์ หัตถกรรม : การประยุกต์ใช้เทคโนโลยีการแสดงแอนติบอดีบนผิวเฟจใน
การศึกษาเอนติบอดีมนุษย์ต่อเชื้อไวรัสไข้เลือดออก(APPLICATION OF PHAGE
DISPLAY ANTIBODY TECHNOLOGY FOR THE STUDY OF HUMAN ANTI-
DENGUE MONOCLONAL ANTIBODIES) อาจารย์ที่ปรึกษา: ศาสตราจารย์ ดร.ภญ.
มณฑารพ ยมาภัย 160 หน้า.

ไวรัสเดงกี่ (Dengue) ทั้งสี่สายพันธุ์ และไวรัสซิก้า (Zika) เป็นไวรัสในกลุ่มเฟลวิไวรัส
(Flavivirus) สามารถติดต่อจากคนสู่คนโดยมียุงลายเป็นพาหะ และมักจะพบการระบาดของไวรัส
ทั้งสองชนิดนี้ในพื้นที่เดียวกัน การติดเชื้อไวรัสเดงกี่สายพันธุ์ใดสายพันธุ์หนึ่ง สามารถก่อให้เกิด
asymptomatic อาการเบื้องต้น คล้ายไข้หวัดทั่วไปคือไข้เดงกี่ (Dengue fever; DF) จนไปถึงระดับ
ความรุนแรงที่เป็นอันตรายถึงชีวิตคือโรคไข้เลือดออก (Dengue hemorrhagic fever; DHF) และ
ไข้เลือดออกภาวะช็อก (Dengue shock syndrome; DSS) ส่วนการได้รับเชื้อไวรัสซิก้านั้น สามารถ
ส่งผลที่ร้ายแรงต่อหญิงตั้งครรภ์ โดยทำให้เสี่ยงต่อการแท้งบุตร หรืออาจให้กำเนิดทารกที่มีศีรษะ
ขนาดเล็กกว่าปกติ และมีผลต่อการเกิดโรคกล้ามเนื้ออ่อนแรง หรือกลุ่มอาการกูเลนแบร์ในผู้ใหญ่
(Guillian-Barré syndrome) ปัจจุบันนี้ยังไม่มียาที่มีประสิทธิภาพในการรักษาโรคไข้เลือดโดยตรง
หรือแม้แต่วัคซีนที่มีประสิทธิภาพในการป้องกันการติดไวรัสเดงกี่ทั้งสี่สายพันธุ์และซิก้า อีกทั้งยัง
ไม่มีรายงานการศึกษาที่ชัดเจนว่า ภูมิคุ้มกันที่เกิดจากการติดไวรัสเดงกี่จะส่งผลกระทบในการ
ป้องกันหรือเสริมการเกิดโรคจากการติดไวรัสซิก้าในมนุษย์ ในวิทยานิพนธ์นี้จึงได้ทำการศึกษาใน
กลุ่มประชากรที่มีสุขภาพดีจำนวน 61 คนที่อาศัยอยู่ในจังหวัดนครราชสีมาซึ่งเป็นพื้นที่ที่มีการ
ระบาดไวรัสเดงกี่ พบว่าอาสาสมัครจำนวน 52 และ 51 คน มีแอนติบอดีต่อไวรัสเดงกี่ และไวรัส
ซิก้าตามลำดับ โดยในจำนวน 52 คนนั้นมีทั้งสิ้น 23 คนที่เคยได้รับเชื้อไวรัสเดงกี่มากกว่าหนึ่งครั้ง
(Secondary infection) หรือคิดเป็นร้อยละ 44.23 โดยพบว่าประชากรกลุ่มนี้มีแอนติบอดีที่สามารถ
ป้องกันการติดทั้งเชื้อไวรัสเดงกี่และซิก้าได้ ในอัตราสูงกว่าเมื่อเทียบกับกลุ่มที่ได้เคยติดเชื้อเดงกี่มา
ก่อนเพียงครั้งเดียว (Primary infection) ผลการศึกษานี้ชี้ให้เห็นว่า ภูมิคุ้มกันที่ได้รับมาจากการติด
ไวรัสเดงกี่หลายครั้งสามารถป้องกันการติดไวรัสซิก้าได้ นอกจากนั้นแล้วในโครงการวิจัยนี้ยังได้
นำข้อมูลที่ได้จากการวิเคราะห์เลือดอาสาสมัคร 40 รายซึ่งมีแอนติบอดีที่มีคุณสมบัติในการป้องกัน
การติดไวรัสเดงกี่ทั้งสี่สายพันธุ์ ไปทำการสร้างคลังแอนติบอดีบนผิวเฟจ แล้วทำการคัดเลือก
แอนติบอดีชนิด scFv โดยใช้ไวรัสเดงกี่สายพันธุ์ที่สอง เป็นเป้าหมายในการคัดเลือก ในการ
ทดลองนี้ได้ค้นพบแอนติบอดีโคลน DV2H12 ซึ่งต่อมาถูกผ่านการดัดแปลงพันธุกรรมให้เป็น
แอนติบอดีมนุษย์ชนิดเต็มรูปแบบคือ IgG แล้วทำการศึกษาในหลอดทดลอง พบว่าแอนติบอดี

DV2H12 สามารถป้องกันการติดไวรัสเดงกี่ได้ทั้งสี่สายพันธุ์ในประสิทธิภาพระดับปานกลาง แต่
เมื่อทดสอบประสิทธิภาพของแอนติบอดีในหนูทดลองชนิ ดAG129 พบว่าแอนติบอดีไม่สามารถ
ป้องกันหนูจากการติดไวรัสเดงกี่ได้ อีกทั้งยังส่งเสริมการติดเชื้อไวรัสเดงกี่สายพันธุ์สองอีกด้วย ผล
จากการศึกษากลไกจับจำเพาะของแอนติบอดี (epitope mapping) ด้วยเทคโนโลยีการแสดงโปรตี น
บนผิวเฟจ แสดงให้เห็นว่า มีความเป็นไปได้ที่แอนติบอดีอาจจะจับกับโปรตีนชนิด prM ของไวร ส
เดงกี่สายพันธุ์สอง เมื่อศึกษาบทบาทของ CD4$^+$ T cell ในการควบคุมการสร้างแอนติบอดีต่อไวรัส
เดงกี่และซิก้าในหนูทดลอง *LysMCre$^+$Ifnar1$^{fl/fl}$* โดยทำการกำจัดเซลล์ภูมิคุ้มกันชนิด CD4$^+$ T
cell ในหนูทดลอง พบว่าระดับของการแสดงออกและการตอบสนองของแอนติบอดีและ B cell ต่อ
ไวรัสซิก้าลดลง ดังนั้นเซลล์ภูมิคุ้มกันชนิด CD4$^+$ T มีส่วนสำคัญในการสร้างแอนติบอดีที่มี
ความสามารถจับจำเพาะต่อไวรัสซิก้าและเดงกี่ องค์ความรู้ใหม่จากการศึกษาทั้งหมดนี้สามารถ
นำไปใช้เพื่อการพัฒนาวัคซีนต่อไปในอนาคต และยังสามารถนำไปใช้ในการศึกษาเพื่อทำความ
เข้าใจการเกิดโรคของไวรัสเดงกี่ หรือไวรัสซิก้าได้

สาขาวิชาเทคโนโลยีชีวภาพ   ลายมือชื่อนักศึกษา_____

ปีการศึกษา 2562   ลายมือชื่ออาจารย์ที่ปรึกษา_____

SARARAT HATTAKAM : APPLICATION OF PHAGE DISPLAY
ANTIBODY TECHNOLOGY FOR THE STUDY OF HUMAN ANTI-
DENGUE MONOCLONAL ANTIBODIES. THESIS ADVISOR : PROF.
MONTAROP YAMABHAI, Ph.D., 160 PP.

DENGUE VIRUS/ZIKA VIRUS/PRE-EXISTING IMMUNITY/DENV-ELICITED
ANTIBODY/NEUTRALIZATION ANTIBODY/RECOMBINANT ANTIBODY

Four serotypes of Dengue virus (DENV1-4) and Zika virus (ZIKV) are
antigenically related mosquito-borne flaviviruses, circulating in overlapping
geographical regions that represent a significant threat to global health. Infection with
one of the four DENV serotypes can cause a broad spectrum of illnesses ranging from
asymptomatic, mild disease known as dengue fever (DF) to severe, life-threatening
syndromes called dengue hemorrhagic fever/dengue shock syndrome (DHF/DSS),
while ZIKV infection is associated with microcephaly in fetuses of infected mothers
and Guillain-Barré syndrome in adults. To date, there are no safe, effective drugs
approved for clinical use, as well as the effect of prior DENV1-4 immunity on ZIKV
cross-neutralization has remained unclear. Here, we conducted a ZIKV and DENV
seroprevalence survey in 61 healthy participants (aged ranged 18-69 years) from a
DENV-endemic area Nakhon Ratchasima, Thailand. We observed 52 and 51 with
DENV and ZIKV seropositive, respectively. Notably, participants with serologically
classified secondary DENV infection (23/52, 44.23%) had strikingly higher titers and
broader reactivity of neutralizing antibodies against ZIKV and DENV heterotypes
compared with participants with primary DENV infection. These data suggest that

multiple exposures to heterologous DENV prior to ZIKV provoke enduring DENV/ZIKV cross-neutralization antibody response. This finding was implemented for the construction of a human antibody phage display library derived from DENV immune people, of which 40 blood samples that showed seropositive for all dengue serotypes were used as templates for scFv genes. We identified a DENV cross-reactive human monoclonal antibody (mAb), DV2H12 from bio-panning using purified whole DENV2 particle as the target. The mAb DV2H12 showed moderately neutralization against DENV1-4; however, it significantly promoted antibody-dependent enhancement (ADE) of DENV2 infection in AG129 mice. The epitope mapping by bio-panning of the phage display peptide library revealed that the antibody might recognize the DENV2 prM protein. Additionally, we studied the role of CD4$^+$ T cells in the regulation of anti-ZIKV/DENV production using *LysMCre$^+$Ifnar1$^{fl/fl}$* mice. Treatment of mice with a CD4$^+$ T cell-depleting Ab reduced the plasma cell, germinal center B cell, and IgG responses to ZIKV or DENV. This result demonstrates that CD4$^+$ T cells are required mainly for the generation of a DENV- or ZIKV-specific humoral immune response. These findings may provide significant implications for future vaccine design and facilitate understanding of the pathogenesis of DENV and ZIKV infection.

School of Biotechnology   Student's Signature_____

Academic Year 2019   Advisor's Signature_____

ACKNOWLEDGMENTS

I thank my fellow lab mates in MY's Lab Numphon Thaiwong, Natcha Preugsamethanan, Junjira Seaubsoonthorn for their friendship and support in mentally. Furthermore, I thank Witsanu Srila, Kuntalee Rangnoi, Thitima Sampan-apai and everyone in MY's Lab who gave me a warm feeling and helped.

And finally, there are no words to explain how much I appreciate to my mom, dad, sister, and brother. They always beside me no matter what; on the hardest day I always get a smile and supports from them. They are my positive energy.

To my love Dave Evans, he is my supporter, cheering me up, brighten up my thought.

TABLE OF CONTENTS

Page

TABLE OF CONTENTS (Continued)

TABLE OF CONTENTS (Continued)

TABLE OF CONTENTS (Continued)

TABLE OF CONTENTS (Continued)

TABLE OF CONTENTS (Continued)

TABLE OF CONTENTS (Continued)

TABLE OF CONTENTS (Continued)

Page

LIST OF TABLES

LIST OF FIGURES

LIST OF FIGURES (Continued)

LIST OF FIGURES (Continued)

LIST OF ABBREVIATIONS

Ab	=	Antibody
ADE	=	Antibody-dependent enhancement
Bp	=	Base pairs
BSA	=	Bovine serum albumin
Cfu	=	Colony forming units
CDR	=	Complementary determining region
CL	=	Constant light chain
DENV	=	Dengue virus
DF	=	Dengue fever
DHF	=	Dengue hemorrhagic fever
DNA	=	Deoxyribonucleic acid
dNTP	=	Deoxynucleotidyl triphosphates
E. coli	=	Escherichia coli
EDTA	=	Ethylenediaminetetra-acetic acid
ELISA	=	Enzyme-linked immunosorbent assay
FBS	=	Fetal bovine serum
Fc	=	Constant region of an antibody molecule
Fv	=	Variable binding region of an antibody
HRP	=	Horse radish peroxidise
IgG	=	Immunoglobulin class
Log	=	Logarithmic

LIST OF ABBREVIATIONS (Continued)

MW	=	Molecular weight
mAb	=	Monoclonal antibody
Nab	=	Neutralizing antibody
NS	=	Non-structural
NT	=	Neutralization test
OD	=	Optical density
PAGE	=	Polyacrylamide gel electrophoresis
PBS	=	Phosphate buffer saline
PBST	=	Phosphate buffer saline/Tween
PEG	=	Polyethylene glycol
pH	=	Log of the hydrogen ion concentration
PRNT	=	Plaque reduction neutralization test
scFv	=	Single chain Fv antibody derivative
SDS	=	Sodium dodecyl sulphate
TMB	=	Tetramethylbenzidine dihydrochloride
UV	=	Ultraviolet
VH	=	Variable region of the heavy chain of antibody
VL	=	Variable region of the light chain of antibody
ZIKV	=	Zika virus

CHAPTER I

INTRODUCTION

1.1 Significance of the study

Dengue virus (DENV), a mosquito-borne flavivirus, was the first outbreak in 1943 and four serotypes (DENV1-4) have been identified. DENV has been distributed globally over 128 countries in tropical and subtropical regions, causes an estimated 390 million infections annually, of which 96 million developed disease severity and 2-5% are fatal (Bhatt et al., 2013). The infection with any of serotype can be asymptomatic or cause clinical symptoms ranging from mild fever to life-threatening dengue fever/hemorrhagic fever (DF/DHF) leading to dengue shock syndrome or severe dengue.

It has been more than 60 years that scientists have been trying to develop the vaccine, therapeutic antibodies, and antiviral drugs to fight the disease. Currently, no vaccine broadly protects against all 4 serotypes of DENV infection. There is only Dengvaxia®, a Sanofi dengue vaccine currently licensed in 20 countries where the DENV is endemic. The licensed DENV vaccine is not equally protective against all four serotypes. It has been shown to be protective in people who have been infected previously but not in naïve individuals. Vaccination in naïve subjects can increase the risks of hospitalization for the severe disease if they are subsequently infected (Ariën & Wilder-Smith, 2018; Organization, 2018; Sridhar et al., 2018). Also, the target age

group for vaccination is limited to children 9-16 years old, as it is not safe to use for all vaccination is limited to children 9-16 years old, as it is not safe to use for all age groups. Therefore, it is urgent to develop an alternative approach to cure the disease, such as generating a human antibody library that can rapidly screen neutralizing antibodies against the specific pathogens.

Phage display antibody library can be produced from an immune or non-immune source. The procedure for selecting phage is simple and inexpensive. This procedure is commonly called the bio-panning method. Following bio-panning, the antibody can be inserted into the vector and expressed in the bacteria, yeast or plants. Advantages of recombinant antibody technology are several (i) selections of antibodies from a phage library is unbiased by the immunogenicity and less dependent on quantitative abundance of the target ligands (Schier et al., 1996), (ii) antibodies are produced in DNA-encoded plasmids that are readily cloned and modified, (iii) antibodies can be produced in large quantities from *Escherichia coli* or cell lines, without the use of animals, (iv) the antibody gene can be further engineered to different formats of antibodies, to obtain an increase affinity and modified specificity. The conveniences of using phage display technology are the most consideration to apply in the study of the antibody for dengue research.

We dissected this thesis into three main parts. First, the research literature is in **chapter II**, where we reviewed the implications for the protective and pathogenesis of humoral immunity in DENV infection and the complicated with the recent outbreak Zika virus (ZIKV). Second, **chapter III** is presented about the study of seroprevalence of anti-DENV and ZIKV, as well as the neutralization antibodies profile of the population who lived in Nakhon Ratchasima, Thailand. Third is in

chapter IV where the phage display antibody library was constructed from healthy DENV immune human, who had neutralization antibodies against all four serotype DENV. The antibody specific DENV was selected from the library and further engineered into human monoclonal full-length IgG. The recombinant anti-DENV human monoclonal antibody was next evaluated the neutralization activity *in vitro* and prophylactic efficacy *in vivo*.

1.2 Research objectives

1.2.1 Main objective

This thesis was aimed to construct a single-chain fragment variable (scFv) antibody phage display library from B cells of healthy volunteers that had neutralizing antibodies altogether against all four serotypes of DENV virus and ZIKV. The specific human scFv antibodies from the constructed library would be affinity selected with immobilized whole DENV or ZIKV particle. It was expected that this library would provide anti-DENV neutralizing antibodies (NAbs) to all 4 serotypes. Biological activities of these scFv antibodies were studied. Moreover, the selected scFv would be further engineered to generate full-length of human monoclonal IgG antibody, of which the Fc portion will be further engineered to reduce the affinity binding with Fc Receptor during DENV infection. The efficacy of monoclonal antibody (mAb) would be evaluated in both *in vitro* and *in vivo* mouse model.

1.2.2 Specific objective

1. To obtain blood from volunteers and test for anti-dengue and Zika antibody using ELISA, plaque reduction neutralization test and flow cytometry-based neutralization assay.

2. To construct the scFv antibody phage display library from those samples that contain neutralizing antibodies.

3. To affinity select (Bio-panning) for specific scFv antibody from the library using the purified whole virus as a target and test the neutralization activity of selected scFv.

4. To engineer selected scFv antibody into wildtype IgG1 and mutant IgG4 and evaluate their neutralization activity *in vitro*.

5. To test the prophylactic efficacy of the IgG antibody *in vivo* mouse model.

6. To map antibodies epitope of selected antibody.

1.3 Scope of the study

In this thesis, we enrolled 65 participants (aged > in 2016 who live in Nakhon Ratchasima. The participants were unselected, without previous history of serotyping dengue infection clinically confirmed. DENV serotype 1-4 that were used in this study is laboratory strain or WHO reference and ZIKV is clinically isolated in 2016. Both of DENV and ZIKV are Asian lineage.

1.4 Reference

Ariën, K. K., & Wilder-Smith, A. (2018). Dengue vaccine: reliably determining previous exposure. **The Lancet Global Health**, 6(8), e830-e831.

Bhatt, S., Gething, P. W., Brady, O. J., Messina, J. P., Farlow, A. W., Moyes, C. L., Hay, S. I. (2013). The global distribution and burden of dengue. **Nature**, 496(7446), 504-507.

WHO, world health organization. (2018). Dengue vaccine: WHO position paper, September 2018 – Recommendations. **Vaccine**.

Schier, R., Bye, J., Apell, G., McCall, A., Adams, G. P., Malmqvist, M., Marks, J. D. (1996). Isolation of high-affinity monomeric human anti-c-erbb-2 single chain fv using affinity-driven selection. **Journal of Molecular Biology**, 255(1), 28-43.

Sridhar, S., Luedtke, A., Langevin, E., Zhu, M., Bonaparte, M., Machabert, T., DiazGranados, C. A. (2018). Effect of dengue serostatus on dengue vaccine safety and efficacy. **New England Journal of Medicine**, 379(4), 327-340.
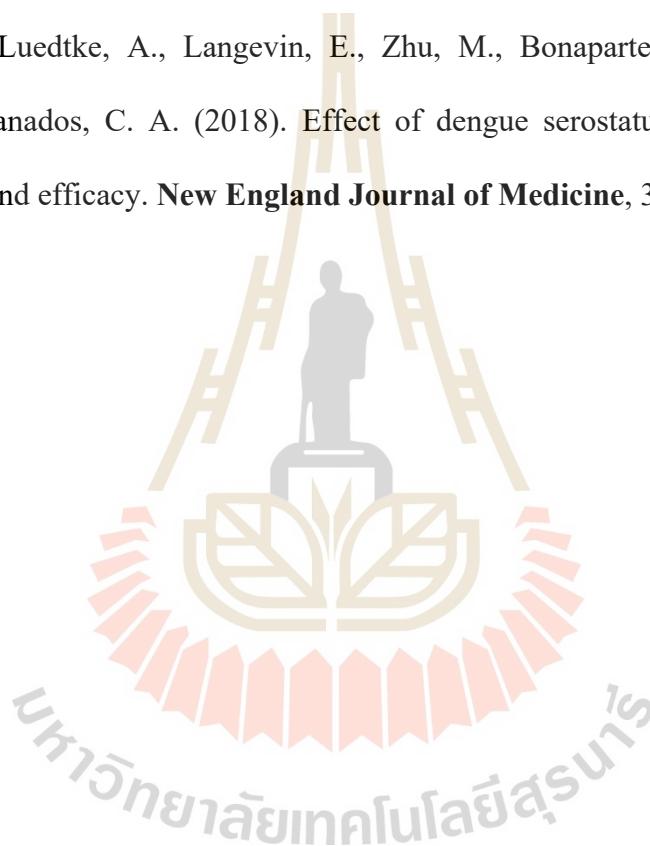
CHAPTER II

LITERATURE REVIEW

2.1 Flavivirus structure

DENV and ZIKV are members of *flavivirus* genus in *Flaviviridae* family that are mosquito-borne positive, single-stranded, enveloped RNA viruses. Both viruses are closely related to antigenically similarity 55.1% to 56.3% in amino acid sequence identity (Ngono & Shresta, 2018). The genome size is approximately 11 kb and encoded a polyprotein with three structural proteins, i.e., capsid protein (C), an envelope protein (E), and precursor membrane protein prM and seven non-structural (NS) proteins, and two untranslated regions (UTR). The virus genome is formed in a nucleocapsid structure by encapsulated with multiple copies of the C proteins (11 kDa). The nucleocapsid is embedded by a host-cell-derived lipid bilayer which is anchored with prM/M and E protein arranged in icosahedral protrusions. The M protein (approx. 8 kDa) is a small proteolytic fragment of prM (approx. 21 kDa). The E glycoprotein is a Class II fusion protein and is responsible for viral attachment to host-cell receptors, and virus-mediated membrane fusion (Stiasny & Heinz, 2006). The E protein monomer is a glycoprotein, composed of β-barrels which has a size of 53 kDa and contains three distinct structural domains DI, DII, and DIII (Figure 2). It exists as a 90 "head-to-tail" homodimer on the virion surface. The DI is positioned between DII, the homodimerization domain, and the immunoglobulin-like DIII. The

DII is also known as the dimerization domain, which is a long finger-like structure that contains the hydrophobic membrane-fusion sequence at its tip for membrane fusion. The DIII contains the receptor-binding motif, which involved in virus attachment. As a class II fusion protein, the E glycoprotein can undergo an acid-catalyzed oligomeric reorganization to a fusogenic homotrimer (Modis, Ogata, Clements, & Harrison, 2004). It is believed that this event occurs in the endosome, allowing the viral nucleocapsid to escape into the cytoplasm and initiate RNA and protein synthesis. Similarly, it is believed that the prM protein functions as a chaperone protein for the E glycoprotein during viral maturation, helping to maintain the E glycoprotein structure until viral assembly is complete and the virion escape the acidic exocytic vesicles (Stiasny & Heinz, 2006). These structural domains I, II, and III are defined as the antigenic domain. The antibodies against these domains showed virus neutralization.

The seven NS proteins, NS1, NS2A, NS2B, NS3, NS4A, NS4B, and NS5 are involved in the initiation of virus replication, assembly and modulation of the immune response of the host cell. The NS1 protein (46 kDa) has three functionally different forms of NS1, secreted hexameric, membrane-bound homodimeric and intracellular monomeric. The secreted NS1 is soluble which circulates in the bloodstream and interacts with the human complement regulatory protein clusterin (Clu). Clu is circulated in serum, and act as the inhibitor of the terminal pathway of the complement system to protect the cell from attack by complement. Therefore interaction of Clu and NS1 is thought to decrease Clu levels and contribute to complement activation, resulting in vascular leakage which seen in DHF (Kurosu, Chaichana, Yamate, Anantapreecha, & Ikuta, 2007). In addition, NS1 also interacts

with lipid raft on the surface of infected cells, which lead to DENV entry and infectivity (Alcon-LePoder et al., 2005; Noisakran et al., 2008). The hydrophobic membrane proteins NS2A, NS4A, and NS4B serve as scaffolds for the replication complex. The NS2A is a transmembrane protein and associated with the endoplasmic reticulum (ER) (Xie, Gayen, Kang, Yuan, & Shi, 2013). It plays an essential role in viral RNA synthesis and virion assembly (Xie, Zou, Puttikhunt, Yuan, & Shi, 2014). The integral membrane protein NS4A is located in the ER membrane which responses to induces membrane rearrangement for harboring of replication complex (S. Miller, Kastner, Krijnse-Locker, Bühler, & Bartenschlager, 2007). NS4B co-located with double-stranded RNA (dsRNA) and played a critical role in viral replication (S. Miller, Sparacio, & Bartenschlager, 2006). NS4B also suppresses the interferon α/β response (Muñoz-Jordán et al., 2005). NS2B protein is associated with NS3 which acts as the cofactor to activate the NS3 protease (Niyomrattanakit et al., 2004). NS3 has activities of protease, at C-terminal are served as nucleotide triphosphatase and RNA helicase (Kadaré & Haenni, 1997). Whereas the N-terminal exhibits the six-stranded β-barrel conformation which is a typical of chymotrypsin-like serine proteases (Murthy, Clum, & Padmanabhan, 1999). NS5 has two main activities, RNA-dependent RNA-polymerase (RdRp) and methyltransferase. The N-terminal one-third of NS5 is methyltransferase activity, responsible for viral RNA cap formation and internal RNA methylation (Dong et al., 2012; Ray et al., 2006). In addition, NS5 also plays a role in evasion of innate immune response (Ashour, Laurent-Rolle, Shi, & García-Sastre, 2009).

2.2 Viral entry and life cycle

Following the bite of DENV-infected mosquito, the first line of human immune cells resides on the skin is a Langerhans cell which is the type of dendritic cells (DCs) (S.-J. L. Wu et al., 2000). The infection of these cells results in three important events. First, upon the pathogen recognition via the cell-surface receptor, C-type lectin DC-specific intracellular adhesion molecule 3-grabbing non-integrin (DC-SIGN; CD209) (Tassaneetrithep et al., 2003), DCs become activated and produce inflammatory cytokines and chemokines. Second, the infected DCs are migrated to lymphoid tissue such as the spleen, lymph nodes, and bone marrow where the viral replication occurs and the infection is spread to monocyte, macrophage and DCs. Third, DCs present DENV antigens to prime naïve T-cells. In addition, monocytes and macrophages circulate in peripheral blood, lymphoid and non-lymphoid organs, which are also susceptible to DENV infection. DENV also utilizes the L-SIGN homolog DC-SIGN to infect liver endothelial cells (Dejnirattisai et al., 2011). The DENV receptors on monocyte are CD14, HSP70/HSP90, and Fc-receptor whereas the macrophage has mannose receptor (MR; CD206) (Chen, Wang, & King, 1999; J. L. Miller et al., 2008; Reyes-del Valle, Chávez-Salinas, Medina, & del Angel, 2005). Moreover, the mammalian non-immune cell can be DENV infected such as liver and kidney cells. HepG2 is human hepatoma cell line that has been studied for DENV receptors. Those receptors on HepG2 are serotype-specific; GRP78 and laminin receptors are specific DENV serotype2 and 1, respectively (Jindadamrongwech, Thepparit, & Smith, 2004; Thepparit & Smith, 2004). The monkey kidney cell lines (Vero and LLC-MK2) and hamster kidney cell line (BHK) have heparan sulfate and glycosphingolipid as the receptors (Aoki et al., 2006; Germi et al., 2002; Wichit et al., 2011). The *A. albopictus*

mosquito cell line, C6/36 has been identified laminin as the receptor for DENV(Sakoonwatanyoo, Boonsanay, & Smith, 2006). In cells lacking selectin-type receptors, recent studies have shown that DENV utilizes the transmembrane receptors TIM and TAM, two receptors involved in phosphatidylserine-dependent removal of cells undergoing apoptosis (Meertens et al., 2012)

Following binding of DENV envelope and host receptor, the binding mediated virus endocytosis, virions are internalized into the host cell and fused with the endosomal membrane. Exposure to low pH inside the endosome initiate virus conformational change in which DII fusion loops exert into the endosomal membrane, allowing uncoating and releasing their RNA genome into the cytosol (Smit, Moesker, Rodenhuis-Zybert, & Wilschut, 2011). Since the viral RNA can act as mRNA, the DENV genome is associated with the rough ER where it is translated. The translated NS2A, NS4A and NS4B are integrated into the ER membrane forming viral replication complex for viral assembly. In addition, the DENV positive-sense RNA genome is copied to RNA negative sense stranded which serves as template for the synthesis of multiple positive senses RNA strands. The positive-sense RNA strands can be used as templates for translation or can become associated with capsid protein to generate nucleocapsid. The nucleocapsids are assembly with membrane and envelope protein at the replication complex, forming immature viral progeny inside the ER lumen. Finally, immature virus particles are traveled in vesicle to the Golgi apparatus where they undergo glycosylation. Eventually, immature virions are traveled through the secreted vesicle and the prM is cleaved by furin to M, generating mature virions prior secreting out of the host cell.

2.3 Host immunity in antiviral response

2.3.1 Innate immune response

According to DENV binding receptor and internalization in endosomes, the virus triggers the innate immune response. The human innate immune response is the front line of defense against pathogen invasion by recruitment of leukocytes such as natural killer cells (NK), mast cells, and phagocytic cells, including monocytes, neutrophils, macrophages and dendritic cells (DC) (Navarro-Sánchez, Desprès, & Cedillo-Barrón). They inhibit viral replication by inducing the production of type I alpha, beta (α, β) and type II gamma (γ) interferons (IFN). Induction of IFN expression occurs after virus binding the pattern recognition receptors; toll-like receptor-3 (TLR3), TLR7, and TLR8 within the endosomes. The binding of TRLs dependent pathway has been shown to induce expression of pro-inflammatory cytokines, IL8, IL12, IFNα, and IFNγ, in a monocytic cell line, THP-1 cells (Chareonsirisuthigul, Kalayanarooj, & Ubol, 2007). IFN expression subsequently upregulates the production of nitric oxide radicles (NOs). The combined action of IFNs and NOs results in the antiviral state in neighboring cells and suppress DENV replication in infected cells (Ubol, Chareonsirisuthigul, Kasisith, & Klungthong, 2008).

2.3.2 Adaptive immune response

Besides the production of IFNs as an innate antiviral response, it can also trigger host adaptive immune response via DC maturation. DCs initiate antibodies synthesis by dependent and independent of T-cells. The infected DC will present DENV antigen on MHC II molecule and recognized by helper T-cell, which plays an important role in B-cell activation to produce antibodies against DENV. In the

absence of T-cell, DENV antigens present on MHC II of DCs can recognize receptor on B-cell to activate primary antibody response. These antibodies against DENV are generated approximately 6 days post-infection. DENV virions will be recognized by antibodies direct against the structural protein E and prM which neutralize virus infectivity. Two mechanisms of neutralization are blocking the attachment of the virus to cell receptor and blocking the virus fusion process by binding of antibodies to the E protein fusion loop, or through blocking of the conformational changes of the E protein that are required for membrane fusion. Other non-E glycoprotein specific antibodies (e.g., anti-NS1 antibody) can exhibit virus protective effects. However, these effects are not mediated by virion-antibody interactions.

The humoral immunity plays an essential role in the immune response to dengue by providing neutralizing antibody-mediated against DENV E glycoprotein. Upon DENV infection, IgM, IgG, and IgA antibodies are produced. The IgM response begins early, frequently before the onset of symptoms. IgM is usually detectable in serologic assays by 7-8 days post-onset of symptoms. IgA antibodies are also detectable and have half-life similar to IgM. The IgG antibodies are detectable soon after infection and are maintained for years. Infection with any DENV serotype results in immunity to that particular serotype. However, there is no long-term protection against infection with any of the other three serotype viruses.

2.4 The role of adaptive immunity in virus pathogenesis

Re-infection of individuals with a distinct second or third serotype of dengue may result in DF or more severe dengue. There have been a number of hypotheses presented that might explain the more severe manifestation of disease following

heterotypic subsequent infection, such as T cell original antigenic sin and antibody-dependent enhancement (ADE), These two events are postulated to increase the viral load and trigger cytokine storm and the activation complement system, resulting in severe dengue.

2.4.1 T cell original antigenic sin

The original antigenic sin in secondary DENV infections is defined as the dominance of cross-reactive memory T-cell responses to a first infecting DENV serotype (the "original antigen") over the new infecting serotype (Rothman, 2011), resulting in an immune response worsen to the recent infection. In heterotypic secondary DENV infection patients, the cross-reactive CD8$^+$ T cell from the previous infection had a low affinity to the infecting serotype. This may lead to delay the viral clearance (Mongkolsapaya et al., 2003). In addition, The pathogenesis of disease severity may by T cell activation, producing cytokine storm TNF which highly observed in DHF/DSS primary and secondary DENV infection patients (Mangada & Rothman, 2005; Rothman & Ennis, 1999). However, there is no direct evidence of the immunopathogenesis role of T cells.

2.4.2 Antibody-dependent enhancement of dengue virus infection

For ADE, pre-existing DENV antibodies are most likely cross-react with other serotypes, but do not neutralize DENV and escape from antiviral effects which increase the number of viruses. The secondary infection of different serotypes of DENV, the pre-existing antibodies against new DENV can be either non-neutralizing property or weak neutralizing (sub neutralizing). These non- or sub-neutralizing antibodies are known as enhancing antibody which can promote virus infectivity in Fcγ Receptor (FcγR) bearing cells such as monocyte, macrophage, and DC. This led

to an increase in the number of infected cells due to increased antibody-mediated cell binding and entry of the virus, also known as extrinsic ADE. Additionally, the uptake of virus-antibody complex through FcγRI and FcγRIIa on THP-1 monocyte resulting in down-regulation of both TLR gene expression and negative regulators of the NFkB pathway, as well as disruption of RIG-I and MDA5 signaling cascades, leading to suppress antiviral immune response, which subsequently enhance virus production per infected cell (Kou et al., 2011; Modhiran, Kalayanarooj, & Ubol, 2010). This phenomenon is known as intrinsic ADE. The observation on infected human peripheral blood mononuclear cells (PBMCs) has shown that the number of cells was doubled but the viral output increased 10-fold (Kou et al., 2011). The THP-1 cells showed decreased production of inflammatory cytokines, IL-12, IFN-γ TNFα, and nitric oxide radicles when they were infected with DENV in ADE condition but not in the absence of enhancing antibodies (Chareonsirisuthigul et al., 2007). Recent studies showed that the leukocyte immunoglobulin-like receptor B1 (LILRB1) binds DENV-antibody aggregates and block the activating FcγR signals for interferon-stimulated genes (ISGs) expression, which enable DENV to evade the antiviral response during ADE condition (Chan et al., 2014). These results suggest that antibody-mediated DENV entry also triggers intracellular signals that suppress the innate immune response to increase viral production.

2.5 The impact of DENV pre-existing immunity in ZIKV infection

DENV and ZIKV are closely related flaviviruses, circulating in overlapping geographical regions. The recent ZIKV epidemic has been linked to an explosion in reports of microcephaly and neurological defects. The disease severity of secondary

DENV infections is associated with ADE, yet it is unclear that previous exposure to DENV may be protective or worsen ZIKV clinical outcomes.

The study of using DENV-immune plasma (Dejnirattisai et al., 2016) and DENV-derived mAbs (Priyamvada et al., 2016) showed an enhancement of ZIKV infection *in vitro* in the U937 monocytic cell lines. Furthermore, the study of passively transfer of convalescent human sera from DENV to Stat2$^{-/-}$ mice prior to ZIKV infection, resulted in fever and weight loss with an increased mortality as compared to some of the animals administered serum from flavivirus-naïve individuals (Bardina et al., 2017). However, new evidences involving in humoral immune response obtained in non-human primates (McCracken et al., 2017; Pantoja et al., 2017) and human cohort (Gordon et al., 2019; Rodriguez-Barraquer et al., 2019; Terzian et al., 2017) demonstrating that pre-existing DENV immunity may have no detrimental impact on ZIKV infection and also show protective for development of symptomatic ZIKV infection. Moreover, the studies in cellular response showed the strong evidence DENV-elicited CD8$^+$ T cell cross-protective ZIKV infection in mouse model (Regla-Nava et al., 2018; Wen et al., 2017), as well as in the study of both CD4$^+$ and CD8$^+$ T cell in human revealed stronger and faster responses to ZIKV infection (Grifoni et al., 2017).

2.6 Development of human monoclonal antibodies to study DENV and ZIKV

Monoclonal antibodies (mAbs) have been a major fundamental and instrumental in mapping the structure and surface of the virion, in which the epitopes can be mapped for potent neutralizing antibodies. mAbs can guide to vaccine design and or

use as diagnostics and future therapeutics. The DENV and ZIKV E protein mediates virus entry and is the major neutralizing target of antibodies. The recognition site of neutralizing mAbs have identified both serotype-specific and serotype-cross-reactive epitopes in all three domains of the E protein (Fibriansah & Lok, 2016). Anti-E targeting DIII have proven to be the most potent neutralizing antibodies (Beltramello et al., 2010; de Alwis et al., 2011), whereas, fusion loop epitope (FLE) located in DII, are highly enhancing of DENV and ZIKV (Dejnirattisai et al., 2016; Priyamvada et al., 2016). On the other hand, the bc loop adjacent to the FLE is an epitope of a highly human neutralizing Abs to all four DENV serotypes (Smith et al., 2013). The study in mice showed antibodies could block virus membrane fusion by targeting the fusion loop and bc loop simultaneously (Dai et al., 2016). Antibodies targeting prM generally have poor neutralizing and enhancing activity (Huang et al., 2006). Recently, a new class potent neutralizing human mAb was reported. The mAbs recognized a novel quaternary E-dimer epitope (EDE) on the intact virus surface (Dejnirattisai et al., 2015). The mAb targeting EDE1 that was isolated from DENV patients neutralized ZIKV in U937+DC-SIGN cells and protect from disease in an AG129 mouse model (Swanstrom et al., 2016).

2.7 Phage display technology and its involvement in DENV and ZIKV researches

Phage display is a powerful tool to generate antibodies and peptides to facilitate subpopulation discrimination and molecular analyses as well as to link genes with the proteins that they encode (Clackson, Hoogenboom, Griffiths, & Winter, 1991). This technology is attractive because of the ability to rapidly select a molecule with the

desired phenotype from a vast and diverse library repertoire. The selection of antibodies using antibody phage display differs from traditional monoclonal approaches. Antibody phage display is possible to generate antibodies against low immunogenic targets, avoid animal immunization, and generate non-immunogenic human antibodies for therapy (Marks et al., 1991). Phage display is based on the ability of bacteriophage to present engineered proteins on their surface coat. The M13 bacteriophage is a bacterial virus that infects *E. coli* and replicates within the host cell. Each filamentous phage contains single-stranded DNA surrounded by multiple copies of major and minor coat proteins (Azzazy & Highsmith Jr, 2002).

The display of protein by phage is a multistep process that involves a phagemid system. Phagemid vector contains *E.coli* and phage origin of replication, a leader sequence, an insert cloning site, a coat protein gene, and a selectable antibiotic marker (Qi, Lu, Qiu, Petrenko, & Liu, 2012). The phagemid contains only a single phage gene so infection with helper phage is required to provide the remaining machinery for replication. A mature phage particle is assembled from wild type proteins provided by helper phage.

Phage display antibody technology has been used to select serotype-specific antibody fragments. The phage display antibody library was constructed from B lymphocytes of 60 Thai blood donors (Kulkeaw et al., 2009). The library was affinity selected with the recombinant envelope protein EDIII of DENV. The selected scFv showed *in vitro* neutralizing activity against DENV2 (Saokaew et al., 2014). Besides, the same library also used to generate scFv antibodies that could bind specifically to the non-structural protein 1 (NS1) of DENV (Poungpair et al., 2014). Recently, a non-dengue immunized phage display library had been studied in the selection of

antibodies against ZIKV DIII recombinant protein. The results of selected antibodies showed moderate neutralization activity against ZIKV *in vitro* by plaque reduction assay and in C57BL/6 background mice deficient in alpha/beta interferon (IFN-α/β) and IFN-γ receptors (Y. Wu et al., 2017). Therefore, phage display technology is an alternative method to rapidly select antibodies targeting both DENV and ZIKV.

2.8 Future direction

Several questions remain unanswered regarding cross-reactive antibody neutralization and enhancement to flavivirus infection. To anticipate the effects of DENV or ZIKV infection and vaccination in a DENV-infected region, we must first expand our knowledge of understanding cross-reactive antibody responses in people who live in endemic-region and develop the potential source of antibodies that broadly protect against DENV1-4 and ZIKV infection.

2.9 References

Alcon-LePoder, S., Drouet, M.-T., Roux, P., Frenkiel, M.-P., Arborio, M., Durand-Schneider, A.-M., Flamand, M. (2005). The secreted form of dengue virus nonstructural protein ns1 is endocytosed by hepatocytes and accumulates in late endosomes: implications for viral infectivity. **Journal of Virology**, 79(17), 11403-11411.

Aoki, C., Hidari, K. I. P. J., Itonori, S., Yamada, A., Takahashi, N., Kasama, T., Suzuki, Y. (2006). Identification and characterization of carbohydrate molecules in mammalian cells recognized by dengue virus type 2. **Journal of Biochemistry**, 139(3), 607-614.

Ashour, J., Laurent-Rolle, M., Shi, P.-Y., & García-Sastre, A. (2009). NS5 of dengue virus mediates stat2 binding and degradation. **Journal of Virology**, 83(11), 5408-5418.

Azzazy, H. M. E., & Highsmith Jr, W. E. (2002). Phage display technology: clinical applications and recent innovations. **Clinical Biochemistry**, 35(6), 425-445.

Bardina, S. V., Bunduc, P., Tripathi, S., Duehr, J., Frere, J. J., Brown, J. A., Lim, J. K. (2017). Enhancement of Zika virus pathogenesis by preexisting antiflavivirus immunity. **Science**, 356(6334), 175.

Beltramello, M., Williams, K. L., Simmons, C. P., Macagno, A., Simonelli, L., Quyen, Nguyen Than H., Sallusto, F. (2010). The human immune response to dengue virus is dominated by highly cross-reactive antibodies endowed with neutralizing and enhancing activity. **Cell host & microbe**, 8(3), 271-283.

Chan, K. R., Ong, E. Z., Tan, H. C., Zhang, S. L.-X., Zhang, Q., Tang, K. F., Ooi, E. E. (2014). Leukocyte immunoglobulin-like receptor B1 is critical for antibody-dependent dengue. **Proceedings of the National Academy of Sciences**, 111(7), 2722-2727.

Chareonsirisuthigul, T., Kalayanarooj, S., & Ubol, S. (2007). Dengue virus (DENV) antibody-dependent enhancement of infection upregulates the production of anti-inflammatory cytokines, but suppresses anti-DENV free radical and pro-inflammatory cytokine production, in THP-1 cells. **Journal of General Virology**, 88(2), 365-375.

Chen, Y.-C., Wang, S.-Y., & King, C.-C. (1999). Bacterial lipopolysaccharide inhibits dengue virus infection of primary human monocytes/macrophages by blockade

of virus entry via a cd14-dependent mechanism. **Journal of Virology**, 73(4), 2650-2657.

Clackson, T., Hoogenboom, H. R., Griffiths, A. D., & Winter, G. (1991). Making antibody fragments using phage display libraries.

Dai, L., Song, J., Lu, X., Deng, Y.-Q., Musyoki, Abednego M., Cheng, H., Gao, George F. (2016). Structures of the Zika virus envelope protein and its complex with a flavivirus broadly protective antibody. **Cell host & microbe**, 19(5), 696-704. doi:10.1016/j.chom.2016.04.013

de Alwis, R., Beltramello, M., Messer, W. B., Sukupolvi-Petty, S., Wahala, W. M. P. B., Kraus, A., de Silva, A. M. (2011). In-depth analysis of the antibody response of individuals exposed to primary dengue virus infection. **PLoS Neglected Tropical Diseases**, 5(6), e1188.

Dejnirattisai, W., Supasa, P., Wongwiwat, W., Rouvinski, A., Barba-Spaeth, G., Duangchinda, T., Screaton, G. R. (2016). Dengue virus sero-cross-reactivity drives antibody-dependent enhancement of infection with zika virus. **Nature immunology**, 17(9), 1102-1108.

Dejnirattisai, W., Webb, A. I., Chan, V., Jumnainsong, A., Davidson, A., Mongkolsapaya, J., & Screaton, G. (2011). Lectin switching during dengue virus infection. **The Journal of Infectious Diseases**, 203(12), 1775-1783. 3

Dejnirattisai, W., Wongwiwat, W., Supasa, S., Zhang, X., Dai, X., Rouvinski, A., Screaton, G. R. (2015). A new class of highly potent, broadly neutralizing antibodies isolated from viremic patients infected with dengue virus. **Nature immunology**, 16(2), 170-177. doi:10.1038/ni.3058

Dong, H., Chang, D. C., Hua, M. H. C., Lim, S. P., Chionh, Y. H., Hia, F., . . . Shi, P.-Y. (2012). 2′-Methylation of internal adenosine by flavivirus NS5 methyltransferase. **PLoS Pathog**, 8(4), e1002642.

Fibriansah, G., & Lok, S.-M. (2016). The development of therapeutic antibodies against dengue virus. **Antiviral Research**, 128, 7-19.

Germi, R., Crance, J.-M., Garin, D., Guimet, J., Lortat-Jacob, H., Ruigrok, R. W. H., Drouet, E. (2002). Heparan sulfate-mediated binding of infectious dengue virus type 2 and yellow fever virus. **Virology**, 292(1), 162-168.

Gordon, A., Gresh, L., Ojeda, S., Katzelnick, L. C., Sanchez, N., Mercado, J. C., Harris, E. (2019). Prior dengue virus infection and risk of Zika: A pediatric cohort in Nicaragua. **PLoS Medicine**, 16(1), e1002726.

Grifoni, A., Pham, J., Sidney, J., Rourke, P. H., Paul, S., Peters, B., Sette, A. (2017). Prior dengue virus exposure shapes T cell immunity to zika virus in humans. **Journal of Virology**, 91(24), e01469-01417.

Huang, K.-J., Yang, Y.-C., Lin, Y.-S., Huang, J.-H., Liu, H.-S., Yeh, T.-M., Lei, H.-Y. (2006). The dual-specific binding of dengue virus and target cells for the antibody-dependent enhancement of dengue virus infection. **The Journal of Immunology**, 176(5), 2825.

Jindadamrongwech, S., Thepparit, C., & Smith, D. R. (2004). Identification of GRP 78 (BiP) as a liver cell expressed receptor element for dengue virus serotype 2. **Archives of Virology**, 149(5), 915-927.

Kadaré, G., & Haenni, A. L. (1997). Virus-encoded RNA helicases. **Journal of Virology**, 71(4), 2583-2590.

Kou, Z., Lim, J. Y. H., Beltramello, M., Quinn, M., Chen, H., Liu, S.-n., Jin, X. (2011). Human antibodies against dengue enhance dengue viral infectivity without suppressing type I interferon secretion in primary human monocytes. **Virology, 410**(1), 240-247.

Kulkeaw, K., Sakolvaree, Y., Srimanote, P., Tongtawe, P., Maneewatch, S., Sookrung, N., Chaicumpa, W. (2009). Human monoclonal ScFv neutralize lethal Thai cobra, Naja kaouthia, neurotoxin. **Journal of Proteomics**, 72(2), 270-282.

Kurosu, T., Chaichana, P., Yamate, M., Anantapreecha, S., & Ikuta, K. (2007). Secreted complement regulatory protein clusterin interacts with dengue virus nonstructural protein 1. **Biochemical and Biophysical Research Communications**, 362(4), 1051-1056.

Mangada, M. M., & Rothman, A. L. (2005). Altered cytokine responses of dengue-specific CD4$^+$ T cells to heterologous serotypes. **The Journal of Immunology**, 175(4), 2676.

Marks, J., Hoogenboom, H., Bonnert, T., McCafferty, J., Griffiths, A., & Winter, G. (1991). By-passing immunisation: Human antibodies from V gene libraries displayed on phage. **Journal of Molecular Biology**, 222, 581 - 597.

McCracken, M. K., Gromowski, G. D., Friberg, H. L., Lin, X., Abbink, P., De La Barrera, R., Thomas, S. J. (2017). Impact of prior flavivirus immunity on Zika virus infection in rhesus macaques. **PLoS Pathogens**, 13(8), e1006487.

Meertens, L., Carnec, X., Lecoin, M. P., Ramdasi, R., Guivel-Benhassine, F., Lew, E., Amara, A. (2012). The TIM and TAM families of phosphatidylserine receptors mediate dengue virus entry. **Cell host & microbe**, 12(4), 544-557.

Miller, J. L., deWet, B. J. M., Martinez-Pomares, L., Radcliffe, C. M., Dwek, R. A., Rudd, P. M., & Gordon, S. (2008). The mannose receptor mediates dengue virus infection of macrophages. **PLoS pathogens**, 4(2), e17.

Miller, S., Kastner, S., Krijnse-Locker, J., Bühler, S., & Bartenschlager, R. (2007). The non-structural protein 4A of dengue virus is an integral membrane protein inducing membrane alterations in a 2k-regulated manner. J**ournal of Biological Chemistry**, 282(12), 8873-8882.

Miller, S., Sparacio, S., & Bartenschlager, R. (2006). Subcellular localization and membrane topology of the dengue virus type 2 non-structural protein 4B. **Journal of Biological Chemistry**, 281(13), 8854-8863.

Modhiran, N., Kalayanarooj, S., & Ubol, S. (2010). Subversion of innate defenses by the interplay between DENV and pre-existing enhancing antibodies: TLRs signaling collapse. **PLoS Neglected Tropical Diseases**, 4(12), e924.

Modis, Y., Ogata, S., Clements, D., & Harrison, S. C. (2004). Structure of the dengue virus envelope protein after membrane fusion. **Nature**, 427(6972), 313-319.

Mongkolsapaya, J., Dejnirattisai, W., Xu, X.-n., Vasanawathana, S., Tangthawornchaikul, N., Chairunsri, A., Screaton, G. (2003). Original antigenic sin and apoptosis in the pathogenesis of dengue hemorrhagic fever. **Nature Medicine**, 9(7), 921-927.

Muñoz-Jordán, J. L., Laurent-Rolle, M., Ashour, J., Martínez-Sobrido, L., Ashok, M., Lipkin, W. I., & García-Sastre, A. (2005). Inhibition of alpha/beta interferon signaling by the NS4B protein of flaviviruses. **Journal of Virology**, 79(13), 8004-8013.

Murthy, H. M. K., Clum, S., & Padmanabhan, R. (1999). Dengue virus NS3 serine protease: crystal structure and insights into interaction of the active site with substrates by molecular modeling and structural analysis of mutational effects. **Journal of Biological Chemistry**, 274(9), 5573-5580.

Navarro-Sánchez, E., Desprès, P., & Cedillo-Barrón, L. Innate immune responses to dengue virus. **Archives of Medical Research**, 36(5), 425-435.

Ngono, A. E., & Shresta, S. (2018). Immune response to dengue and Zika. **Annual review of immunology**, 36, 279-308.

Niyomrattanakit, P., Winoyanuwattikun, P., Chanprapaph, S., Angsuthanasombat, C., Panyim, S., & Katzenmeier, G. (2004). Identification of residues in the dengue virus type 2 NS2B cofactor that are critical for NS3 protease activation. **Journal of Virology**, 78(24), 13708-13716.

Noisakran, S., Dechtawewat, T., Avirutnan, P., Kinoshita, T., Siripanyaphinyo, U., Puttikhunt, C., Sittisombut, N. (2008). Association of dengue virus NS1 protein with lipid rafts. **Journal of General Virology**, 89(10), 2492-2500.

Pantoja, P., Pérez-Guzmán, E. X., Rodríguez, I. V., White, L. J., González, O., Serrano, C., Sariol, C. A. (2017). Zika virus pathogenesis in rhesus macaques is unaffected by pre-existing immunity to dengue virus. **Nature Communications**, 8, 15674.

Poungpair, O., Bangphoomi, K., Chaowalit, P., Sawasdee, N., Saokaew, N., Choowongkomon, K., Yenchitsomanus, P.-t. (2014). Generation of human single-chain variable fragment antibodies specific to dengue virus non-structural protein 1 that interfere with the virus infectious cycle. **mAbs**, 6(2), 474-482.

Priyamvada, L., Quicke, K. M., Hudson, W. H., Onlamoon, N., Sewatanon, J., Edupuganti, S., Wrammert, J. (2016). Human antibody responses after dengue virus infection are highly cross-reactive to Zika virus. **Proceedings of the National Academy of Sciences of the United States of America**, 113(28), 7852-7857.

Qi, H., Lu, H., Qiu, H.-J., Petrenko, V., & Liu, A. (2012). Phagemid vectors for phage display: properties, characteristics and construction. **Journal of molecular biology**, 417(3), 129-143.

Ray, D., Shah, A., Tilgner, M., Guo, Y., Zhao, Y., Dong, H., Shi, P.-Y. (2006). West Nile Virus 5′-Cap structure is formed by sequential guanine N-7 and ribose 2′-O methylations by nonstructural protein 5. **Journal of Virology**, 80(17), 8362-8370.

Regla-Nava, J. A., Elong Ngono, A., Viramontes, K. M., Huynh, A.-T., Wang, Y.-T., Nguyen, A.-V. T., Shresta, S. (2018). Cross-reactive dengue virus-specific CD8+ T cells protect against Zika virus during pregnancy. **Nature Communications**, 9(1), 3042.

Reyes-del Valle, J., Chávez-Salinas, S., Medina, F., & del Angel, R. M. (2005). Heat shock protein 90 and heat shock protein 70 are components of dengue virus receptor complex in human cells. **Journal of Virology**, 79(8), 4557-4567.

Rodriguez-Barraquer, I., Costa, F., Nascimento, E. J. M., Nery, N., Castanha, P. M. S., Sacramento, G. A., Ko, A. I. (2019). Impact of preexisting dengue immunity on Zika virus emergence in a dengue endemic region. **Science**, 363(6427), 607.

Rothman, A. L. (2011). Immunity to dengue virus: a tale of original antigenic sin and tropical cytokine storms. **Nature Reviews Immunology**, 11(8), 532-543.

Rothman, A. L., & Ennis, F. A. (1999). Immunopathogenesis of dengue hemorrhagic fever. **Virology**, 257(1), 1-6.

Sakoonwatanyoo, P., Boonsanay, V., & Smith, D. R. (2006). Growth and production of the dengue virus in C6/36 cells and identification of a laminin-binding protein as a candidate serotype 3 and 4 receptor protein. **Intervirology**, 49(3), 161-172.

Saokaew, N., Poungpair, O., Panya, A., Tarasuk, M., Sawasdee, N., Limjindaporn, T., Yenchitsomanus, P. (2014). Human monoclonal single-chain antibodies specific to dengue virus envelope protein. **Letters in Applied Microbiology**, 58(3), 270-277.

Smit, J. M., Moesker, B., Rodenhuis-Zybert, I., & Wilschut, J. (2011). Flavivirus cell entry and membrane fusion. **Viruses**, 3(2), 160-171.

Smith, S. A., de Alwis, A. R., Kose, N., Harris, E., Ibarra, K. D., Kahle, K. M., Crowe, J. E., Jr. (2013). The potent and broadly neutralizing human dengue virus-specific monoclonal antibody 1C19 reveals a unique cross-reactive epitope on the bc loop of domain II of the envelope protein. **mBio**, 4(6), e00873.

Stiasny, K., & Heinz, F. X. (2006). Flavivirus membrane fusion. **Journal of General Virology**, 87(10), 2755-2766.

Swanstrom, J. A., Plante, J. A., Plante, K. S., Young, E. F., McGowan, E., Gallichotte, E. N., Baric, R. S. (2016). Dengue virus envelope dimer epitope monoclonal antibodies isolated from dengue patients are protective against Zika virus. **mBio**, *7*(4), e01123-01116.

Tassaneetrithep, B., Burgess, T. H., Granelli-Piperno, A., Trumpfheller, C., Finke, J., Sun, W., Marovich, M. A. (2003). DC-SIGN (CD209) mediates dengue virus

infection of human dendritic cells. **The Journal of Experimental Medicine**, 197(7), 823-829.

Terzian, A. C. B., Schanoski, A. S., Mota, M. T. d. O., da Silva, R. A., Estofolete, C. F., Colombo, T. E., Nogueira, M. L. (2017). Viral load and cytokine response profile does not support antibody-dependent enhancement in dengue-primed Zika virus–infected patients. **Clinical Infectious Diseases**, 65(8), 1260-1265.

Thepparit, C., & Smith, D. R. (2004). Serotype-specific entry of dengue virus into liver cells: identification of the 37-kilodalton/67-kilodalton high-affinity laminin receptor as a dengue virus serotype 1 receptor. **Journal of Virology**, 78(22), 12647-12656.

Ubol, S., Chareonsirisuthigul, T., Kasisith, J., & Klungthong, C. (2008). Clinical isolates of dengue virus with distinctive susceptibility to nitric oxide radical induce differential gene responses in THP-1 cells. **Virology**, 376(2), 290-296.

Wen, J., Elong Ngono, A., Regla-Nava, J. A., Kim, K., Gorman, M. J., Diamond, M. S., & Shresta, S. (2017). Dengue virus-reactive CD8+ T cells mediate cross-protection against subsequent Zika virus challenge. **Nature Communications**, 8(1), 1459.

Wichit, S., Jittmittraphap, A., Hidari, K. I., Thaisomboonsuk, B., Petmitr, S., Ubol, S., Suzuki, T. (2011). Dengue virus type 2 recognizes the carbohydrate moiety of neutral glycosphingolipids in mammalian and mosquito cells. **Microbiology and Immunology**, 55(2), 135-140.

Wu, S.-J. L., Grouard-Vogel, G., Sun, W., Mascola, J. R., Brachtel, E., Putvatana, R., Frankel, S. S. (2000). Human skin Langerhans cells are targets of dengue virus infection. **Natare Medicine**, 6(7), 816-820.

Wu, Y., Li, S., Du, L., Wang, C., Zou, P., Hong, B., Ying, T. (2017). Neutralization of Zika virus by germline-like human monoclonal antibodies targeting cryptic epitopes on envelope domain III. **Emerging Microbes & Infections**, 6(1), 1-11.

Xie, X., Gayen, S., Kang, C., Yuan, Z., & Shi, P.-Y. (2013). Membrane topology and function of dengue virus NS2A Protein. **Journal of Virology**, 87(8), 4609-4622.

Xie, X., Zou, J., Puttikhunt, C., Yuan, Z., & Shi, P.-Y. (2014). Two distinct sets of NS2A molecules are responsible for dengue virus RNA synthesis and virion assembly. **Journal of Virology**, 89(2), 1298-1313.
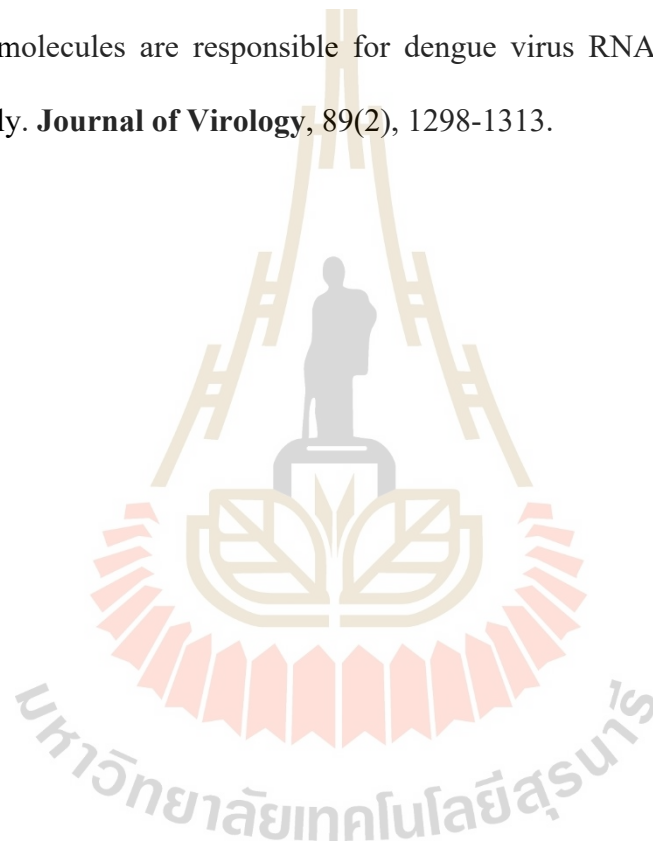
CHAPTER III

REPEATED EXPOSURE TO THE DENGUE VIRUSES ELICITS ROBUST CROSS-NEUTRALIZING ANTIBODIES AGAINST ZIKA VIRUS IN RESIDENTS OF A DENGUE-ENDEMIC REGION IN THAILAND

3.1 Abstract

Zika virus (ZIKV) and dengue virus (DENV) are antigenically related mosquito-borne flaviviruses. ZIKV is becoming increasingly prevalent in DENV-endemic regions, raising the possibility that pre-existing immunity to one virus could modulate the response to a heterogenous virus, although whether this would be beneficial or detrimental is unclear. Here, we analyzed sera from the resident of a DENV-endemic region of Thailand to determine the prevalence of DENV-elicited antibodies capable of cross-neutralizing ZIKV. Of the 61 participants, who were asymptomatic and unselected for viral serostatus, 52 and 51 were DENV and ZIKV seropositive, respectively. Notably, participants with serologically classified secondary DENV infection (23/52, 44.23%) had strikingly higher titers and broader reactivities of neutralizing antibodies against ZIKV and DENV heterotypes compared with participants with primary DENV infection. Primary ZIKV infection was detected in some participants, confirming ZIKV co-circulation in this region. Our results suggest

that a large proportion of residents in a DENV-endemic region provoke enduring a cross-protective neutralization antibody against ZIKV and DENV heterotypes.

3.2 Introduction

Dengue virus (DENV) and Zika virus (ZIKV) are members of the *Flavivirus* genus, which includes other pathogens such as, Yellow fever virus, West Nile virus, and Japanese encephalitis virus. ZIKV was first discovered from a rhesus monkey in the Zika forest of Uganda in 1947 (Dick, Kitchen, & Haddow, 1952). After decades, the first confirmed human ZIKV infection was reported in 1964 (Simpson, 1964). A ZIKV outbreak occurred again in 2007 on Yap Island, Micronesia (Duffy et al., 2009). Since then, the virus had spread through Africa, Southeast Asia, and the South Pacific in 2013 – 2014 in French Polynesia (V.-M. Cao-Lormeau et al., 2014; Ioos et al., 2014). Then in 2015, an explosive ZIKV epidemic was noted in Brazil that rapidly spread through South, Central and North America (Faria et al., 2017; Zhang et al., 2017). ZIKV infections can be symptomatic. However, 80% are asymptomatic (Lazear & Diamond, 2016). ZIKV infection is a self-limited mild, febrile illness with fever, myalgia, arthralgia, headache, conjunctivitis, and rash, similar in presentation to dengue virus infection (Musso & Gubler, 2016). It was later discovered that ZIKV is associated with Guillain Barré syndrome (GSB) in adults, an autoimmune disease characterized by ascending paralysis and polyneuropathy dating back to the outbreak in French Polynesia 2013 (V. M. Cao-Lormeau et al., 2016). Furthermore, the prevalence of ZIKV infection in Brazil in 2015 first noted the coincidence of congenital malfunction in pregnancy known as microcephaly (Rasmussen, Jamieson, Honein, & Petersen, 2016). Neonates born to ZIKV-infected mothers resulted in a

reduction in head size and brain development, causing developmental delay. ZIKV is unique in that the virus can be transmitted vertically from mother to fetuses as well as via sexual contact (D'Ortenzio et al., 2016; Musso, Roche, et al., 2015; Mysorekar, 2017; Yockey et al., 2016). The severity of birth malformations noted with the epidemic led to the World Health Organization (WHO) to declare ZIKV a public health emergency in February 2016 (Organization, 2016). However, ZIKV epidemiology and disease burden in Southeast Asia is not well studied, as compared to South America where it is well defined and is therefore poorly understood. It has been more than 60 years since the first evidence of ZIKV isolation from mosquitoes in Malaysia in 1966 (Marchette, Garcia, & Rudnick, 1969), and the first laboratory-confirmed autochthonous ZIKV infection in Asia occurred in Cambodia in 2010 (Heang et al., 2012). In Thailand, ZIKV infection was first reported in early 2013 in a female Canadian traveler (Fonseca et al., 2014). Subsequently, there were two cases report from a German traveler in November in 2013 and a Japanese traveler in July in 2014 (Shinohara et al., 2016; Tappe et al., 2014). Thailand is endemic for DENV and although there is co-circulation of all four serotypes throughout the year, there tends to be a predominant serotype in any given year (Pongsiri, Themboonlers, & Poovorawan, 2012; Vongpunsawad, Intharasongkroh, Thongmee, & Poovorawan, 2017). ZIKV shares the same mosquito vectors and ecology as DENV (Musso, Cao-Lormeau, & Gubler, 2015). Therefore, high rates of co-circulation of the four DENV serotypes with ZIKV give rise to problems with heterotypic immunity and raise important questions for ZIKV infection dynamics in forthcoming DENV and ZIKV epidemics in Thailand.

Genetic clustering of both ZIKV and DENV are closely related, sharing approximately 54-59 % of nucleotide sequence identity of the encoded envelope protein (E) (Kostyuchenko et al., 2016). The E protein of viral particles is essential for receptor binding, entry, and fusion. Additionally, It has been shown that the E protein epitopes on the virus surface are a primary target for a neutralizing antibody (NAb) response (Halstead, 1988; Halstead, 2015). Primary infection with one of the four DENV serotypes produces life-long serotype specific-NAbs. Secondary infection with a different serotype increases the risk of severe morbidity and mortality. This phenomenon is thought to occur due to the sub-neutralizing level of previous serotype-specific antibodies which can produce immunopathogenesis by increasing virus entry into Fc-receptor bearing cells, resulting in viral replication promotion (Halstead, 1979, 2015). This phenomenon is also known as antibody-dependent enhancement (ADE). However, little is known about the effect of pre-existing flavivirus immunity on ZIKV infection. Controversy exists whether or not cross-reactive antibodies between DENV and ZIKV generate protection or enhancement of infection. The convergence of several findings has amplified the need to understand the health ramifications of sequential infections with ZIKV or DENV1–4 heterotypes. First, the high sequence homology between ZIKV and DENV generates substantial antigenic overlap, leading to cross-reactive T and B cell immune responses. Second, pre-existing immunity to one flavivirus or serotype has been shown to either protect against or exacerbate a subsequent heterologous virus infection, but the mechanisms controlling the particular outcome are unclear (Bradt et al., 2019). It has been shown that DENV-specific antibodies are able to enhance ZIKV infection *in vitro* and *in vivo* (Bardina et al., 2017; Dejnirattisai et al., 2016; Priyamvada et al., 2016). A passive

transfer of human DENV convalescent plasma into ZIKV infected mice resulted in increased morbidity and mortality (Bardina et al., 2017). Conversely, three different studies have recently reported that pre-existing anti-DENV immunity has been shown to confer protection against subsequent ZIKV infection in humans (Gordon et al., 2019; Pedroso C & Netto EM, 2019; Rodriguez-Barraquer et al., 2019). The mechanism of cross-protection afforded by prior DENV immunity against ZIKV infection in humans is presently unclear, but based on mouse model studies, CD8 T cell may play a key role in mediating this cross-protection (Regla-Nava et al., 2018; Wen, Elong Ngono, et al., 2017; Wen, Tang, et al., 2017). Third, the observation that ZIKV may be silently continuing to spread in DENV-endemic regions, where the majority of the population has already been exposed to DENV (Grubaugh et al., 2019), has increased the potential for detrimental ADE of infection with ZIKV or DENV heterotypes. Thus, it is essential that we understand whether pre-existing anti-DENV immunity may have deleterious or beneficial effect upon ZIKV infection in residents of DENV-endemic regions.

In this study, we examined serum samples from unselected healthy adults living in Nakhon Ratchasima, Thailand for the presence of anti-DENV1-4 and anti-ZIKV Abs and investigated the extent to which they could cross-neutralize heterologous virus infections *in vitro*. We found a striking association between repeated DENV infection and the presence of a strong and broad cross-neutralizing response

3.3　Material & Methods

3.3.1 Study Participants and Sample Collection

The study included blood samples from a total of 61 unselected healthy volunteers (25 men, 36 women, aged 18-69 years) living in Nakhon Ratchasima, Thailand, who attended at the Suranaree of Technology (SUT) Hospital. Blood samples (5 mL) were collected between April and July 2016. As controls, additional blood samples were obtained from 3 healthy female volunteers of European descent (Austrians, aged 22 years) who had never traveled to Southeast Asia and were confirmed here to be ZIKV and DENV seronegative. The study was approved by the Ethics committee of SUT (protocol no. EC-59-10) and the Institutional Review Boards of La Jolla Institute for Immunology (protocol no. IB-189-1118). Written informed consent was obtained from all participants before blood collection.

3.3.2 Viruses Propagation

WHO reference strain: DENV1 16007, DENV2 16681, DENV3 16562, and DENV4 1036 were kindly provided by Duncan R. Smith (Mahidol University, Thailand). ZIKV Asian lineage strain SD001 was isolated from a donor who had visited Venezuela in 2016 (Carlin et al., 2018). All virus stocks were propagated in *Aedes albopictus* C6/36 cells (ATCC no. CRL-1660). Virus-containing supernatants were clarified by low-speed centrifugation, concentrated by ultracentrifugation, and supplemented with the fetal bovine serum to a final concentration of 20%. All the viruses were stored at −80 °C. Viral titers were determined using a focus forming assay with baby hamster kidney (BHK)-21 cells (ATCC no. CCL-10) as previously described (Elong Ngono et al., 2019).

3.3.3 *In vitro* neutralization assay

3.3.3.1 Plaque Reduction Neutralization Test (PRNT)

Plaque Reduction Neutralization Test (PRNT) of DENV1-4 was performed on LLC-MK$_2$ cells. Cells were seeded as monolayer into 6-well plates at 3×10^5 cells/ well and grown at 37 °C for 24h. Human serum was heat-inactivated at 56 °C for 30 min and then serially two-fold diluted starting at 1:10 – 1:1,280 dilutions with Medium 199 (Gibco, Invitrogen). DENV viruses were diluted in Medium 199, supplemented with 2% fetal bovine serum (Gibco, Invitrogen) to obtain sufficient infection 50-60 PFU/well without human serum dilution (control). An equal volume of virus and each serum dilution were mixed and incubated at 37 °C for 1 h. The virus and serum mixture was added onto each well of LLC-MK$_2$ cells and incubated at 37 °C for 2 h. The inoculated cells were removed from the virus and serum mixtures and overlaid with 2X nutrient and 1.6% Seakem® LE agarose (Lonza) and incubated at 37 °C with 5% CO_2 for 5 days. Cells were fixed with 4% formaldehyde solution (Millipore Sigma) for 2 h at room temperature. Cells were overlaid with agarose and then stained with 1.25% crystal violet in 50% ethanol for 5 min. Cells were washed with water and let to air-dry. Plaque number was counted and calculated for the percentage of neutralization, comparing with plaque number from infection control. Plaque numbers after incubation with (test) or without (control) test sera were counted and the percentage neutralization was calculated as $100 \times$ ([control plaque number – test plaque number]/control plaque number). The 90% neutralization titer (NT$_{90}$) was defined as the reciprocal of the serum dilution resulting in a 90% reduction of viral infectivity and was calculated by non-linear regression with 95% confidence intervals using Prism 7 software (GraphPad, La Jolla, CA).

3.3.3.2 Flow cytometry-based Neutralization assay

ZIKV SD001 neutralization activity of human serum was determined by using a flow cytometry-based assay with U937 human monocytic cells stably transfected with DC-SIGN (U937+DC-SIGN) as previously described (Elong Ngono et al., 2019). U937+DC-SIGN cells were seeded into 96-well plates at the 5×10^4 cells/well and grown in 37 °C with 5% CO_2 for 24 h. The inactivated human serum was diluted with RPMI 1640 without FBS supplemented at a dilution of 1:10 followed with serial five-fold dilutions until 1:6,250. The serially diluted serum was incubated with sufficient virus to cause 7-15% infection in U937+DC-SIGN cells at 37 °C for 1 h before added to U937+DC-SIGN cells. Cells were infected for 2 h at 37 °C. The infected U937+DC-SIGN cells were centrifuged at $1,500 \times g$ for 5 min to removed virus-serum mixtures and washed one time with RPMI 1640 supplemented 10% FBS. Cells were replaced with fresh RPMI 1640 supplemented 10% FBS and incubated at 37 °C with 5% CO_2 for 20 h. The cells were stained with PE-conjugated mouse anti-human CD209 (BD biosciences), fixed and permeabilized by cytofix/cytoperm solution (BD Biosciences). The cells were intracellular stained with Alexa Flour 647-conjugated (Molecular Probes, Life Technologies) 4G2 antibody, a mouse monoclonal that binds to ZIKV E protein. Unbound antibody was washed off, and cells were resuspended in 1XPBS supplemented with 3% FBS and 2mM EDTA. The assay was quantified on an LSRII flow cytometer (BD Biosciences) and the percentage of infected cells was analyzed using FlowJo 10.4.2 software (Tree Star, Ashland, OR). The percentage of serum neutralization was calculated as $100 \times$ (% infected cells in the absence of serum − % infected cells in the presence of serum)∕% infected cells in the absence of serum. The titer of serum that showed 90%

neutralization was analyzed by non-linear regression using GraphPad Prism 7 (GraphPad software, La Jolla, CA).

3.3.4 ELISA

Individual human serum was tested for the presence of IgG antibody against dengue E antigen serotype 1–4 using indirect enzyme-linked immunosorbent assay (ELISA) (E-DEN-01G, Panbio, Brisbane, QLD, Australia), according to the manufacturer's instructions. The DENV specific IgG was expressed as Panbio units. The human serum binding to ZIKV E and NS1 recombinant proteins were measured by ELISA as previously described (Elong Ngono et al., 2019), ELISA 96-wells plate (Costar) were coated with 1 μg/mL of ZIKV E antigen (Suriname strain, Native Antigen) or NS1 antigen (R01636, Meridian Life Science) in 0.1 M $NaHCO_3$ overnight at 4 °C. Plates were then blocked with 5% casein in PBS for 1 h. Human serum was three-fold serially diluted in PBS containing 1% BSA and added to the plate for 1.5 h. The binding was detected with HRP conjugated goat anti-human IgG Fc (Invitrogen, USA). The colorimetric detection was read at the absorbance 450 nm. ZIKV-specific IgG is expressed as an endpoint titer, calculated as the reciprocal of the highest serum dilution that gave a reading above the cutoff value of the negative serum control.

3.3.5 Serostatus Definitions

An NT_{90} >20 was considered positive for NAbs against ZIKV or a DENV serotype. Primary infection was defined as either (i) an NT_{90} >20 against a single virus or serotype, *or* (ii) a dominant response against a single virus or serotype with an NT_{90} ≥4-fold that for the remaining virus/serotypes. A secondary infection was

defined as an NT_{90} >20 against at least two virus/serotypes and the dominant response had an NT_{90} ≤4-fold that of the next highest response.

3.3.6 Statistical Analysis

Data are expressed as the mean ± standard deviation (SD). Differences between group means were analyzed by two-way analysis of variance or the Kruskal–Wallis test. P < 0.05 was considered significant.

3.4 Result

Selected demographic features and the DENV and ZIKV serostatus of the 61 patient Thai cohort is shown in **Table 1**. The group consisted of 25 men and 36 women with a median age of 31 years (SD 9.9, range 18–69 years). Of the 61 participants, 52 (85.3 %, 95% CI 74.3–92.0) were seropositive for DENV IgG, indicating that the majority had been infected with DENV at least once (**Figure 1 and Table 1**). A breakdown of DENV seroprevalence by age indicated a positive association between prior exposure to DENV and age. Thus, 100% of participants aged 38 years and older were DENV seropositive (n = 21; 95% CI 84.5–100), compared with 80% of participants aged 28–37 years (n = 16; 95% CI 58.4–91.3) and 75% of those aged 18–27 years (n = 15; 95% CI 53.1–88.8) (**Table 1**). There was no significant by the association between sex and seroprevalence (P >0.99); thus, approximately the same proportion of women and men were DENV seropositive (31/36 [86.1%] and 21/25 [84.0%], respectively). The three control sera were DENV seronegative, as expected (**Figure 1**).

Similar to DENV, 51 of the 61 sera tested were ZIKV seropositive (**Table 1**). There was also no significant association between sex and seroprevalence (P >0.99).

ZIKV seropositive proportion of women and men was 31/36 [86.5%] and 20/25 [80.0%], respectively. The ZIKV seropositive by age indicated a positive association i.e., 100% of participants aged 38 years and older were ZIKV seropositive (n = 21; 95% CI 84.5–100), compared with 80% of participants aged 28–37 years (n = 16; 95% CI 58.4-91.3) and 70% of those aged 18–27 years (n = 14; 95% CI 48.1–85.5) (**Table 1**). These data suggest that most of DENV seropositive also cross-reacted with ZIKV which prompted us to determine whether it was able to neutralize ZIKV infection.

3.4.2 Prevalence of Anti-DENV1–4 and Anti-ZIKV Neutralizing Antibodies

To determine the serotype specificity and neutralizing activity of Abs present in the 61 sera, we performed in vitro cell-based neutralization tests, using a PRNT with LLC-MK2 cells for screening DENV1–4 infection and a flow cytometry assay with DC-SIGN-positive U937 cells for ZIKV infection. In both cases, the data are expressed as 90% neutralization titers (NT90). The NT90 values for the sera are shown in Figure 2. Among the 61 participants, 19 (31.1%, 95 % CI 20.9–43.6) had NAbs against ZIKV and all four DENV serotypes (Tables 2 and 3). NAbs against DENV1, 2, or 3 were detected in more than half of the sera, with NAbs against DENV2 being the most prevalent (44/61, 72.1%) followed by DENV3 (38/61, 62.3%), DENV1 (36/61, 59.0%), and DENV4 (21/61, 34.4%). Approximately half of the sera were positive for anti-ZIKV NAbs (32/61, 52.5%).

There were no significant differences in the proportion of sera from males (total n = 25) and females (total n = 36) that were positive for NAbs against DENV1 (~59%), DENV2 (~72%), DENV3 (~62%), DENV4 (~34%), and ZIKV (~52%). Not surprisingly, the prevalence of NAbs against each DENV serotype and ZIKV

increased significantly with age. For example, the proportion of participants in each age group positive for anti-DENV1 NAbs increased from 50% (10/20) at age 18–27 years to 75% (3/4) by age ≥48 years, and a similar age-dependent increase was observed for NAbs against DENV2–4 and ZIKV (**Table 2**). These results reveal that age is a reflection of the time that the individuals may have been exposed to the different DENV serotypes that circulated in the region.

3.4.3 Neutralizing Antibody Profiles According to DENV and ZIKV Serostatus

To determine whether and how the prevalence of anti-DENV or anti-ZIKV NAbs was affected by prior exposure to DENV or ZIKV, we classified the sera into primary/secondary infection based on NAb serostatus and reactivity. For this analysis, we defined NAb positivity as an NT_{90} >20 for the specific test virus/serotype. A primary infection was defined as either (i) positive for NAbs against a single virus/serotype or (ii) positive for NAbs against more than one virus/serotype and a dominant NT_{90} value ≥4-fold higher than that against the other virus/serotype(s). A secondary infection was defined as positive for NAbs against at least two virus/serotypes and the dominant response had an NT_{90} ≤4-fold that of the next highest response.

As shown in Figure 3, of the 61 participants, 25 (41.0%; 95% CI 29.5–53.5), 23 (37.7%; 95% CI 26.6–50.3), 2 (3.3%; 95% CI 0.58–11.2), 2 (3.3%; 95% CI 0.58–11.2), and 9 (14.8%; 95% CI 7.96–25.7) were classified as primary DENV infection, secondary DENV infection, primary ZIKV infection, secondary ZIKV or DENV infection, or no infection (naïve), respectively. Among the 25 participants whose serology was consistent with primary DENV infection, most were DENV2

infections, followed by DENV1, and DENV3 (n = 13, 7, and 5, respectively); in contrast, none of the serological profiles were consistent with primary DENV4 infection (Table 3). Interestingly, only 6 of the 25 (24%) participants with primary DENV infection had cross-neutralizing Abs against ZIKV (Table 3). In contrast, of the 23 participants with secondary DENV infection, 22 (95.7%) showed high titers of anti-ZIKV NAbs, and the one negative sample also had low titers of NAbs against DENV1–4, suggesting that the donor mounted a weak NAb response to all flaviviruses/serotypes tested. Thus, nearly all of the participants showing evidence of repeated infection with DENV contain Abs with robust ZIKV-neutralizing capacity. Only two participants showed serological evidence of primary ZIKV infection. One of these (no. 15) had a low NT_{90} for ZIKV and was negative DENV NAbs, and the second (no. 30) had a very high titer of ZIKV NAbs and lower but marked neutralizing activity against all four DENV serotypes. Two sera (no. 24 and 60) had high NT_{90} values for DENV1 and ZIKV, suggesting they may reflect sequential infection with both viruses. Collectively, these results indicate that repeated exposure to heterotypic DENV elicits strongly cross-neutralizing Abs against ZIKV in healthy individuals living in a DENV-endemic area.

3.4.4 ZIKV-Neutralizing Activity of DENV-Elicited Antibodies

To further investigate the reactivity of DENV-elicited ZIKV cross-neutralizing Abs, we performed antigen-specific ELISAs using recombinant ZIKV NS1 and E proteins as the target antigens. For this analysis, we assigned the 62 sera to one of five groups based on DENV1–4 and/or ZIKV NAb serostatus (where the cutoff for positive/negative NAb is NT_{90} 20). Group 1, DENV⁻ ZIKV⁻ (n = 9); group 2, DENV⁺ (one to three serotypes) ZIKV⁻ (n = 19); group 3, DENV⁺ (one to three

serotypes) ZIKV$^+$ (n = 13); group 4, DENV$^+$ (all four serotypes) ZIKV$^+$ (n = 19); and group 5, DENV$^-$ ZIKV$^+$ (n = 1).

Notably, all of the DENV seropositive samples also contained anti-ZIKV E protein (**Figure 4A**) and/or anti-ZIKV NS1 (**Figure 4B**) Abs, and the binding patterns for ZIKV E and NS1 were similar for each group. The anti-ZIKV Ab endpoint titer of sera with NAbs against all four DENV serotypes (group 4) was not significantly higher than that of the sera with NAbs against fewer DENV serotypes (group 3) (P >0.99), indicating that the anti-DENV NAb response influenced the magnitude of the cross-reactive anti-ZIKV Ab response. Furthermore, the five groups also showed distinct ZIKV-neutralizing activities (**Figure 5**), with a strong correlation between the breadth of DENV serotype neutralizing activity and the titer of ZIKV NAbs. Thus, the sera with the most potent ZIKV-neutralizing activity was group 5 (reactive to ZIKV alone), followed in order by group 4 (ZIKV and DENV1–4), group 3 (ZIKV and one to three DENV serotypes), and group 2 (one to three DENV serotypes but not ZIKV) (**Figure 5**). In summary, these results indicate that both the quantity and quality of DENV and ZIKV NAbs are influenced by prior exposure to the heterologous virus/serotype.

3.5 Discussion

Thailand is a hyperendemic region where all four DENV serotypes co-circulate. In addition, ZIKV has been found throughout Thailand. Little is known about asymptomatic infection in healthy adults and how their background immunity can affect infection with ZIKV and thus affect the epidemic dynamics in the country.

In this study, we sought to determine whether healthy residents of a DENV-endemic region in Thailand showed evidence of cross-neutralizing Abs to ZIKV. DENV has been endemic in the area since 1958 (Halstead & Yamarat, 1965), and although there have been no outbreaks of ZIKV in Thailand, its presence has been documented since 2006 (Ruchusatsawat, 2019). These observations suggested that most residents of the region have likely been infected with DENV, if not ZIKV, at least once. This suggestion is supported by our results here showing that, 52 of the 61 participants in our study were DENV seropositive, 25 of whom showed evidence of repeat infections based on NAbs. Similarly, 51 were ZIKV seropositive, 4 of whom were confirmed as having primary or secondary ZIKV infection based on NAbs. Thus, a substantial proportion of the participants showed evidence of exposure to DENV but not ZIKV, yet had sera with strongly cross-neutralizing activity against ZIKV.

Our findings are consistent with a recent cohort study of 1,453 individuals school-age and adults in Brazil, which indicated that individuals with high Ab titers to DENV showed a reduced risk for ZIKV infection (Rodriguez-Barraquer et al., 2019). In the present study, 52.5% (32/61) of serum samples contained anti-ZIKV NAbs (based on $NT_{90} \geq 20$), which was considerably higher than the 22.2% of sera (based on $PRNT_{90} \geq 20$) detected in a cohort of 135 adults in Bangkok, Central Thailand (Sornjai, Jaratsittisin, Auewarakul, Wikan, & Smith, 2018). This discrepancy is probably because Nakhon Ratchasima is located in Northeastern Thailand, which is less developed and not urbanization.

A study of North Carolina travelers returning from DENV or ZIKV endemic country who confirmed DENV or ZIKV infection indicated that patients with primary

DENV infection showed no evidence of ZIKV NAbs and only a low frequency of those with secondary DENV infection had anti-ZIKV NAbs (23 %, IC_{50} in FRNT assay). That study was performed with samples collected ≥6 months after infection when the NAbs response has become more specific to virus/serotype (Matthew et al., 2017). The discrepancy in findings between the study of Collins et al. and ours is likely due to the residency of the subjects and the timespan after primary infection. Recent cohort studies of patients from Latin America and Asia, including Thailand, showed that convalescent sera collected ≥5 months (Montoya et al., 2018) after secondary DENV infection failed to cross-neutralize ZIKV. The limitation of our study is the unselected participant recruited without infection history or clinically confirmed. Our results support a previous observation that healthy but repeatedly infected residents of regions hyper-endemic for DENV can maintain broadly cross-neutralizing Abs again ZIKV and the four DENV serotypes (Katzelnick, Montoya, Gresh, Balmaseda, & Harris, 2016). In the present study, we observed that cross-neutralizing Abs DENV4 was the least frequent (21/61, 34.4%), which correlates well with epidemiological studies demonstrating that DENV4 is the least prevalent serotype in Thailand (Limkittikul, Brett, & L'Azou, 2014).

The two different cohort studies have also found that high titers of NAbs to DENV provided cross-protective against ZIKV in adults (Rodriguez-Barraquer et al., 2019) and reduce the risk of developing symptomatic ZIKV in child patients (Gordon et al., 2019). Moreover, studies of mouse models have indicated that T cell immunity elicited by DENV infection plays a role in cross-protecting against subsequent infection with ZIKV. For example, DENV-elicited $CD4^+$ and $CD8^+$ T cells cross protect against ZIKV infection in mice (Regla-Nava et al., 2018; Wen, Elong Ngono,

et al., 2017), nonhuman primates (Dudley et al., 2017), and humans (Badolato-Corrêa et al., 2017; Grifoni et al., 2017). In the human studies, memory T cell responses elicited by DENV predominantly recognized highly conserved epitopes in DENV and ZIKV NS3 and NS5 proteins, reducing the severity of disease during secondary ZIKV infection (Grifoni et al., 2017). Analysis of anti-ZIKV responses by peripheral T and B cells isolated from adult residents of DENV-endemic areas of Colombia also revealed a strong T cell response against epitopes conserved in DENV and ZIKV, and the level of ZIKV NAbs was higher in DENV-immune compared with DENV-naïve donors (Delgado et al., 2018). However, in a study of the pediatric dengue cohort in Nicaragua, the total rate of ZIKV infection was comparable between naïve and DENV-immune donors (Gordon et al., 2019), suggesting that DENV-elicited ZIKV cross-reactive Abs may not always reduce ZIKV infection per se, but perhaps could still reduce the severity of the disease.

In summary, our study provides insights into the prevalence and potency of anti-DENV1–4 and ZIKV cross-neutralizing Abs in healthy adults living in a DENV-endemic region of Thailand. We found that 52/61 (85.3%) of participants were DENV seropositive, of whom 19 (31.1%) showed evidence of cross-neutralizing Abs against ZIKV and/or heterologous DENV serotypes. Conversely, 51 of the 61 participants were ZIKV seropositive, of whom 31 had NAbs against at least one DENV serotype. All participants with secondary DENV infection contained anti-ZIKV E- and NS1-reactive Abs. Collectively, these results show that repeat exposure to DENV1–4 elicits an Ab response that strongly cross-neutralizes heterologous DENV serotypes as well as ZIKV. These observations not only have important implications for the surveillance of residents of DENV-endemic regions where ZIKV co-circulates, and

vice versa, but also inform the design of safe, effective, and potentially cross-protective vaccines.
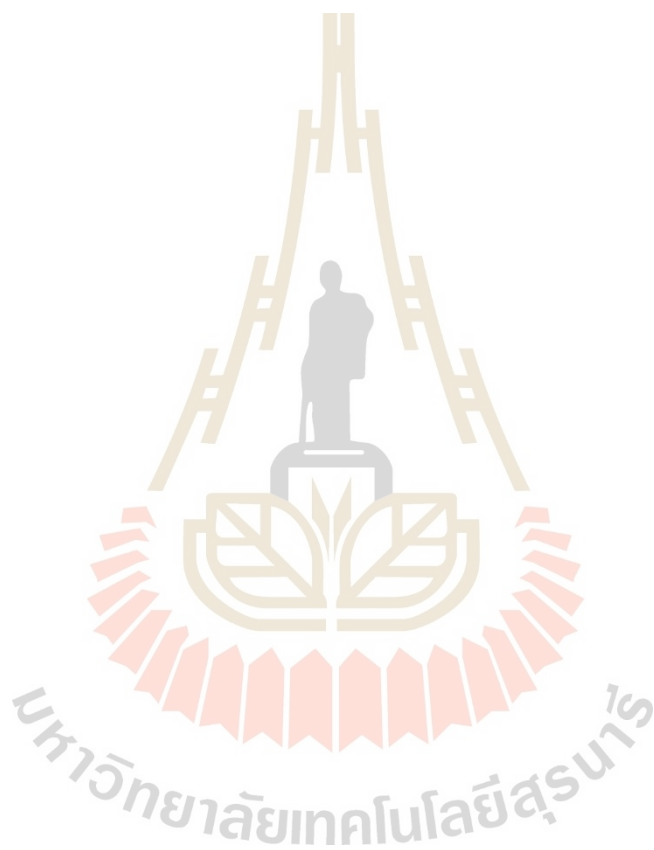
3.6 Figures & Tables
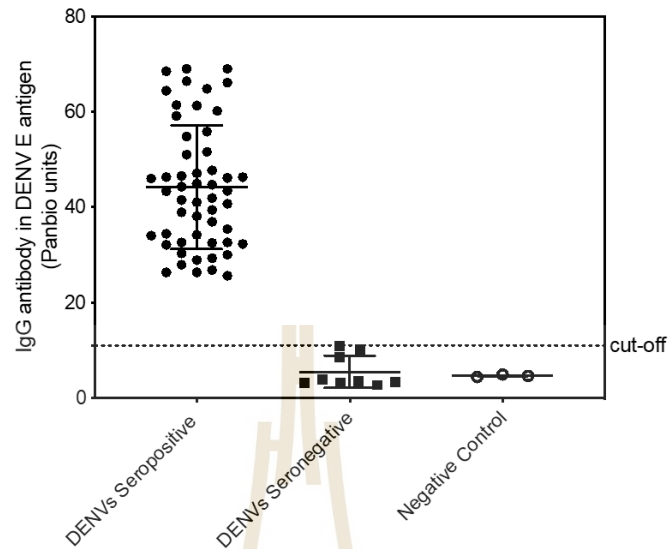
Figure 3.1 **DENV seroprevalence in healthy adult residents of a DENV-endemic region in Thailand.** DENV E antigen-specific IgG (in Panbio units) was quantified by specific ELISA. Each symbol represents an individual sample. Data are presented as the mean ± SD of 52 DENV seropositive and 9 DENV seronegative samples. The three negative control samples are from European donors who have never traveled to the region.
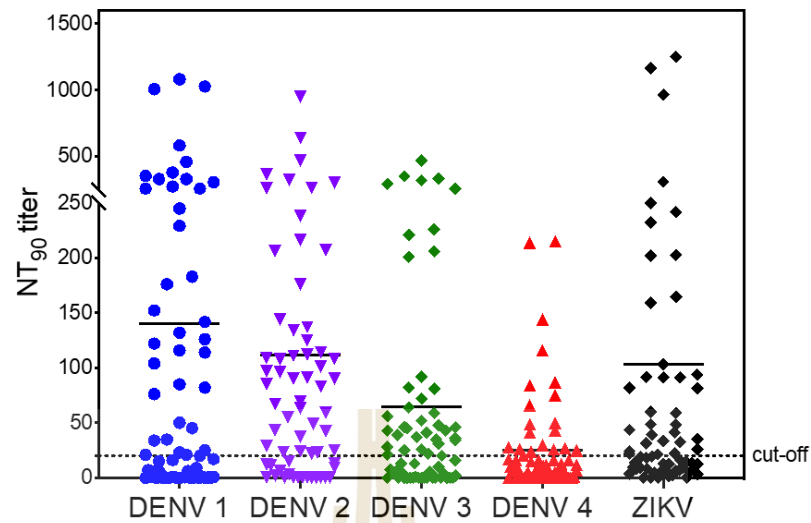
Figure 3.2 Distribution of neutralizing Ab titers against DENV 1–4 and ZIKV.

Neutralizing Abs titers against DENV1–4 and ZIKV were measured by PRNT or flow cytometry-based assays, respectively. NT90 of 20, the cutoff value for positive/negative stratification of sera, is shown as a dashed line. Each symbol represents an individual sample. Horizontal line represents the mean. N = 61.
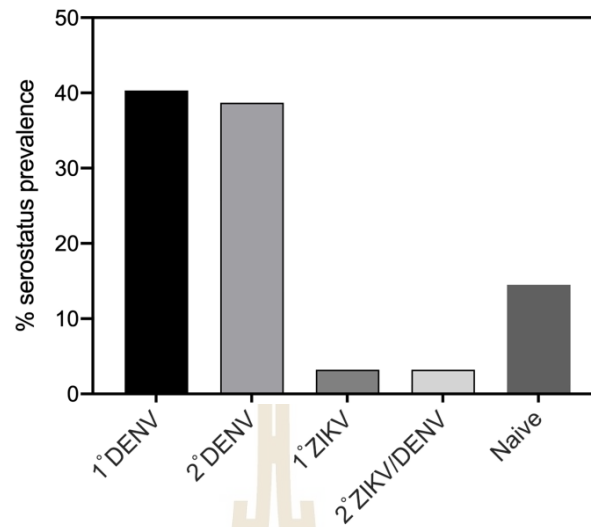
Figure 3.3 Serological classification of primary/secondary infection status. Seropositivity was defined as an NT90 ≥20. Primary infection was defined as an NT90 >20 for ZIKV or a single DENV serotype, or an NT90 ≥4-fold higher than for ZIKV or any other DENV serotype. Secondary infection is defined as an NT90 >20 for ZIKV or at least two DENV serotypes, with the highest NT90 being <4-fold that of the next highest titer. N = 25, 23, 2, 2, and 9 for primary (1°) and secondary (2°) DENV infection, 1° ZIKV infection, 2° ZIKV/DENV infection, and no infection (naïve), respectively.
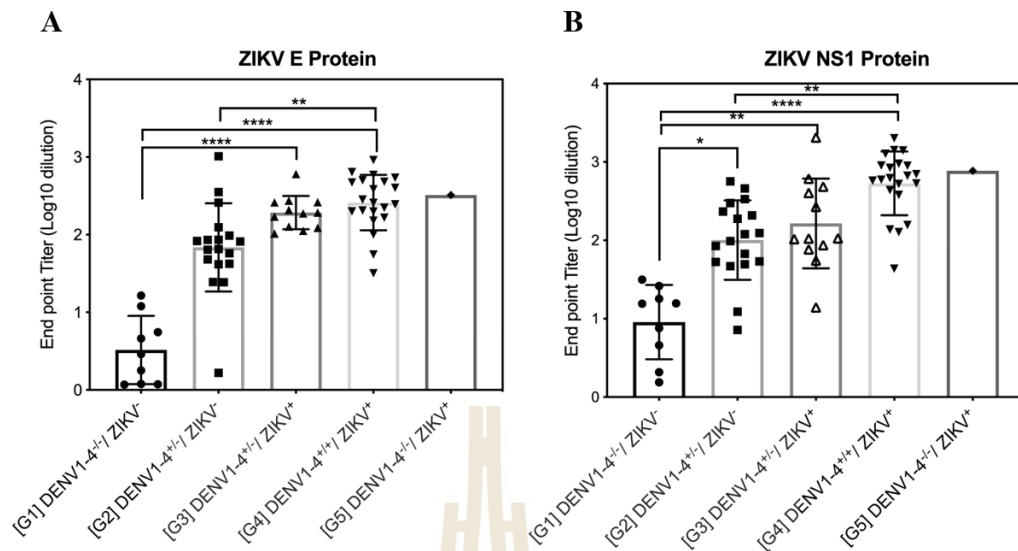
Figure 3.4 Endpoint titers in anti-ZIKV E and NS1 protein ELISAs for sera grouped by neutralizing activity. (A and B) Quantification of IgG against ZIKV E protein (A) or ZIKV NS1 protein (B) by ELISA for the 62 sera grouped according to the presence or absence of neutralizing antibodies against DENV1–4 and ZIKV (cutoff, NT90 = 20): Group 1 (n = 9), negative for all DENV serotypes and ZIKV; G2 (n = 19), positive for between one and three DENV serotypes and negative for ZIKV; G3 (n = 13), positive for between one and three DENV serotypes and positive for ZIKV; G4 (n = 19), positive for all DENV serotypes and positive for ZIKV; G5 (n = 1), negative for all DENV serotypes and positive for ZIKV. Data are presented as the mean ± SD, with each symbol representing an individual sample. *$p < 0.05$, **$p < 0.01$, ***$p < 0.001$, ****$p < 0.0001$ by the Kruskal–Wallis test.
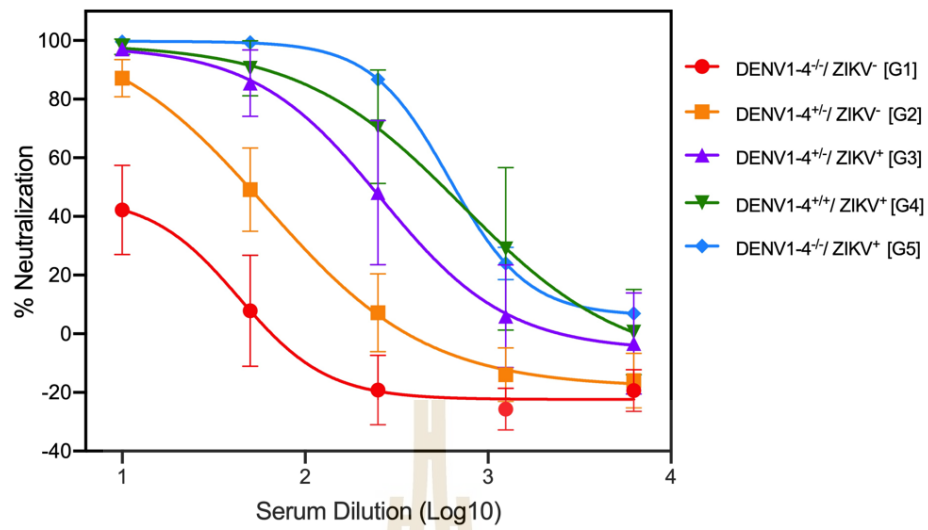
Figure 3.5 ZIKV-neutralizing activity of serum samples. The ZIKV-neutralizing activity was determined using a flow cytometry-based assay with DC-SIGN-positive U937 cells. Group 1–5 sera (G1–G5) are as described in Figure 4. Data are presented as the mean ± SD.

Table 3.1 Characteristics and DENV/ZIKV serostatus of participants

	Participants No. (% of total)	Positive DENV IgG No. (% [95% CI])	Positive ZIKV IgG No. (% [95% CI])
Total participant	61 (100)	52 (85.3 [74.3-92.0])	51 (83.6 [72.4-90.8])
Sex			
Male	25 (41.0)	21 (84.0 [65.3-93.6])	20 (80.0 [60.9-91.1])
Female	36 (59.0)	31 (86.5 [72.0-94.1])	31 (86.5 [72.0-94.1])
Age			
18-27	20 (32.8)	15 (75 [53.1-88.8])	14 (70.0 [48.1-85.5])
28-37	20 (32.8)	16 (80.0 [58.4-91.3])	16 (80.0 [58.4-91.3])
38-47	17 (27.9)	17 (100 [81.6-100])	17 (100 [81.6-100])
≥ 48	4 (6.56)	4 (100 [51.0-100])	4 (100 [51.0-100])

Table 3.2 Characteristics and DENV/ZIKV-neutralizing antibody status

	DENV 1 NT_{90} Number of serum (% [95% CI])	DENV 2 NT_{90} Number of serum (% [95% CI])	DENV 3 NT_{90} Number of serum (% [95% CI])	DENV 4 NT_{90} Number of serum (% [95% CI])	ZIKV NT_{90} Number of serum (% [95% CI])
Total Serum	36 (59.0 [46.5-70.5])	44 (72.1 [59.8-81.8])	38 (62.3 [49.7-73.4])	21 (34.4 [23.7-47.0])	32 (52.5 [40.2-64.5])
Sex					
Male	15 (60.0 [40.7-76.6])	18 (72.0 [52.4-85.7])	15 (60.0 [40.7-76.6])	7 (28.8 [14.3-47.6])	13 (52.0 [33.3-70.0])
Female	21 (58.3 [42.2-72.9])	26 (72.2 [56.0-84.2])	23 (63.9 [47.6-77.5])	14 (38.9 [24.8-55.1])	19 (52.8 [37.0-68.0])
Age					
18-27	10 (50 [29.9-70.1])	13 (65.0 [43.3-81.9])	10 (50.0 [29.9-70.1])	7 (35.0 [18.1-56.7])	8 (40.0 [21.9-61.3])
28-37	13 (65.0 [43.3-81.9])	13 (65.0 [43.3-81.9])	11 (55.0 [34.2-74.2])	4 (20.0 [8.01-41.6])	10 (50.0 [29.9-70.1])
38-47	10 (58.8 [36.0-78.4])	14 (82.4 [59.0-93.8])	13 (76.5 [52.7-90.4])	8 (47.0 [26.2-69.0])	11 (64.7 [41.3-82.7])
≥ 48	3 (75.0 [30.1-98.7])	4 (100 [51.0-100])	3 (75.0 [30.1-98.7])	2 (50.0 [8.88-91.1])	3 (75.0 [30.1-98.7])

NT_{90}: 90% neutralizing titer. Positive sera are defined as $NT_{90} > 20$.

Table 3.3 Serostatus and neutralizing antibody profile of individual participants

Sample ID	DENV 1	DENV 2	DENV 3	DENV 4	ZIKV	Serostatus
			NT 90 titer			
12	258	23	22	<20	<20	Primary DENV 1
13	356	67	28	<20	<20	
31	142	23	20	<20	<20	
34	332	59	<20	<20	82	
38	274	<20	43	<20	<20	
40	1007	134	206	43	91	
51	152	22	<20	<20	<20	
5	45	948	46	<20	159	Primary DENV 2
7	<20	238	46	27	<20	
11	<20	63	<20	<20	<20	
14	<20	111	<20	<20	<20	
19	21	144	<20	<20	36	
21	82	642	31	84	41	
32	<20	29	<20	<20	<20	
33	<20	49	<20	<20	<20	
35	<20	109	<20	<20	<20	
46	<20	24	<20	<20	<20	
49	<20	55	<20	<20	<20	
58	<20	42	<20	<20	<20	
65	21	108	<20	<20	<20	
6	23	85	294	28	39	Primary DENV 3
53	<20	<20	62	<20	<20	
59	<20	<20	35	<20	<20	
63	<20	<20	56	<20	<20	
64	<20	<20	43	<20	<20	
1	122	91	21	<20	22	Secondary DENV
2	104	90	48	<20	165	
3	245	206	201	214	203	
4	229	324	470	215	60	
8	76	25	258	25	24	
9	126	112	59	<20	103	
10	20	<20	41	<20	<20	
20	<20	305	<20	116	82	
22	116	364	36	144	92	
23	462	125	37	26	32	
25	307	90	221	87	33	
26	331	216	226	24	44	
28	50	266	64	75	242	
37	259	137	320	49	48	
39	114	69	45	<20	49	
42	370	83	25	<20	94	
45	176	108	72	26	91	
47	35	96	26	66	32	
50	34	260	34	<20	202	
57	<20	97	81	<20	233	
52	1081	114	92	30	310	
54	183	469	39	41	59	
61	132	<20	335	<20	26	
15	<20	<20	<20	<20	250	Primary ZIKV
30	85	207	52	26	1166	
24	583	176	82	50	965	Secondary
60	1028	101	353	37	1249	ZIKV/DENV

3.7 References

Badolato-Corrêa, J., Sánchez-Arcila, J. C., Alves de Souza, T. M., Santos Barbosa, L., Conrado Guerra Nunes, P., da Rocha Queiroz Lima, M., de-Oliveira-Pinto, L. M. (2017). Human T cell responses to dengue and Zika virus infection compared to dengue/Zika coinfection. **Immunity, inflammation and disease**, 6(2), 194-206.

Bardina, S. V., Bunduc, P., Tripathi, S., Duehr, J., Frere, J. J., Brown, J. A., Lim, J. K. (2017). Enhancement of Zika virus pathogenesis by preexisting antiflavivirus immunity. **Science**, 356(6334), 175

Bradt, V., Malafa, S., von Braun, A., Jarmer, J., Tsouchnikas, G., Medits, I., Heinz, F. X. (2019). Pre-existing yellow fever immunity impairs and modulates the antibody response to tick-borne encephalitis vaccination. **NPJ Vaccines**, 4(1), 38.

Cao-Lormeau, V.-M., Roche, C., Teissier, A., Robin, E., Berry, A.-L., Mallet, H.-P., Musso, D. (2014). Zika virus, French polynesia, South pacific, 2013. **Emerging infectious diseases**, 20(6), 1085-1086.

Cao-Lormeau, V. M., Blake, A., Mons, S., Lastere, S., Roche, C., Vanhomwegen, J., Ghawché, F. (2016). Guillain-Barré syndrome outbreak associated with Zika virus infection in French Polynesia: a case-control study. **Lancet (London, England)**, 387(10027), 1531-1539.

Carlin, A. F., Vizcarra, E. A., Branche, E., Viramontes, K. M., Suarez-Amaran, L., Ley, K., Glass, C. K. (2018). Deconvolution of pro- and antiviral genomic responses in Zika virus-infected and bystander macrophages. **Proceedings of the National Academy of Sciences**, 115(39), E9172.

D'Ortenzio, E., Matheron, S., de Lamballerie, X., Hubert, B., Piorkowski, G., Maquart, M., Leparc-Goffart, I. (2016). Evidence of sexual transmission of Zika virus. **New England Journal of Medicine**, 374(22), 2195-2198.

Dejnirattisai, W., Supasa, P., Wongwiwat, W., Rouvinski, A., Barba-Spaeth, G., Duangchinda, T., Screaton, G. R. (2016). Dengue virus sero-cross-reactivity drives antibody-dependent enhancement of infection with zika virus. **Nature immunology**, 17(9), 1102-1108.

Delgado, F. G., Torres, K. I., Castellanos, J. E., Romero-Sánchez, C., Simon-Lorière, E., Sakuntabhai, A., & Roth, C. (2018). Improved immune responses against Zika virus after sequential dengue and Zika virus infection in humans. **Viruses**, *10*(9), 480.

Dick, G. W. A., Kitchen, S. F., & Haddow, A. J. (1952). Zika virus (I). Isolations and serological specificity. **Transactions of the Royal Society of Tropical Medicine and Hygiene**, 46(5), 509-520.

Dudley, D. M., Newman, C. M., Lalli, J., Stewart, L. M., Koenig, M. R., Weiler, A. M., Aliota, M. T. (2017). Infection via mosquito bite alters Zika virus tissue tropism and replication kinetics in rhesus macaques. **Nature Communications**, 8(1), 2096.

Duffy, M. R., Chen, T.-H., Hancock, W. T., Powers, A. M., Kool, J. L., Lanciotti, R. S., Hayes, E. B. (2009). Zika virus outbreak on Yap island, Federated States of Micronesia. **New England Journal of Medicine**, 360(24), 2536-2543.

Elong Ngono, A., Young, M. P., Bunz, M., Xu, Z., Hattakam, S., Vizcarra, E., Shresta, S. (2019). CD4+ T cells promote humoral immunity and viral control during Zika virus infection. **PLoS Pathogens**, 15(1), e1007474.

Faria, N. R., Quick, J., Claro, I. M., Thézé, J., de Jesus, J. G., Giovanetti, M., Pybus, O. G. (2017). Establishment and cryptic transmission of Zika virus in Brazil and the Americas. **Nature**, 546, 406.

Fonseca, K., Meatherall, B., Zarra, D., Drebot, M., MacDonald, J., Pabbaraju, K., Tellier, R. (2014). First case of Zika virus infection in a returning Canadian traveler. **The American Journal of Tropical Medicine and Hygiene**, 91(5), 1035-1038.

Gordon, A., Gresh, L., Ojeda, S., Katzelnick, L. C., Sanchez, N., Mercado, J. C., Harris, E. (2019). Prior dengue virus infection and risk of Zika: A pediatric cohort in Nicaragua. **PLoS Medicine**, 16(1), e1002726.

Grifoni, A., Pham, J., Sidney, J., Rourke, P. H., Paul, S., Peters, B., Sette, A. (2017). Prior dengue virus exposure shapes T cell immunity to Zika virus in humans. **Journal of Virology**, 91(24), e01469-01417.

Grubaugh, N. D., Saraf, S., Gangavarapu, K., Watts, A., Tan, A. L., Oidtman, R. J., Andersen, K. G. (2019). Travel surveillance and genomics uncover a hidden Zika outbreak during the waning epidemic. **Cell**, 178(5), 1057-1071.e1011.

Halstead, S. B. (1979). *In vivo* enhancement of dengue virus infection in Rhesus monkeys by passively transferred antibody. **The Journal of Infectious Diseases**, 140(4), 527-533.

Halstead, S. B. (1988). Pathogenesis of dengue: challenges to molecular biology. **Science**, 239(4839), 476.

Halstead, S. B. (2015). Pathogenesis of dengue: dawn of a new era. **F1000Research**, 4, F1000 Faculty Rev-1353.

Halstead, S. B., & Yamarat, C. (1965). Recent epidemics of hemorrhagic fever in thailand. Observations related to pathogenesis of a "new" dengue disease. **American journal of public health and the nation's health**, 55(9), 1386-1395.

Heang, V., Yasuda, C. Y., Sovann, L., Haddow, A. D., Travassos da Rosa, A. P., Tesh, R. B., & Kasper, M. R. (2012). Zika virus infection, Cambodia, 2010. **Emerging infectious diseases**, 18(2), 349-351.

Ioos, S., Mallet, H. P., Leparc Goffart, I., Gauthier, V., Cardoso, T., & Herida, M. (2014). Current Zika virus epidemiology and recent epidemics. **Médecine et Maladies Infectieuses**, 44(7), 302-307.

Katzelnick, L. C., Montoya, M., Gresh, L., Balmaseda, A., & Harris, E. (2016). Neutralizing antibody titers against dengue virus correlate with protection from symptomatic infection in a longitudinal cohort. **Proceedings of the National Academy of Sciences**, 113(3), 728.

Kostyuchenko, V. A., Lim, E. X. Y., Zhang, S., Fibriansah, G., Ng, T.-S., Ooi, J. S. G., Lok, S.-M. (2016). Structure of the thermally stable Zika virus. **Nature**, 533, 425.

Lazear, H. M., & Diamond, M. S. (2016). Zika virus: new clinical syndromes and its emergence in the Western hemisphere. **Journal of Virology**, 90(10), 4864.

Limkittikul, K., Brett, J., & L'Azou, M. (2014). Epidemiological trends of dengue disease in Thailand (2000-2011): a systematic literature review. **PLoS neglected tropical diseases**, 8(11), e3241-e3241.

Marchette, N. J., Garcia, R., & Rudnick, A. (1969). Isolation of Zika virus from *Aedes aegypti* mosquitoes in Malaysia. **The American Journal of Tropical Medicine and Hygiene**, 18(3), 411-415.

Matthew, H. C., Eileen, M., Ramesh, J., Ellen, Y., Cesar, A. L., Ralph, S. B., Aravinda, M. d. S. (2017). Lack of durable cross-neutralizing antibodies against Zika virus from dengue virus infection. **Emerging Infectious Disease journal**, 23(5), 773. doi:10.3201/eid2305.161630

Montoya, M., Collins, M., Dejnirattisai, W., Katzelnick, L. C., Puerta-Guardo, H., Jadi, R., Harris, E. (2018). Longitudinal analysis of antibody cross-neutralization following Zika virus and dengue virus infection in Asia and the Americas. T**he Journal of Infectious Diseases**, 218(4), 536-545.

Musso, D., Cao-Lormeau, V. M., & Gubler, D. J. (2015). Zika virus: following the path of dengue and chikungunya? **The Lacet**, 386(9990), 243-244.

Musso, D., & Gubler, D. J. (2016). Zika virus. **Clinical microbiology reviews**, 29(3), 487-524.

Musso, D., Roche, C., Robin, E., Nhan, T., Teissier, A., & Cao-Lormeau, V.-M. (2015). Potential sexual transmission of Zika virus. **Emerging infectious diseases**, 21(2), 359-361.

Mysorekar, I. U. (2017). Zika virus takes a transplacental route to infect fetuses: insights from an animal model. **Missouri medicine**, 114(3), 168-170.

World Health Organization. (2016). Zika situation report. Retrieved from https://www.who.int/emergencies/zika-virus/situation-report/5-february-2016/en/

Pedroso C, F. C., Feldmann M, Sarno M, Luz E, Moreira-Soto A, Cabral R,, & Netto EM, B. C., Kümmerer BM, Drexler JF. (2019). Cross-protection of dengue virus infection against congenital Zika syndrome, Northeastern Brazil. **Emerging infectious diseases**, 25(8), 1485-1493.

Pongsiri, P., Themboonlers, A., & Poovorawan, Y. (2012). Changing pattern of dengue virus serotypes in Thailand between 2004 and 2010. **Journal of health, population, and nutrition**, 30(3), 366-370.

Priyamvada, L., Quicke, K. M., Hudson, W. H., Onlamoon, N., Sewatanon, J., Edupuganti, S., Wrammert, J. (2016). Human antibody responses after dengue virus infection are highly cross-reactive to Zika virus. **Proceedings of the National Academy of Sciences of the United States of America**, 113(28), 7852-7857.

Rasmussen, S. A., Jamieson, D. J., Honein, M. A., & Petersen, L. R. (2016). Zika virus and birth defects — reviewing the evidence for causality. **New England Journal of Medicine**, 374(20), 1981-1987.

Regla-Nava, J. A., Elong Ngono, A., Viramontes, K. M., Huynh, A.-T., Wang, Y.-T., Nguyen, A.-V. T., Shresta, S. (2018). Cross-reactive dengue virus-specific CD8+ T cells protect against Zika virus during pregnancy. **Nature Communications**, 9(1), 3042.

Rodriguez-Barraquer, I., Costa, F., Nascimento, E. J. M., Nery, N., Castanha, P. M. S., Sacramento, G. A., Ko, A. I. (2019). Impact of preexisting dengue immunity on Zika virus emergence in a dengue endemic region. **Science**, 363(6427), 607.

Ruchusatsawat, K., Wongjaroen, P., Posanacharoen, A., Rodriguez-Barraquer, I., Sangkitporn, S., Cummings, D. A. T., & Salje, H. (2019). Long-term circulation of Zika virus in Thailand: an observational study. **The Lancet Infectious Diseases**, 19(4), 439-446.

Shinohara, K., Kutsuna, S., Takasaki, T., Moi, M. L., Ikeda, M., Kotaki, A., Ohmagari, N. (2016). Zika fever imported from Thailand to Japan, and diagnosed by PCR in the urine. **Journal of Travel Medicine**, 23(1).

Simpson, D. I. H. (1964). Zika virus infection in man. **Transactions of the Royal Society of Tropical Medicine and Hygiene**, 58(4), 335-338.

Sornjai, W., Jaratsittisin, J., Auewarakul, P., Wikan, N., & Smith, D. R. (2018). Analysis of Zika virus neutralizing antibodies in normal healthy Thais. **Scientific Reports**, 8(1), 17193.

Tappe, D., Rissland, J., Gabriel, M., Emmerich, P., Günther, S., Held, G., Schmidt-Chanasit, J. (2014). First case of laboratory-confirmed Zika virus infection imported into Europe, November 2013. **Eurosurveillance**, 19(4), 20685.

Vongpunsawad, S., Intharasongkroh, D., Thongmee, T., & Poovorawan, Y. (2017). Seroprevalence of antibodies to dengue and chikungunya viruses in Thailand. **PloS one**, 12(6), e0180560-e0180560.

Wen, J., Elong Ngono, A., Regla-Nava, J. A., Kim, K., Gorman, M. J., Diamond, M. S., & Shresta, S. (2017). Dengue virus-reactive CD8+ T cells mediate cross-protection against subsequent Zika virus challenge. **Nature Communications**, 8(1), 1459.

Wen, J., Tang, W. W., Sheets, N., Ellison, J., Sette, A., Kim, K., & Shresta, S. (2017). Identification of Zika virus epitopes reveals immunodominant and protective roles for dengue virus cross-reactive CD8+ T cells. **Nature Microbiology**, 2, 17036.

Yockey, L. J., Varela, L., Rakib, T., Khoury-Hanold, W., Fink, S. L., Stutz, B. Iwasaki, A. (2016). Vaginal exposure to zika virus during pregnancy leads to fetal brain infection. **Cell**, 166(5), 1247-1256.e1244.

Zhang, Q., Sun, K., Chinazzi, M., Pastore y Piontti, A., Dean, N. E., Rojas, D. P., Vespignani, A. (2017). Spread of Zika virus in the Americas. **Proceedings of the National Academy of Sciences**, 114(22), E4334.
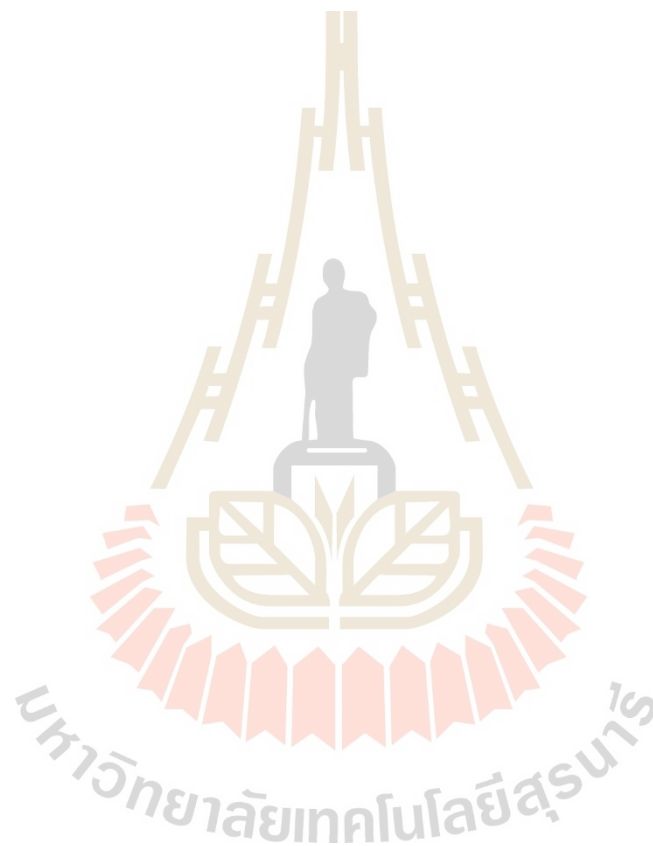
CHAPTER IV

IDENTIFICATION AND GENERATION OF RECOMBINANT HUMAN MONOCLONAL IgG ANTIBODY AGAINST DENGUE VIRUS

4.1 Abstract

Dengue disease is the most widespread vector-borne viral disease caused by dengue virus (DENV) for which there are no safe, effective drugs approved for clinical use. Here, we construct phage display antibody derived from healthy donors who had high titer neutralizing antibodies against all four DENV serotypes. We identified a cross-reactive human monoclonal antibody (mAb), DV2H12 from bio-panning using purified whole DENV2 particle as the target. The mAb DV2H12 bound with high affinity to DENV2 from all four DENV serotypes. Immunogenetic analysis indicated that DV2H12 is a germline-like mAb with the closest human V_H and V_λ germline genes. Importantly, we found that mAb may recognize the prM DENV2 epitope. Furthermore, mAb DV2H12 showed cross-reactive and weakly neutralized DENV1-4 and significantly promoted ADE infection in AG129 mice. These findings may provide significant implications for future therapeutic antibody and vaccine design and facilitate understanding the pathogenesis of DENV infection.

4.2 Introduction

Dengue virus (DENV) is the most important emerging arboviral infection of humans, which has been globally emerged in more than 100 countries. Forty percent of the world's population, about 3 billion people lives in areas with a risk of dengue, with an estimated 390 million infections and 96 million symptomatic cases annually (Bhatt et al., 2013). There is up to 50,000 dies from dengue hemorrhagic fever (DHF) and dengue shock syndrome (DSS) each year (Kyle & Harris, 2008). The DENV consists of 4 distinct serotypes (DENV1-4). Each of these DENVs is similar to one another, but differ by 30-35% in amino acid sequence (Dejnirattisai et al., 2015b). The difference of amino acid among those serotypes leads to the fact that one antibody may not be sufficient to neutralize all DENV infection. Instead, the antibodies response to one DENV infection can enhance the infection and disease processes brought by a subsequent infection with another DENV serotype. The human monoclonal antibodies (mAbs) against envelop dimer epitope (EDE), which bridges two envelope protein subunits on mature dengue virion, have been isolated from viremic patients infected with DENV. These mAbs were shown to be highly potent and broadly reactive across the dengue sero-complex and fully neutralized virus infection in primary human cells (Dejnirattisai et al., 2015b). These finding indicated the design and monitoring of future vaccine trials, in which the induction of antibody to the EDE should be prioritized.

Since the production of the monoclonal antibody, especially from humans, is laborious and time-consuming, phage display technology has offered an additional alternative for the isolation and further genetic modification of antibody fragments against important viral pathogens from human subjects or immunized animals.

Antibody phage-displayed libraries have been used for dengue diagnosis purposes from the generation of single-chain variable antibody fragments (scFv) (Fatima et al., 2014). For a therapeutic effect, the human ScFv derived healthy donor antibody phage libraries have been shown to bind specifically to dengue enveloped recombinant protein domain III (EDIII) and exhibited neutralizing activity at 40-60% to DENV1, 2, and 4 but not serotype 3 (Saokaew et al., 2014). Recently, a non-dengue immunized phage display library had been studied in the selection of antibodies against ZIKV DIII recombinant protein. The results of selected antibodies showed moderate neutralization activity against ZIKV *in vitro* by plaque reduction assay and in C57BL/6 background mice deficient in alpha/beta interferon (IFN-α/β) and IFN-γ receptors (Y. Wu et al., 2017). Therefore, phage display technology is an alternative method to rapidly select antibodies targeting both DENV and ZIKV. However, there is no report about the effect of scFv on the ADE activity against any serotype. Moreover, these antibodies were generated from using recombinant protein as a target, not an EDE or a quaternary structure epitope or whole virus particle. Therefore, the development of new and broadly neutralization antibodies against all the serotypes of DENV using whole virus particle as an antigen could be promising candidate anti-DENV agents and may also guide the design of effective and safe vaccine immunogens.

In this study, we generated scFv antibody phage display library derived from 40 healthy donors showing broad neutralizing antibodies against DENV1-4 and engineered scFv into full-length recombinant human monoclonal IgG1 and IgG4 subclass. We studied the biological activity of antibodies against DENV and ZIKV infection *in vitro* and *in vivo*.

4.3 Materials and Methods

4.3.1 Construction of human scFv phage display library

4.3.1.1 Generation of scFv gene repertoire

The peripheral blood mononuclear cells (PBMCs) were collected from 40 DENV-immune people in Nakhon Ratchasima, Thailand who have neutralizing antibodies (NT_{70} titer $\geq$ 20) against all four DENV serotypes. The PBMCs were isolated using Ficoll-Paque™ Plus, a density gradient media (GE Healthcare, Chicago, IL), following the manufacture's protocol. Total RNA was extracted from PBMCs by TRI-zol reagent (Invitrogen, Carlsbad, CA), an equal amount of total RNA from 40 individuals was pooled in the total amount of 40 μg. The pooled RNA was synthesized for cDNA, using MMuLV reverse transcriptase (NEB, Ipswich, MA) with a mix of 4 μL of RNaseOut (40 U/μL, Invitrogen, Carlsbad, CA), 20 μM of oligo-dT_{18} and 80 ng of random hexamer primer. The cDNA was amplified for the genes encoded variable region of the heavy chain, κ light chain, and λ light chain (V_H, $V_κ$, and $V_λ$). The set of 75 pairs of heavy and light chain PCR primers and the amplifying were previously described (Pansri, Jaruseranee, Rangnoi, Kristensen, & Yamabhai, 2009). Briefly, the heavy chain primers were included a *Sfi*I site at 5' and the linker sequence $(Gly_4Ser)_3$ at 3' region. The light chain primers were generated a complementary sequence for linker at 5' and included *Not*I site at 3' region. An equal amount (150 ng) of each 75 PCR products were pooled in the collection of V_H, $V_κ$, and $V_λ$. The equal molar of pooled V_H gene repertoires was assembled by the linker sequences with pooled $V_κ$, or $V_λ$ gene repertoires. The correctly linked products from the assembly step were extended by PCR under the following conditions: 30 cycles of denaturation at 94°C for 1 minute, annealing at

60°C for 1 minute and ssextension at 72°C for 2 minutes. This was followed by the final extension at 72°C for 10 minutes. Finally, the full-length scFv fragment was obtained in PCR with two primers, which anneal at the 5' of V_H and 3' of the assembled V_κ, or V_λ product. Then the scFv genes were purified by Wizard® SV gel clean up kit (Pomega, Madison, WI) for the cloning step.

4.3.1.2 Cloning of the scFv into pMOD1 vector

The pMOD1 vector was already constructed (Pansri et al., 2009). The scFv fragments DNA was inserted into pMOD1 vector between *Sfi*I and *Not*I sites. The DNA of scFv fragments and pMOD1 vector was sequentially digested with *Sfi*I (20U/µL, NEB, , Ipswich, MA) and *Not*I (10U/µL, NEB, Ipswich, MA) enzymes, respectively, to generate compatible sticky ends. The digestion reactions of scFv fragments and pMOD1 vector were performed separately, each in a total volume of 500 µL. For the *Sfi*I digestions, the reaction mixtures consisted of 10 µg of insert DNA, 12 µg of vector DNA, 1x NEB buffer 2, 1 µg/mL BSA and 200U of *Sfi*I (20U/µL, NEB, , Ipswich, MA). The reactions were incubated at 50°C for 16 hours. The *Sfi*I digested DNA was cleaned by Wizard clean up kit (Promega, USA) before the next digestion step. The *Not*I digestion mixtures consisted of 400 µL of purified *Sfi*I digested DNA, 1x NEB buffer 3, 1 µg/mL BSA and 100 U of *Not*I (10U/µL, NEB, USA). The reaction mixtures were incubated at 37°C for 16 hours. After the digestion, the *Sfi*I/*Not*I digested vector was dephosphorylated by adding 3 µL of CIP enzyme (10U/µL, NEB, Ipswich, MA) and incubated at 37 ºC for 1 hour. After the dephosphorylation, the vector was heat-inactivated at 85ºC for 15 minutes. The inserts and vectors were separated from stuffer fragments by gel electrophoresis followed by Wizard clean up kit (Promega, Madison, WI). The scFv DNA was ligated into

pMOD1 vectors at a 3:1 ratio. The total volume of the ligation reaction was 200 μl, which consisted of 2.8 μg of inserted DNA, 5.5 μg of pMOD1 vector, 1x T4 DNA ligase buffer and 15 μL of T4 DNA ligase (400U/μL, NEB, USA). After 16 h of incubation at 16 ºC, the ligation reaction was concentrated to 40 μL by precipitating overnight with 3M sodium acetate pH 5.2 plus absolute ethanol. The ligation reaction was then transformed into 600 μL of *E. coli* TG1 cells by electroporation. The reaction was done in two separate cuvettes by pipetting 20 μL of the ligated sample into a 2 mm cuvette containing 300 μL of *E. coli* TG1 competent cells. The electroporation was performed at 2.5 kV, 25 μF, 200 Ω and τ approximately 4 msec using an electroporation machine (BTX, Harvard Bioscience, USA). The cuvette was flushed immediately with 3 mL of SOC medium at room temperature, and the two separate transformation reactions were combined in 50 mL polypropylene tube. The 6 mL of combined transformed cells were incubated at 37 ºC for 1 h. After that, the transformed cells were spread on eight 24x24 cm plates, containing TYE medium, 100 μg/mL ampicillin plus 1% glucose, and incubated overnight at 37 ºC.

4.3.1.3 Determination of the library size

The library size was quantified by spreading dilutions of the transformation reaction on separate plates. A volume of 100 μL from transformation reactions was taken and a four-step 10-fold serial dilution was made. Then 100 μL of non-diluted and the four dilutions were plated on separate TYE agar plates containing 100 μg/mL ampicillin and 1% glucose. The vector ligation control was performed in parallel to evaluate the background of the library. The concentration of vector DNA in the ligation control was scaled down to 100 ng in a total volume of 10 μL. The large plates of the library were scraped into 20 mL of 2xYT with 20% glycerol and

aliquoted into freezing vials. The glycerol stock of the library was stored at -70 ºC. To determine the diversity of the library, 20 of individual clones were picked and analyzed by DNA sequencing and *Bst*N1 digestion pattern.

4.3.1.4 Amplifying phagemid library

The library glycerol stock was diluted to an OD600 of 1.00, which represents approximately 1×10^8 cells. Then 40 mL 2xYT containing 100 μg/mL ampicillin and 1% (w/v) glucose was inoculated with 10 mL of the diluted library stock. The culture was grown at 30ºC for 3 hours, until the cells got into the mid-log phase. The culture was infected with 2×10^{10} KM13 helper phage (MRC, Cambridge, UK) to give a 1:1 ratio of bacteria: helper phage and incubated at 37ºC for 1 h. After that the culture was spun down at $3000 \times g$ for 10 minutes and resuspended in 500 mL 2xYT containing 100 μg/mL ampicillin and 50 μg/mL kanamycin. The culture was incubated at 30ºC overnight with vigorous shaking. The phage particles expressing scFv antibody were harvest by centrifugation $3000 \times g$ for 30 min. The supernatant was mixed with 0.2 volumes of 20% (w/v) PEG/2.5 M NaCl solution. The mixture was chilled on ice for 1 hour, and then centrifuged at $3000 \times g$ for 10 minutes. The pellet was resuspended in 5 mL of 15% (v/v) glycerol in PBS. The phage library was dispensed into 500 μL aliquots in microcentrifuge tubes. To determine the phage titer, the PEG precipitated phage was diluted by making six 100-fold serial dilutions and adding 100 μl of diluted phage into 900 μL of mid-log *E. coli* TG1. The infected *E. coli* TG1 cells were incubated at 37ºC for 30 min, and then plated on separate TYE agar plates containing 100 μg/mL ampicillin and 1% (w/v) glucose. The plates were incubated at 37ºC overnight.

4.3.2 Affinity selection of human scFv phage display library

The phage antibody library was used for selecting the phage particles that specifically bind to immobilized antigen. The selection was made on MaxiSorp™ Nunc-Immuno™ tube (Thermo Scientific, Waltham, MA) with the immobilized purified whole particle of DENV 2 or ZIKV as the antigens. The immobilization conditions of each target viruses were different with respect to buffer (PBS, 100 mM NaHCO$_3$ pH 8.5), temperature (4ºC, 37ºC) and concentration. The immobilizing was performed overnight at 4ºC. The well was then blocked to avoid non-specific binding of phage particles with 2% (w/v) skimmed milk (2% MPBS) and incubated at room temperature for 1 h. The blocking solution was poured off and the well was washed 3 times with PBS. Then 50 μL of 2% MPBS containing 10^{11}-10^{12} phages from the phage antibody library was added to the well and incubated at room temperature for 2 h. The unbound phages were removed by washing the well with PBS containing 0.1% (v/v) tween 20 (PBST). The wash buffer was added to the well and the plate was vigorously rotated for 3 min. After shaking out the wash buffer and repeating this washing step for 10 times, the well was rinsed with PBS 10 times. The bound phages could be eluted by trypsinization or/and low pH conditions using acidic elution buffer (50 mM glycine-HCl pH, 2.0). The trypsinization was performed by adding 50 μL of freshly prepared trypsin buffer (5 μL of 10mg/mL trypsin stock in 45 μL of PBS) to the well and leaving it for 10 min at room temperature. The low pH elution was performed by using 50 μL of 50 mM glycine-HCl pH, 2.0, to be an elution buffer. After incubation at room temperature for 10 min, the acidic solution had to be neutralized by adding 50 μL of neutralization solution (200 mM NaHPO$_4$ pH 7.5). The recovered phages were amplified in *E. coli* TG1 cells by infecting 175 μL of mid-

log phase *E. coli* TG1 at OD600 of 0.4 with 25 μL of eluted phages and incubating at 37ºC for 30 min. For the output titering, the eluted phages were diluted. Three 10-fold serial dilutions were performed. Then 100 μL of non-diluted and the three dilutions were separately spread on TYE agar plates containing 100 μg/mL ampicillin and 1% (w/v) glucose. The plates were incubated at 37ºC overnight.

4.3.2.1 Further round of selection

The infected *E.coli* TG1 colonies on TYE agar plates containing 100 μg/mL ampicillin and 1% (w/v) glucose were scraped and kept as 15% (v/v) glycerol stock at –70°C. Five μL of scraped bacteria was inoculated into 5 mL of 2xYT containing 100 μg/mL ampicillin and 1% (w/v) glucose. The culture was grown at 37ºC until the OD600 was 0.4, and then 5×10^{10} helper phages were added. The culture was incubated again at 37°C without shaking for 30 minutes. After spinning at $3000\times g$ for 15 min, the supernatant was discarded and the pellet was resuspended in 5 mL of 2xYT containing 100 μg/mL ampicillin, 50 μg/mL kanamycin and 0.1% (w/v) glucose. The culture was incubated for at least 20 h at 30°C with shaking. The next day, phage particles expressing scFv antibody were harvest by centrifugation ($3000\times g$ for 30 min). The supernatant was mixed with 0.2 volumes of 20% (w/v) PEG/2.5 M NaCl solution. The mixture was chilled on ice for 1 h, and then centrifuged at $3000\times g$ for 10 min. The pellet was resuspended in 200 μL of PBS. This precipitated phage was used for the next round of selection.

4.3.2.2 Monoclonal phage rescues

After selection, the single colonies of infected *E.coli* TG1 on TYE agar plates containing 100 μg/mL ampicillin and 1% (w/v) glucose were randomly picked and separately inoculated into each well of 96- well culture plate containing

100 μL of 2xYT with 100 μg/mL ampicillin and 1% (w/v) glucose. The inoculum was incubated at 37°C with shaking overnight. The following day, 5 μL of overnight culture from each well was transferred into a second 96-well culture plate containing 100 μL of 2xYT with 100 μg/mL ampicillin and 1% (w/v) glucose. The second culture plate was incubated at 37°C with shaking for 2-3 h, until the culture started to get cloudy. Then 25 μL of 2xYT containing 100 μg/mL ampicillin, 1% (w/v) glucose and 10^{10} KM13 helper phage were added to each well. The inoculum was incubated at 37°C with shaking 250 rpm for 1 h. Then the supernatant was aspirated off after centrifugation at $3000 \times g$ for 15 min. The bacterial pellet was resuspended in 150 μL of 2xYT, containing 100 μg/mL ampicillin and 50 μg/mL kanamycin. The cultures were incubated for at least 20 hours at 30°C with shaking 250 rpm. The culture supernatant containing the amplified phages was used in ELISA, to determine which individual clones bound to target protein. The original 96- well culture plate or master plate was treated by adding 95 μL of 40 % (v/v) glycerol to the remaining culture, to give a final concentration of 15%. The glycerol stock was stored at –70°C for later use.

4.3.3 Phage ELISA

After bio-panning, the monoclonal scFv clone was screened using ELISA. The ELISA wells were coated with 2×10^5 PFU of purified DENV or ZIKV antigens in 50 μl PBS or 100 mM NaHCO3 pH, 8.5. The coating was performed for overnight at 4°C. The wells were rinsed 3 times with PBS. Non-specific binding was blocked by 2% MPBS at room temperature for 1 h. Then the wells were rinsed 3 times with PBS. The 125 μL of supernatant from the phage rescue of selected single colonies were added to the wells containing 25 μl of 2% MPBS. The binding was incubated at room

temperature for 2 h. After that, the wells were washed 3 times with PBST followed by 3 times of PBS. The secondary antibody was used for detecting the bound phages. A 1:5000 dilution of a mouse anti-M13 phage-horseradish peroxidase (HRP) conjugate (Abcam, Cambridge, UK) in 100 µL of 2% MPBS was added into each well, and the plates were incubated at room temperature for 1 h. The wells were washed 3 times with PBST followed by 3 times of PBS. The 50 µL of TMB substrate (Invitrogen, Carlsbad, CA) was added, and the plates were incubated at room temperature for 15 min. The reaction was stopped with 50 µl of 4N sulfuric acid solution (Fisher Scientific, Hampton, NH). The ELISA plate was measured the absorbance at 450 nm in an ELISA plate reader.

4.3.4 scFv antibody ELISA

The 96-wells plate was coated with 2×10^5 PFU of purified DENV or ZIKV antigens in 50 µl PBS or 100 mM NaHCO₃ pH, 8.5. The coating was performed overnight at 4°C. The wells were rinsed 3 times with PBS. Non-specific binding was blocked by 2% MPBS at room temperature for 1 h. Then the wells were rinsed 3 times with PBS. The 125 µL of supernatant from the phage rescue of selected single colonies were added to the wells containing 25 µl of 2% MPBS. The binding was incubated at room temperature for 2 h. After that, the wells were washed 3 times with PBST followed by 3 times of PBS. The secondary antibody was used for detecting the bound phages. A 1:5000 dilution of an anti-6xHis conjugated-HRP conjugate (Abcam, Cambridge, UK) in 100 µL of 2% MPBS was added into each well, and the plates were incubated at room temperature for 1 h. The wells were washed 3 times with PBST followed by 3 times of PBS. The 50 µL of TMB substrate (Invitrogen, Carlsbad, CA) was added, and the plates were incubated at room temperature for 15

min. The reaction was stopped with 50 μl of 4N sulfuric acid solution (Fisher Scientific, Hampton, NH). The ELISA plate was measured the absorbance at 450 nm in an ELISA plate reader.

4.3.5 Expression and Purification of scFv

The soluble scFv antibody was expressed and secreted without the pIII domain, by infecting to *E. coli* HB2151, which is a non-suppressor bacterial strain. A single colony of *E. coli* HB2151 containing pMOD phagemid bearing positive clones was inoculated into 5 ml 2xYT containing 100 μg /mL Ampicillin, 2% (w/v) glucose and was grown overnight at 37°C with shaking 250 rpm. On the next day, 2 mL of the overnight culture was inoculated into 200 mL 2xYT broth, containing 100 μg/mL Ampicillin, 0.1% (w/v) glucose at 30°C with shaking for 3 h and 30 min to reach OD600 is 0.9. After that, the culture was induced with 1mM IPTG and continued shaking for 6 h or overnight at 250 rpm. For overnight induction, the secreted antibody could be found in the supernatant, whereas the antibody fragments could be found in periplasm when incubated at 6 h.

For periplasmic extraction, the culture was centrifuged at 3,000×g for 20 min at 4 °C and the supernatant was discarded. The pellet was resuspended in 8 mL of cold periplasmic buffer (1xPBS, 1 M NaCl and 1 mM EDTA) and left on ice for 20 min. The resuspended solution was spun at 3,000×g for 10 min at 4 °C. The supernatant which carrying the periplasmic fractions containing scFv fragments were collected and was added with $MgCl_2$ to be 1 mM as final concentration. Before purification, cell debris was removed from the periplasmic supernatant by filtering through 0.2 μm. The filtered periplasmic was purified for scFv using Ni-NTA spin kit (QIAGEN, Netherland), following the manual's protocol. The scFv was eluted from

the column with elution containing a high concentration of imidazole (20 mM $NaPO_4$, 500 mM NaCl, 500 mM imidazole, pH 7.5). The antibody fraction was dialysed with PBS buffer using 10 kDa Amicon® ultra-15 centrifugal filter (Merck, Germany). Protein concentration was quantified by a Nanodrop ND2000 spectrophotometer (Thermo Scientific, Waltham, MA).

4.3.6 Cell lines and Virus

WHO reference strain of DENV serotype 2 strain 16803 and ZIKV Asian lineage strain SD001 was isolated in 2016 from a San Diego traveler to Venezuela, were used as the targets for phage display selection (bio-panning). All the virus stocks were propagated in C6/36 *Aedes albopictus* mosquito cells (ATCC no. CRL-1660). C6/36 cells were grown in Leibovitz's L15 medium (Corning, USA) supplemented with 10% fetal bovine serum (FBS; Invitrogen, USA), 10 mM HEPES (Fisher scientific), and 100 units/mL of penicillin/streptomycin (Gibco, Invitrogen). C6/36 cells were infected with DENV serotype 2 (strain S16803) or ZIKV (strain SD001) at MOI 0.1 for 14 days. DENV and ZIKV supernatants were harvested on day 7 and 14 after infection. The supernatant was clarified by centrifugation at 700×g for 15 min at 4 ºC and concentrated by 100 kDa Amicon® ultra-15 centrifugal filter (Merck, Germany).

4.3.7 Gradient-free virus purification

The concentrated supernatant containing the virus was purified as previously described (Jensen, Nguyen, & Jewett, 2016). Briefly, 20 mL of supernatant was layered over 7 mL of a 20% sucrose (w/v) solution in an ultracentrifuge tube (Beckman Coulter, USA) on ice. Ultracentrifugation was carried out at 113,600×g at 4 ºC for 3 h using a Beckman Coulter ultracentrifuge (model XE-90) with a swing

bucket rotor (SW32Ti). Following ultracentrifugation, the supernatant was quickly aspirated and drip-dried the pellet for 20 min at room temperature. The pellet was quickly re-suspended in 1 ml precipitation buffer (100 mM HEPES, pH 7.9 with 50 mM NaCl) on ice. The viral suspension was immediately centrifuged on a benchtop microcentrifuge at 16,000 × g for 10 min at room temperature. The remaining visible viral pellet was re-suspended in 50 μL TNE buffer (50 mM Tris-HCl pH 7.4, 100 mM NaCl, 0.1 mM EDTA). The presence of a purified virus was confirmed by SDS-PAGE with coomassie staining. The purified virus titer were measured the titers using baby hamster kidney (BHK)-21 cells (ATCC no. CCL-10) based on focus forming assay (FFA) as previously described (Elong Ngono et al., 2019).

4.3.8 Flow cytometry-based *in vitro* neutralization assay

DENV 2 (strain S16803) and ZIKV (strain SD001) neutralization activity of scFv or recombinant human mAb was determined using a flow cytometry-based assay with U937 human monocytic cells stably transfected with DC-SIGN (U937+DC-SIGN) as previously described (Elong Ngono et al., 2019). U937+DC-SIGN cells were seeded into 96-well plates at the 5×10^4 cells/well and grown at 37 °C with 5% CO_2 for 24 h. The scFv or human mAb was diluted with RPMI 1640 without FBS supplemented at a dilution of 1:10 followed with serial five-fold dilutions until 1:6,250. The serially diluted serum was incubated with sufficient virus to cause 7-15% infection in U937+DC-SIGN cells at 37 °C for 1 h before added to U937+DC-SIGN cells. Cells were infected for 2 h at 37 °C. The infected U937+DC-SIGN cells were centrifuged at 1,500 × g for 5 min to removed virus-serum mixtures and washed one time with RPMI 1640 supplemented 10% FBS. Cells were replaced with fresh RPMI 1640 supplemented 10% FBS and incubated at 37 °C with 5% CO_2

for 20 h. The cells were stained with PE-conjugated mouse anti-human CD209 (BD biosciences, Frankin Lakes, NJ), fixed and permeabilized by cytofix/cytoperm solution (BD Biosciences, Frankin Lakes, NJ). The cells were intracellular stained with Alexa Flour 647-conjugated (Molecular Probes, Life Technologies) 4G2 antibody, a mouse monoclonal that binds to ZIKV E protein. Unbound antibody was washed off, and cells were resuspended in 1XPBS supplemented with 3% FBS and 2mM EDTA. The assay was quantified on LSRII flow cytometer (BD Biosciences, Frankin Lakes, NJ) and the percentage of infected cells was analyzed using FlowJo 10.4.2 software (Tree Star, Ashland, OR). The percentage of serum neutralization was calculated as 100 × (% infected cells in the absence of antibodies − %infected cells in the presence of antibodies) ⁄ % infected cells in the absence of antibodies. The titer of serum that showed 50% and 90% neutralization was analyzed by non-linear regression using GraphPad Prism 7 (GraphPad software, La Jolla, CA). Control and antibodies were tested in two independent assays in duplicated well.

4.3.9 Recombinant Full-length anti-human monoclonal IgGs antibody expression

4.3.9.1 IgG vectors construction

The phagemids containing scFv gene was amplified only regions that encoding V_H and V_L by PCR. The primers set are shown in **Table 4.5**. The PCR products were directly cloned into antibody expression vectors containing the constant domains of wild-type IgG1, L235E mutant (leucine (L) to glutamate (E) substitution at positions 235) IgG4 chain for the VH domains, and wild-type λ chain for the VL domain in an isothermal amplification reaction (Gibson reaction) using GeneArt Seamless Cloning and Assembly kit (Thermo Fisher, Waltham, MA). Plasmids

encoding the heavy and light chain were transfected into 293F cells and full-length recombinant IgG was secreted into transfected cell supernatants. Supernatant was collected and filtrated with 0.22 µm filter. The filtrated supernatant was kept at 4°C for further protein purification.

4.3.9.2 mAb IgG purification

Recombinant monoclonal antibodies were purified from culture media using recombinant MabSelect SuRe Protein A affinity resin (GE Healthcare Life Sciences, Pittsburgh, PA). The conditioned medium was filtered with a 0.22 µm vacuum filter unit (Millipore, Bedford, MA) and loaded onto a HiTrap MabSelect SuRe column (GE Healthcare Life Sciences, Pittsburgh, PA) of appropriate capacity to match the amount of antibody in the medium. The column was washed thoroughly with 6 column volumes of PBS, the antibody was eluted with 0.1 M Gly-HCl, 0.15 M NaCl pH 3.7 followed by 0.1 M Gly-HCl, 0.15 M NaCl pH 2.5, and neutralized with 1 M Tris-HCl, pH 8.0. The fractions were analyzed by SDS-PAGE and the positive fractions were pooled and dialyzed against PBS pH 7.4 (Sigma Aldrich, St. Louis, MO). Following dialysis, antibody samples were concentrated with a centrifugal filter concentrator (Vivaspin, 30,000 MWCO, Sartorius, Gettingen, Germany). Finally, the antibody was filter-sterilized using syringe filters with 0.22 µm pore diameter and the antibody concentration was determined by the Lowry method. Pyrogen content was determined using FDA-licensed Endosafe-PTS Limulus Amebocyte Lysate (LAL) assay (Charles River Laboratories, San Diego, CA). The limits of detection of this assay are 1- 0.01 EU/mL of endotoxin. If the test was negative, the samples were considered endotoxin-free.

4.3.10 ELISA of mAb binding analysis

To determine human mAb 2H12 binding to DENV1-4 and ZIKV viruses, ELISA 96-wells plate (Costar) were coated with 1 μg/mL of ZIKV E antigen (Suriname strain, Native Antigen, UK) or NS1 antigen (Meridian Life Science, Memphis, TN) in coating buffer (0.1 M NaHCO$_3$) for overnight at 4°C. Plates were then blocked with 5% casein in PBS for 1 h. Human serum was three-fold serially diluted in PBS containing 1% BSA and added to the plate for 1.5 h. The plates were washed with wash buffer (0.05% Tween 20 in PBS), followed by adding HRP conjugated goat anti-human IgG Fc (Invitrogen, Carlsbad, CA) for 1.5 h at room temperature. The plates were washed with washing buffer and developed the color using TMB substrate solution (Invitrogen), and the reaction was stopped by the addition of 4N sulfuric acid. The colorimetric detection was read at the absorbance 450 nm.

4.3.11 Epitope Mapping

4.3.11.1 Phage-displayed bio-panning procedures

The SUT-12 Phage Display peptide Library was performed in epitope searching. Three successive rounds of bio-panning were carried out using a different amount of mAb DV2H12 IgG1 as a target by 10, 5, and 2 μg for round 1, 2, and 3, respectively. Briefly, 100 μl of DV2H12 IgG1 was coated by coating buffer (100mM NaHCO$_3$, pH 8.5) overnight at 4°C on 96-well plates and blocked (1% BSA in 0.05% Tween in 1xPBS) at room temperature for 2h. The plates were then washed five times with washing buffer, and phages 10^{11} PFU were incubated room temperature at for 2 h with the coated antibody. The wells were washed five times with 0.05% PBST (0.05% tween in 1xPBS). Then, the bound phages were eluted with

100 μL of 0.2 M glycine-HCl (pH 2.2) plus 1 mg of BSA/ml and were then neutralized with 15 μL of 1 M Tris–HCl (pH 9.1). The eluted phages were amplified in *E. coli* DH5α culture. The amplified phage supernatant was used in the next round. After three rounds of bio-panning, 70 phage clones were selected and screened by ELISA and further characterized by DNA sequencing.

4.3.11.2 Phage peptide ELISA

To identify immunopositive phage clones, the ELISA plates were coated overnight at 4°C with 100 μl mAb 2H12 (5 μg/mL) and blocked with blocking buffer (1% BSA in 1xPBS containing 0.1% Tween20) 2h at 4°C. Phage clones were added to the wells (200 μL per well) and incubated with agitation for 2h at room temperature. The plates were then washed with washing buffer (1xPBS containing 0.1% Tween20), and 1:5000-diluted horseradish-peroxidase (HRP)-conjugated anti-M13 antibody (GE Healthcare, USA) in washing buffer was added. The plates were incubated at room temperature for 1 h with agitation and washed with washing buffer. The 200 μl of ABTS substrate solution (1mg/mL in 50 mM citric acid pH 4.0, containing 0.05% H_2O_2) was added into each well and incubated at room temperature for 30 min. The plates were read using a microplate reader set at 405 nm.

4.2.11.3 DNA sequencing and computer analysis

The DNA sequences of ELISA-positive phage clones were sequenced with the 96 gIII sequencing primer 5' TGAGCGGATAACAATTTCAC 3'. Sequences of DNA inserted into target phage clones were translated into amino acid sequences and aligned with that of prM protein of DENV2 using Standard protein–protein BLAST (blast) and ClustalW Multiple Sequence Alignment public software.

4.3.12 Mouse lethal prevention experiment

4.3.12.1 Infection of AG129 mice

The 129/Sv mice lacking the interferon α/β and γ receptors (AG129) were bred under specific pathogen-free conditions at the animal facility of La Jolla Institute for Immunology. AG129 mice (5 weeks-old) were injected intravenous (i.v.) into the tail vein with or without 2 mg of DV2H12 IgG4 mAb, in a total volume of 200 µL, then infected 1h later with either 10^5 PFU of DENV 2 strain S221 diluted in PBS 100 µL volume by i.v. injection into the tail vein. Survival rates, weight loss, and disease signs were monitored daily. Kaplan-Meier survival curves were analyzed by the log-rank test and compared to curves of the controls, using GraphPad Prism 8 (GraphPad Software, La Jolla, CA).

4.4 Results

4.4.1 Library construction

4.4.1.1 Amplification and assembly of the variable region of heavy and light chain

The total RNA was extracted from PBMCs of an individual sample. The RNA quality was intact and no contamination of DNA (**Figure 4.1**) and subjected to cDNA synthesis. To amplify the variable region of heavy (V_H) and light chain (V_L) of lambda (V_λ) or kappa (V_κ), the primers were designed to represent of all five classes of antibodies. We performed 75 independent PCRs, using all possible combinations within the designed primer set (**Table 4.1**) that encompasses the whole repertoires of human antibody genes. As shown in Figure 4.2, the predicted size of V_H, V_λ, and V_κ genes are approximately 350-400 bp. A total of 24 V_H variants were

generated from paring of 6 V_H forward and 4 reverse primers. The total of 30 V_κ variants was obtained from 6 forward and 5 reverse primes of V_κ, and 21 paired of V_λ were from 7 forward and 3 reverse primers of V_λ. To assemble V_H and V_L genes into scFv fragment, the linker sequence of 3' end of V_H gene was complementary to 5' end of V_L gene. The assembled V_H and V_L genes were amplified by PCR with pull-through primers, giving the full-length scFv genes of approximately 800 bp (**Figure 4.3**).

4.4.1.2 Cloning of scFv genes and electro-transformation

The purified of digested full-length scFv fragments and vectors were ligated at *Sfi*I and *Not*I enzyme restriction sites. The 1:3 ratios of insert and vector at the total x μg DNA insert was electroporated into *E. coli* TG1. The background was determined in parallel using 100 ng of digested empty pMOD1 vector. The final scFv library was successfully constructed, showing the size of the library at 1×10^8 individual clones with 0.002% of the self-ligation background.

4.4.1.3 Analysis of library diversity

In order to analyze the diversity of scFv repertoire and the quality of the primary library, the phagemid DNA containing scFv gene from 20 randomly picked clones was examined. The phagemid DNA was digested with *Bst*NI, and their fingerprint patterns were compared. The variation in patterns indicated the framework diversity in antibody phage display library. We observed 19 different, meaning that these examined clones are unique (**Figure 4.4**).

The variable regions of 40 random clones were also DNA sequenced. After sequencing, the origin of V genes and complementary determining region 3 (CDR3) length were determined using IMGT/V-QUEST database. The DNA

sequencing data indicate that variable regions derived from 6 different V gene families (**Table 4.2**).

4.4.2 Isolation and characterization of scFv antibody against purified DENV 2 and ZIKV antigens

4.4.2.1 Affinity selection of monoclonal scFv against DENV2 and ZIKV

The previous large phage-display antibody scFv library using peripheral blood B cells of 140 non-immunized healthy donors was successfully prepared and identified panels of scFv against various targets such as cancer-related cell lines, mycotoxins, and rabies virus vaccine antigens. In this study, we successfully constructed a phage display scFv library from 40 DENV immune healthy donors using similar methodology. We aimed to isolate a neutralizing scFv against purified DENV2 (strain S16803) and ZIKV (strain SD001). To prepare the target antigen for bio-panning, DENV2 and ZIKV were propagated in C6/36 cell lines. The virus supernatant culture was purified using ultracentrifuge with a gradient-free sucrose cushion method. The purified virus was UV inactivated and used as a target antigen during bio-panning. The bio-panning of each DENV2 and ZIKV were done in parallel. After one round of DENV2 panning, we have got phage output at 600 colonies (**Table 4.3**). A total of 192 phage clones were randomly picked for their binding test by monoclonal phage ELISA. The phages were scored as positive, if the absorbance on virus coated wells was at least two times higher than the binding of phage to 1% (w/v) BSA in 1xPBS coated wells. According to these criteria, there were 18 clones showed positive absorbance on DENV2 coated wells (**Figure 4.5**). The positive phage clones were again expressed for confirming the binding affinity and the result showed that only 17 clones were positive (**Figure 4.6**). The soluble scFv

antibodies of 17 phage clones were expressed in *E. coli* HB2151 and the supernatant containing soluble scFv were tested for monoclonal scFv ELISA. All of 17 clones showed the binding signal of DENV2 higher than 1% BSA in 1xPBS coated wells (**Figure 4.7A**). To check cross-reactivity against ZIKV, scFv supernatant from clone 2H12, 2D2, 2E11, and 2B1 that contained different DNA sequences were tested for ELISA with ZIKV and DENV2. The result of these 4 clones showed the binding signal of ZIKV similar to DENV2 and two times higher than 1% BSA, suggesting this scFv cross-react to ZIKV (**Figure 4.7B**).

To identify specific scFv against purified ZIKV, 3 rounds of bio-panning were performed (**Table 4.3**). A total of 192 phage clones were randomly picked from the third rounds to test binding affinities by phage ELISA. There were 25 clones showed binding signals against ZIKV higher than 1% BSA (**Figure 4.8**). To confirm their binding with ZIKV and cross-reactivity for DENV2, soluble scFv was expressed for ELISA. All 25 scFv clones showed a signal for ZIKV higher than DENV2 coated wells (**Figure 4.9**), suggesting scFv obtained from 3 rounds bio-panning can enrich specific phage clones against ZIKV.

4.4.2.2 Analysis of human scFv sequences

To characterize the ELISA positive clones, 17 clones from DENV2 and 25 clones from ZIKV bio-panning were analyzed DNA sequences. The sequencing data revealed that 9 and 5 unique different DNA sequences were obtained from DENV2 and ZIKV bio-panning, respectively. The alignment of the amino acid sequence of 14 different clones was shown in Figure 4.10A and B. Immunogenetic analysis of their sequences was performed using the IMGT tool to determine the closest VH and VL germline genes (**Table 4.4**). Analyses of germline gene usage

indicated that they originated from different B-cell lineages. Furthermore, their nucleotide sequences displayed 87%–100% variable region of heavy and light chain identity to the germline (**Table 4.4**). Therefore, all 14 antibodies were germline-like mAbs, which, in general, exhibit lower immunogenicity. While the patterns of VDJ gene segment usage were diverse among the 14 antibodies, six of them or 42.9% shared the same IGHV1-69 germline gene, with slight differences between allelic variants (IGHV1-69*01; IGHV1-69*04; and IGHV1-69*09). Taken together, these results suggest that the elicitation of these germline-like antibodies, especially IGHV1-69 lineage could be relatively quick and effective by immunization of flavivirus immunogens.

4.4.2.3 *In vitro* neutralization assay of soluble scFv

To examine the neutralizing capability of the scFv antibodies against DENV2 and ZIKV infection, we first evaluated 4 scFv clones from DENV2 bio-panning (DV2B1, DV2D2, DV2E11, and DV2H12) and 5 clones from ZIKV bio-panning (ZV1B7, ZV1B10, ZV1C11, ZV1F8, and ZV1H6). As shown in Figure 4.11, DV2D2 exhibited the highest neutralizing activities against DENV2 (**Figure 4.11A**) and cross neutralizing against ZIKV (**Figure 4.11B**) among the four scFv antibodies. In comparison, DV2H12 and DV2B1 had modest neutralization activity, while DV2E11 did not show the neutralization activity against both DENV2 and ZIKV. In contrast, ZV1B10 and ZV1B7 showed the highest neutralization activity against ZIKV (**Figure 4.11C**) but could not neutralize DENV2 infection (**Figure 4.11D**). A similar pattern could be observed in other 3 scFv clones obtained from 3 rounds ZIKV

bio-panning. This result suggests that increasing the number of panning, the more specific scFv to the target will be achieved. The DV2D2 and DV2H12 scFv inhibited DENV2 infection in a dose-dependent manner with 50 μg/mL resulting in ~70% neutralization, which was less effective than the control mouse IgG mAb 4G2 (**Figures 4.11A**).

4.4.3 Production of full-length recombinant human monoclonal IgG

An immunoglobin G (IgG) is the most accepted format for the therapeutic purposed. Conversion of scFv antibody fragments back into IgG can result in similar or even improved antigen binding. To examine the effect of Fc regions in changing the IgG subclass on its neutralization activity *in vitro* and *in vivo*, conversion in wildtype IgG1 and mutated IgG4 was performed. Human IgG4 has a weak binding affinity to most FcγRs-bearing cells and its mutation at L232E silent the Fc effector function. In this study, three scFv clones, DV2H12 and ZV1B10 were converted into both IgG1 and mutant IgG4, and DV2D2 was fused with only mutant IgG4 format. The heavy and lambda light chain variable region of each scFv clone was amplified from pMOD phagemid vector containing scFv genes. The V_H and V_L PCR products were cloned into pcDNA3.4 mammalian expression vectors, containing a constant region of heavy or lambda light chains (**Figure 4.12**). Heavy and light chain vectors were co-transfected into HEK293-F cells in 50 mL culture volume. All antibodies were purified by protein A affinity chromatography for further validation. Antibodies were extremely pure, at least >95%, and high quality by SDS-PAGE and size exclusion chromatography (SEC) (**Figure 4.13**). A review of the SEC, in which there is no SDS-PAGE sample buffer, shows that the antibody is actually an intact, single

peak of the correct MW. The IgG production yields of 50 mL scale were between 196-363 mg/L (**Table 4.6**).

4.4.4 Characterization of Human mAb IgG

4.4.4.1 IgG binding test

To test the antigen-binding efficiency of IgG 1 and IgG4 format, specific and cross-reactivity between DENV1-4 and ZIKV was performed by ELISA. The recombinant human mAb DV2H12 IgG1 and IgG4, and DV2D2 IgG4 were shown to recognize the purified DENV 2 in dose-dependent antibody concentration (**Figure 4.14A**). In contrast, mAb DV2H12 IgG1 and 4 did not cross-react to ZIKV lysate or whole virus (**Figure 4.14B**). The mAb ZV1B10 IgG1 and 4 showed a weak binding signal against ZIKV lysate (**Figure 4.14B**) and lacking the ability to bind DENV2 (**Figure 4.14A**). The DV2H12 IgG1 and DV2D2 IgG4 were cross-reactivity checked against DENV1-4 lysate (**Figure 4.14C and D**). As shown in Figure 4.14A, DV2H12 IgG1 showed the signal against DENV2 and DENV3 lysate lower than the purified DENV2 and there was no signal observed in DENV1 and 4 lysates. The similar pattern was observed in DV2D2 IgG4 which a weaker signal was detected in DENV1-4 lysate (**Figure 4.14D**).

4.4.4.2 *In vitro* neutralization assay

To determine the neutralization activity of mAbs IgG1 and IgG4 against ZIKV and DENV serotype 1-4, U937+DC-SIGN flow cytometry-based assay was performed. We used DENVs that are common strains and WHO referenced in DENV research, DENV1 (WestPac 74), DENV2 (S16803), DENV3 (CH53489), and DENV4 (TVP360). ZIKV is the strain SD001, an Asian lineage was isolated in 2016 in a returning traveler from Venezuela. The mAb ZV1B10 IgG1 and 4 could not cross

neutralize DENV2 infection (**Figure 4.15A**), while the ZV1B10 IgG4 showed a better

neutralization activity against ZIKV infection than the ZV1B10 IgG1 (**Figure 4.15B**).

However, ZV1B10 IgG4 at the highest concentration (50 μg/mL) had the

neutralization activity against ZIKV infection lower than 50%, suggesting the

antibody was not a potent neutralizing antibody. A similar pattern of neutralization

efficiency also could be observed in mAb 2H12 IgG4, which showed a better

neutralization against DENV2 than the IgG1 format (**Figure 4.15C**). At the

concentration 50 μg/mL, the DV2H12 IgG4 could neutralize DENV2 infection by

about 70%. In contrast, the DV2H12 IgG1 and IgG4 failed to neutralize ZIKV

infection (**Figure 4.15D**). This result suggests that the IgG4, which lacks the function

at Fc effector site, could give a better neutralization activity *in vitro* than the wildtype

IgG1 format. Therefore, only the IgG4 of DV2H12 and DV2D2 were next evaluated

the cross-neutralization activity against all four DENV serotypes (**Figure 4.15E and

F**). The DV2D2 and DV2H12 IgG4 antibody shown similar mAb concentration 25-30

μg/mL resulting in 50% neutralization against DENV2. However, the DV2D2

antibody failed to neutralize DENV1, 3, 4, and ZIKV infection (**Figure 4.15F**). In

contrast, the DV2H12 IgG4 antibody shown mild neutralization activity against

DENV3 and weak neutralization activity for DENV1 and 4 infections (**Figure 4.16E**).

Among the mAbs in this study, the DV2H12 IgG4 was the best candidate antibody for

further *in vivo* experiments.

4.4.4.3 *In vivo* evaluation of mAb in mice

To determine whether DV2H12 IgG4 can protect DENV2 infection

in vivo, we used an AG129, which lack receptors for both IFN-α/β and IFN-γ and the

mouse-adapted DENV2 strain S221. The S221 infected AG129 mouse model

developed the dengue-like lethal disease. The mice were treated intraperitoneally with a single dose of 2 mg/mouse (100 mg/kg/dose) of DV2H12 IgG4 antibodies, or with PBS as a control. After one hour, mice were challenged with DENV2 S221 (5.0×10^5 PFU/mouse, i.v. injection). Animals were observed daily for survival, body weight changes and clinical sign of disease. The description of clinical scores is shown in Table 4.7. On day 1 after the virus challenge, mice from the antibody group were more active and healthier than mice in the control (**Figure 4.16A and B**) The weight loss in the antibody group was slightly lower than the control (**Figure 4.16C**). For the survival study, mice in the antibody group were 100% mortality within the first 4 days which was significantly different from the control group (p = 0.025). One mouse from the control group died on day 5, and two more died on day 6 (**Figure 4.16A**). This data indicated that the DV2H12 IgG4 antibody could not prevent DENV2 infection but increase the mortality in mice. This antibody could be considered as the enhancing antibody which contributes to the enhancement of virus infection *in vivo*.

4.4.5 Epitope searching

To map the epitope of the mAb DV2H12 IgG4 and identify in a greater detail for the structural basis of DENV neutralization, a library of short random 12-mer peptides phage display technique (SUT-12 library) was implemented. The bound phage clones were selected after three bio-panning rounds. Twenty-two of 70 selected phage clones had significantly reactivity to the mAb DV2H12 but not to 1% BSA in PBS as a control (**Figure 4.17**). The phagemid of positive phage clones was sequenced and translated to the peptide sequences (**Table 4.8**). Through the alignment of phage-displayed peptide sequences, the binding motif of antibody DV2H12 was shown to be WT/SxW/MG (**Table 4.9**). We next compared the binding motif with the

primary amino acid sequence of DENV2 polyprotein and found matching with the prM protein of DENV2 (GenBank accession no. X51713.1). The binding motif for DV2H12 antibody corresponded to amino acid residues 78 to 89 of the membrane precursor protein of DENV2 (**Figure 4.18A**). The alignment of this region with DENV1, 3, 4 (GenBank accession no. KM204119.1, AY648961.1, and MG601754.1, respectively) was partially conserved but not to ZIKV (GenBank accession no. MH882541.1) (**Figure 4.18B**). This result was consistent with the *in vitro* neutralization result that mAb DV2H12 exhibited the highest neutralization activity against DENV2 but partial cross neutralized other DENV serotypes. The antibody was also lacking the ability to neutralize ZIKV infection.

4.5 Discussion

Dengue is a disease with a complex immune response, cross-reactivity between DENV serotypes or ZIKV can give either protection or pathogenesis. This consideration is the major challenging in the development of an effective vaccine. Thus, it is urgent to develop an effective and cross-reactive antiviral against DENV or ZIKV infection. The studies of mAbs derived DENV or ZIKV infected patients have been provided a powerful tool to understand the mechanism of DENV and ZIKV antiviral immunity, diagnostics and therapeutics (Bhaumik et al., 2018; Dejnirattisai et al., 2015a; Priyamvada et al., 2016). In this study, we used the difference strategies in identifying new antibodies against DENV and ZIKV. We successfully constructed a DENV immunized scFv antibody phage display library from B-cells of 40 healthy donors. These donors have been characterized as repeated exposure to DENV infection and showed high titer neutralizing antibodies for all four DENV serotypes

and ZIKV. The library contained the repertoire of scFv genes at 1×10^8 members and represents almost the entire family of variable gene germline of human heavy and light chains. The advantage of screening antibodies from the phage display library is the rapid development of human mAbs, especially for quick response to the new outbreak of emerging viruses. Recently, the naïve libraries successfully identified human germline-like mAbs against recombinant E protein domain III of DENV and ZIKV, which were potently (micromolar scale) neutralized virus *in vitro* and in the mouse model (Hu et al., 2019; Wu et al., 2017). Therefore, the DENV immunized library that had been constructed in this study could be used for rapid isolation human mAbs that recognize to whole particles of DENV and ZIKV. We obtained a total of 14 difference scFv clones from both DENV and ZIKV bio-panning. Notably, 5 clones from DENV and 1 clone from ZIKV (6/14; 42.9%) were from the same V-gene germline IGHV1-69 Interestingly, IGHV1-69 was frequently found in the studies of human mAbs isolated from DENV and ZIKV infected patient (Dejnirattisai et al., 2015a; Gao et al., 2019; Hu et al., 2019; Li et al., 2019; Sapparapu et al., 2016). Similarly, detection of the dominant IGHV1-69 was reported in influenza virus studies (Avnir et al., 2016; Lingwood et al., 2012). Taken together, the IGHV1-69 V-gene germline was biasedly use in B cell repertoire during viral infection.

In our study, DV2H12 scFv clones from DENV bio-panning was engineered into fully human IgG subclass 1 and 4 antibodies. The neutralization of IgG4 against DENV2 showed a better activity than the IgG1 subclass in U937+DC-SIGN cells, this probably explains that the U937 is monocyte expressing FcRs which could bind with IgG Fc region whereas IgG4 possess weak affinity binding to FcγRIa by two-fold lower compared to IgG1 (Bruhns et al., 2009). This is the first study using. the human

IgG4 subclass to study DENV infection. We also found that DV2H12 IgG4 showed about 70% neutralization of DENV2 and partial neutralized DENV1, 3, and 4 infections in U937+DC-SING cells at the micromolar range ratio. In contrast to the *in vitro* study, the DV2H12 IgG4 mAb failed to protect AG129 mice, but showed ADE from DENV2 infection *in vivo*. The epitope mapping of mAb DV2H12 using peptide phage display showed the epitope might be located on the amino acid residues 78 to 89 of the DENV2 prM protein. It has been previously reported that human anti-prM mAbs are capable of enhancing DENV infection in Fc receptor-bearing U937 cells (Dejnirattisai et al., 2010; Smith et al., 2016) and in Balb/c mice (Luo et al., 2013). The human anti-prM mAbs are highly cross-reactive among the four DENV serotypes and predominant for the immune response in both primary and secondary DENV infections patients, as well as most of these antibodies display limited 10% to 60% virus neutralization capacity (Dejnirattisai et al., 2010). It is unclear whether the only mature virus is infectious or whether the immature virus contains small numbers of prM molecules at its surface and still remain infectious. Our study showed partial neutralization, which implies that some prM containing particles remain infectious. In the viral replication process, immature virion will be cleaved at prM into pr fragments by the cellular furin protease, thus generating mature infectious virion (Rey, Stiasny, Vaney, Dellarole, & Heinz, 2018). The efficiency of the cleavage of prM can vary among the different cell types. It has been previously found that DENV virus production in mosquito C6/36 release 30% prM containing immature particles (Zybert, van der Ende-Metselaar, Wilschut, & Smit, 2008). Therefore, it is possible that in our study the DENV propagation released a mixture of not only fully mature but contained immature. Furthermore, the recent study has filled the gap by showing

how anti-prM enhance immature DENV infectivity via the attachment of FcγR bearing-cells (Wirawan et al., 2019). Fully immature DENV on its own is not infectious, however the complex of the anti-prM antibody with immature DENV and recognized by FcγR, allowing internalization of the virus-antibody complex. Wirawan et al, 2019 showed the 25 A° cryoEM structure of Fab fragment of anti-prM bound to prM at the surface of the virus, in which the low pH 5.5 of the endosome induce the dramatic rearrangement the structure of antibody-virus complex, resulting pr molecules dissociated from E protein fusion loop. This allows viruses and endosomal membrane fusion to occur. However, our study still lacks the data to confirm that our mAb DV2H12 is truly recognized as the prM epitope. In the future, Western blot analysis should be performed to investigate the specificity of DV2H12 mAb for the DENV2 prM protein.

In conclusion, we successfully constructed DENV immune human antibody library and developed a platform to rapid engineered scFv antibody into fully recombinant human IgG mAbs. We identified a panel of human mAb that mediated ADE infection *in vivo*. We found mAb against DENV2 may recognize the prM protein. Most importantly, identification of the epitope on prM protein will provide new insight for further understanding of humoral immune response to DENV and eliminate pathogenic enhancing epitope for future vaccine candidates. Taken together, our human antibody library can be used to study DENV and other flaviviruses.

4.6 Figures and Tables
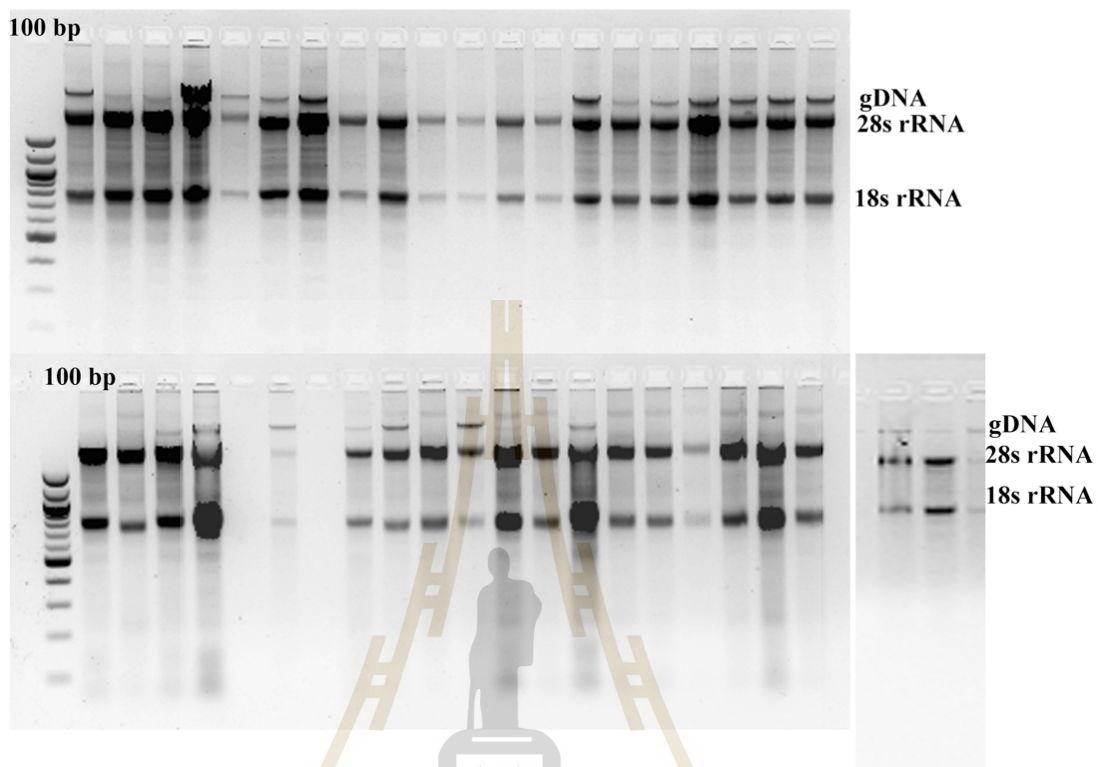
Figure 4.1 The total RNA of 40 samples used in library construction. The intact of total RNA showed discreet 18S and 28S ribosomal RNAs, which were approximately 1.3 kb and 2.6 kb, respectively, on 2 % agarose gel.
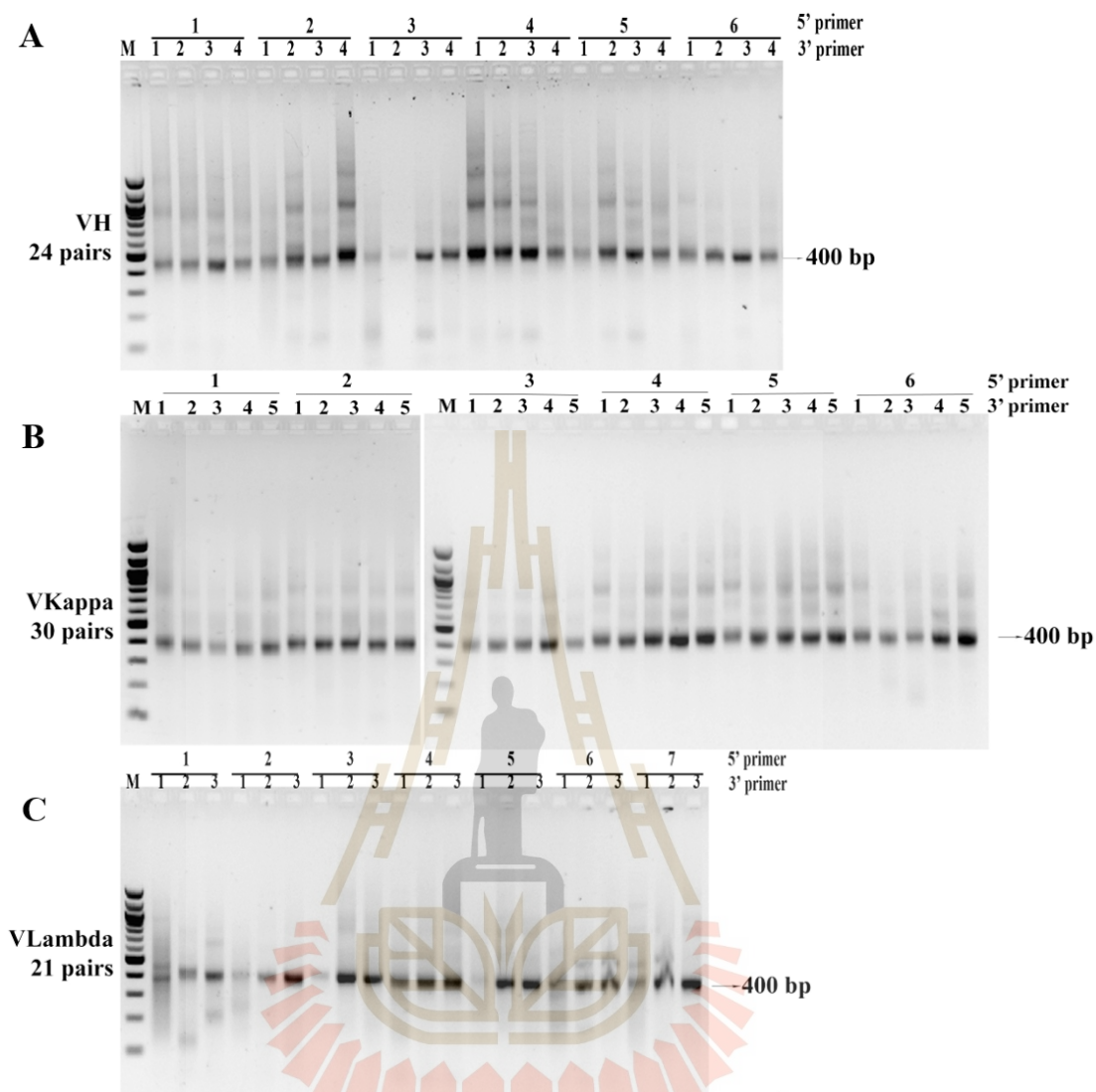
Figure 4.2 Amplification of variable region heavy and light chain. Agarose gel analysis of heavy and light chain DNA from first step PCR, using all combinations of the primers within the primer sets. (A), Lane M, DNA markers (100 bp ladder); lane 1-24, PCR products of VH DNA from 24 combinations of six VH forward primers paired with four VH reverse primers. (B), Lane M, DNA markers (100 bp ladder); lane 1-30, PCR products of Vκ DNA from 30 combinations of six Vκ forward primers paired with five Vκ reverse primers. (C), Lane M, DNA markers (100 bp

ladder); lane 1-21, PCR products of Vλ DNA from 21 combinations of seven Vλ forward primers paired with three Vλ reverse primers. The PCR product size is about 400 bp.
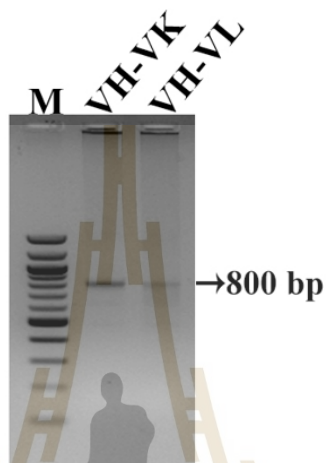
Figure 4.3 The scFv products from Pull-Through PCR. Lane M, DNA marker (100 bp ladder). The second lane is the assembled of pooled VH-linker-Vκ products. The third lane is pooled VH-linker-Vλ products. The scFv fragment size is 800 bp.
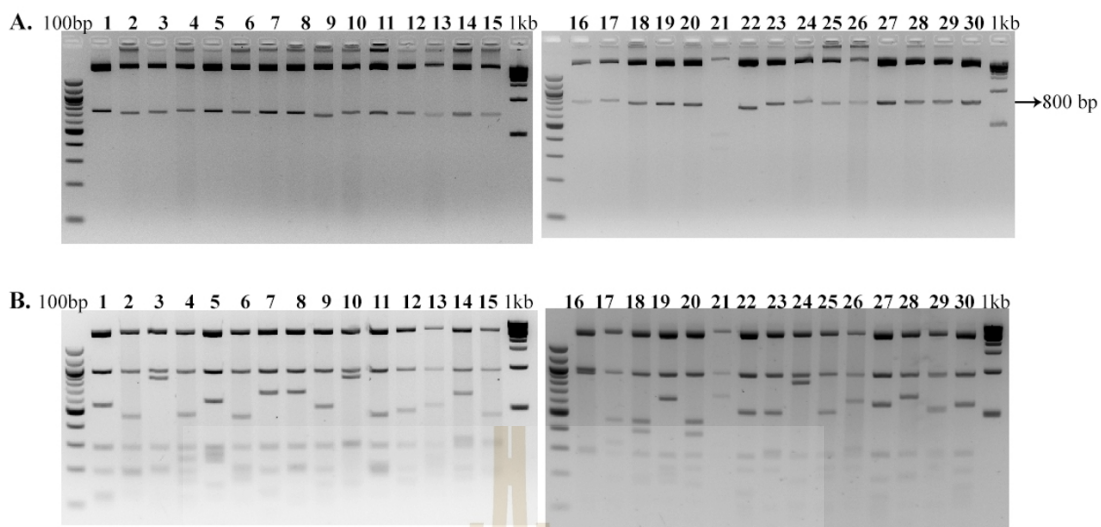
Figure 4.4 Fingerprint analysis of primary library. (A) DNA of the thirty scFv clones were digested with NotI and NcoI. The inserted scFv gene size is 800 bp. (B) the phagemid of 30 clones were digested with BstNI. The restriction patterns were analyzed on 1% agarose gel.
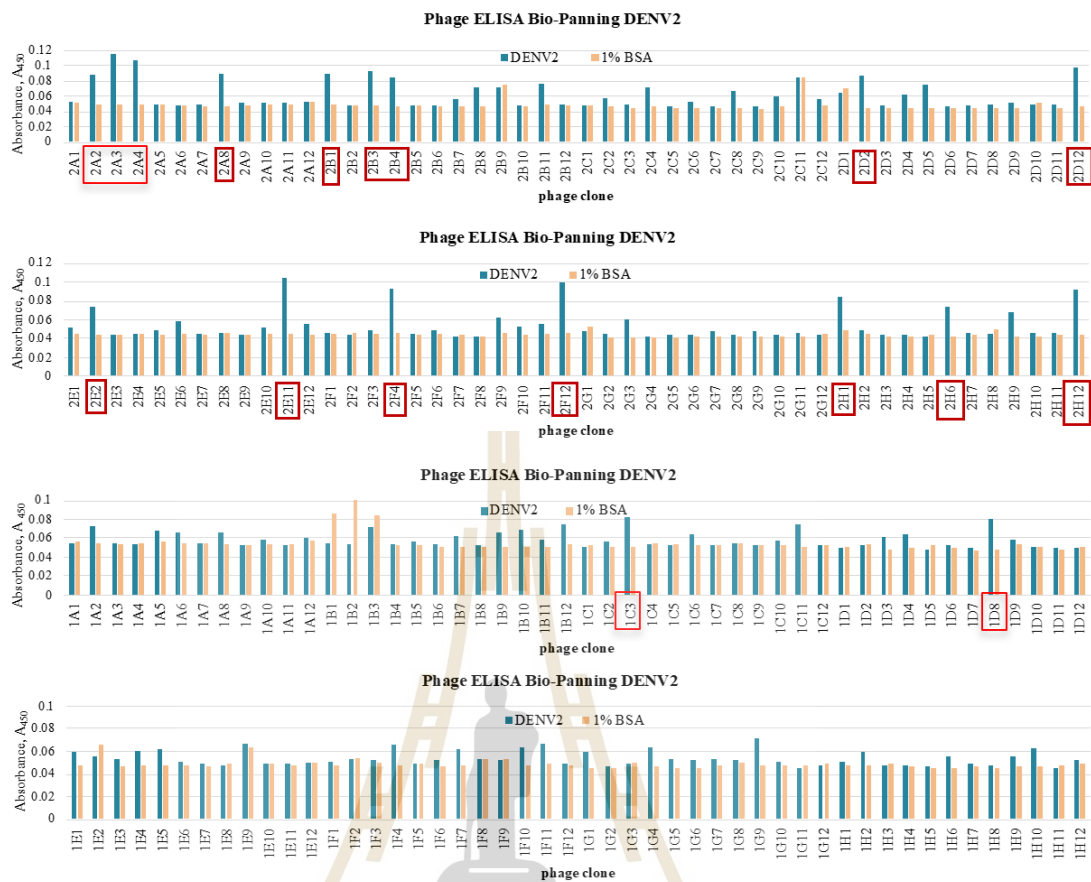
Figure 4.5 Binding of eluted phage from DENV2 bio-panning. ELISA of 192 phage supernatant against the purified whole DENV2. Eighteen phage clones in the red box showed the signal higher than 1% BSA.
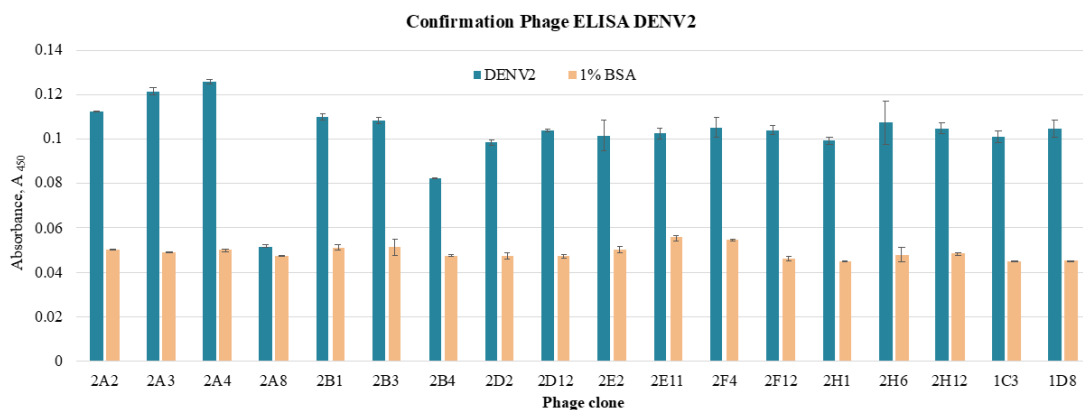
Figure 4.6 Confirmation binding of positive phage clone. Eighteen of selected phage clone after one round DENV2 bio-panning were again expressed phage in the supernatant. The ELISA showed 17 clones bound to purified DENV2. 1% BSA was use as the negative control. Data are expressed as means of duplicated experiments. The error bars represent SD.
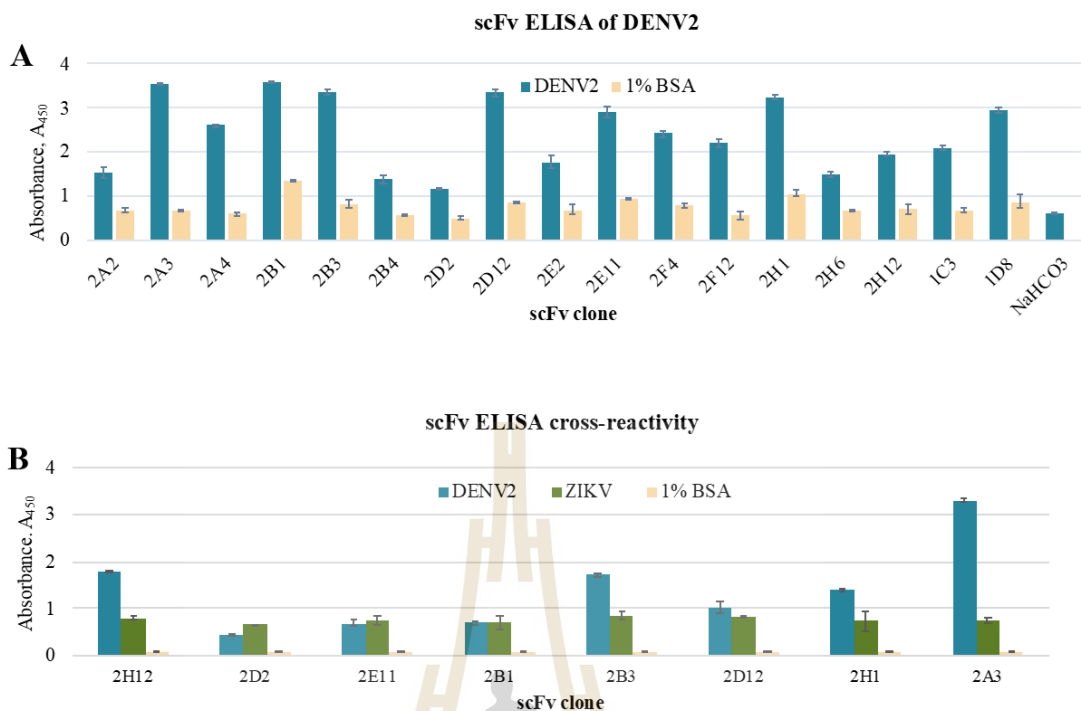
Figure 4.7 Specificity of soluble scFv antibody. Seventeen of selected positive phage clones were expressed soluble scFv. The supernatant containing soluble scFv has tested the binding with purified DENV (A). 1% BSA was used as negative control. Seven different cloned was cross-reactivity checked with purified ZIKV (B). Data are expressed as means of duplicated experiments. The error bars represent SD.

Figure 4.8 Biding of eluted phage from 3rd round of ZIKV bio-panning. ELISA of 192 phage supernatant against the purified whole ZIKV. The 25 phage clones in the red circle showed the signal higher than 1% BSA.
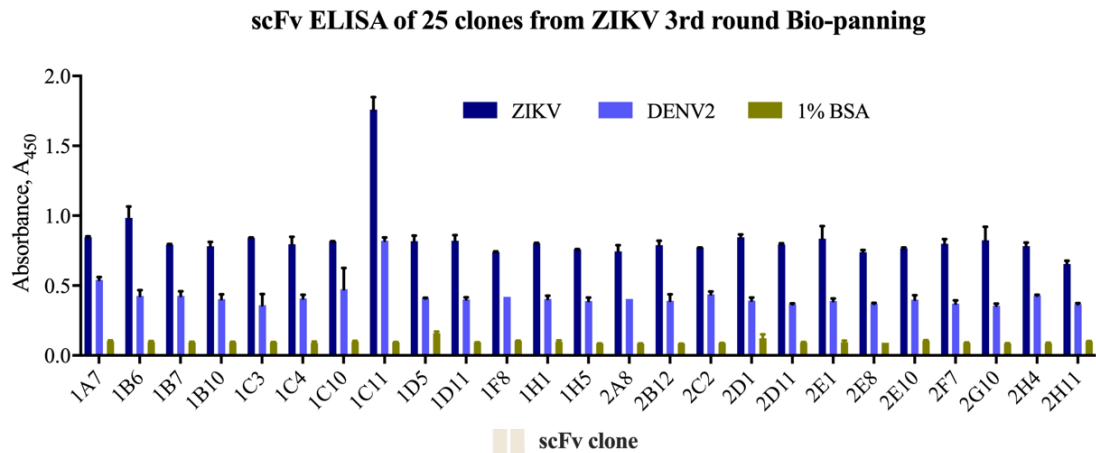
Figure 4.9 Specificity and cross-reactivity of soluble scFv. Twenty-five of selected phage clone after three rounds ZIKV bio-panning were expressed soluble scFv. The supernatant containing soluble scFv was tested the binding with purified whole ZIKV or DENV by ELISA. 1% BSA was use as the negative control. Data are expressed as means of duplicated experiments. The error bars represent SD.

Figure 4.10 Multiple alignments of amino acid of scFv fragments. The alignment was performed using the Clustal Omega database. The highlighted sequences in the green box show the CDR3 of the heavy chain (VH) and the yellow box is CDR3 of the light chain (VL). Both VH and VL are linked by the glycine-serine (Gly4S)3 linker (shown in the grey box). (A) The amino acid of 9 different scFv clones from DENV2 bio-panning. (B) The amino acid of 5 different scFv from 3rd round ZIKV bio-panning.
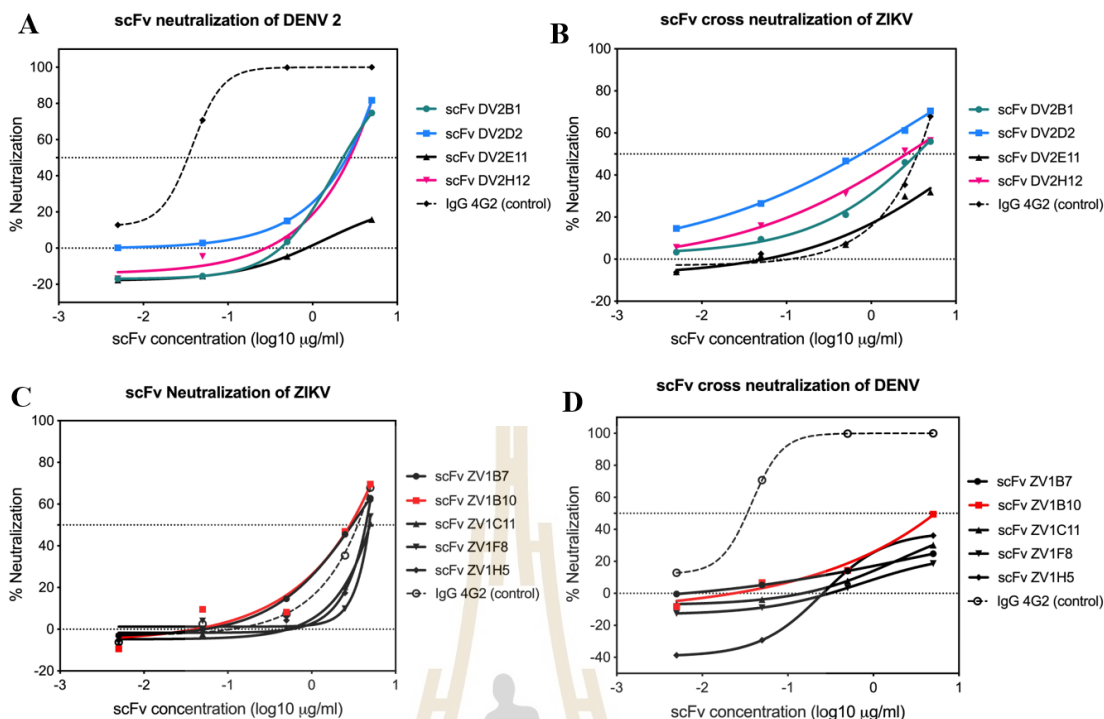
Figure 4.11 Neutralization activity of soluble scFv against DENV2 and ZIKV infection in U937+DC-SIGN cells. Four soluble scFv antibodies from DENV2 bio-panning were 10-fold serially diluted, starting at concentration 5 μg/mL and preincubated with DENV2 (A) or ZIKV (B). Five soluble scFv antibodies from ZIKV bio-panning were 10-fold serially diluted, starting at concentration 5 μg/mL and preincubated with ZIKV (C) or DENV2 (D). The mouse mAb 4G2 IgG was used as the experiment control.
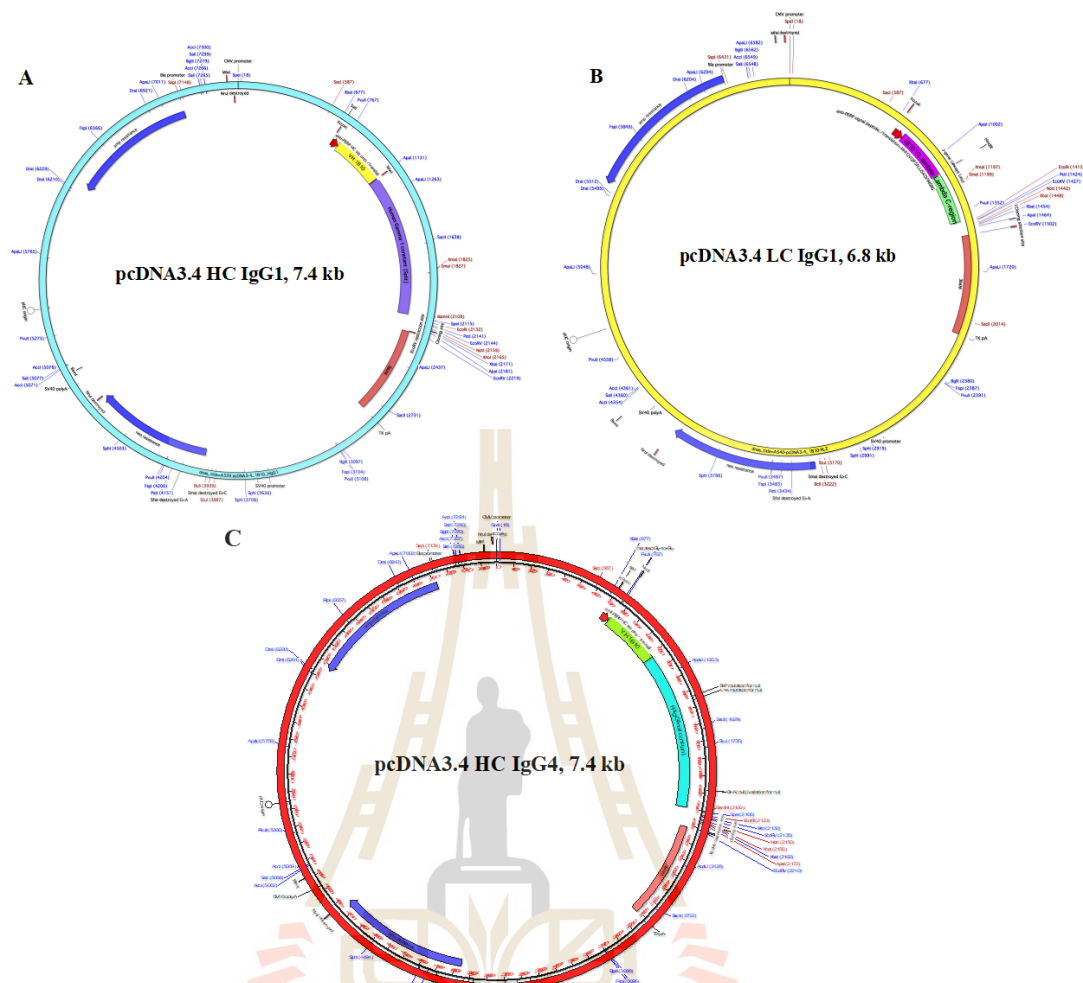
Figure 4.12 Heavy and light chain of human IgG expression vectors. The pcDNA3.4 containing a constant region of heavy chain IgG1 (A), the constant region of the lambda light chain (B), and the constant region of heavy chain IgG4 (C). The variable region of heavy chain was cloned into a heavy chain vector by Gibson assembly at the NheI and NruI restriction site. The variable region of light chain was cloned into the light chain vector at SfoI and XhoI restriction sites.
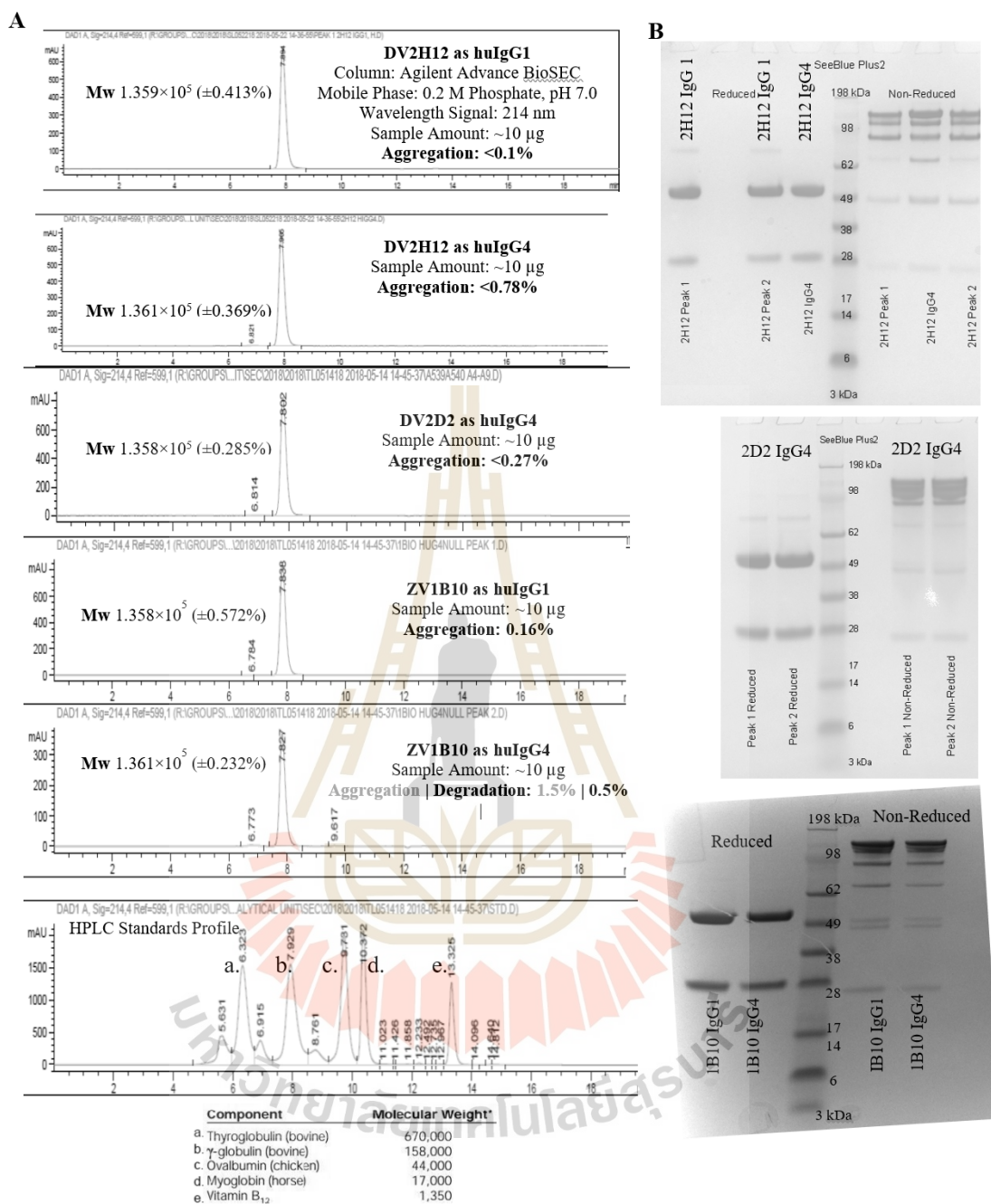
Figure 4.13 Analysis recombinant human mAb IgG purification. MAbs were expressed in HEK-293F cells and purified using protein A affinity resin. (A) Analysis of size-exclusion chromatography of mAb DV2H12 IgG1 and 4, DV2D2 IgG4, and ZV1B10 IgG1 and 4. (B) SDS-PAGE of reducing and non-reducing mAb DV2H12 IgG1 and IgG4 (top), DV2D2 IgG4 (middle), and ZV1B10 IgG1 and IgG4 (bottom).
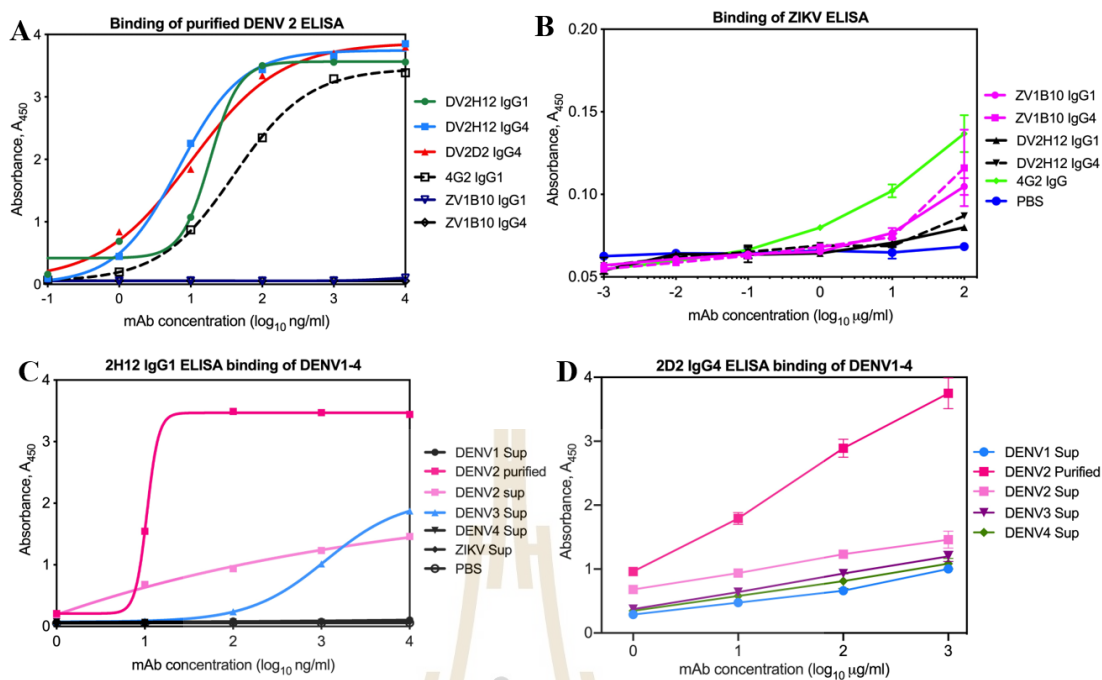
Figure 4.14 Binding of recombinant human mAb IgG1 and IgG4 against DENV serotype 1-4 and ZIKV. ELISA results for the binding between mAbs IgG1 or IgG4 of DV2H12, DV2D2 and ZV1B10 and the purified virion of DENV serotype 2 (A) or lysate of ZIKV supernatant (B). The anti-E protein mouse mAb 4G2 IgG, was used as the positive control. (C) The binding of mAb DV2H12 IgG1 against four DENV serotypes and ZIKV lysates. (D) The binding of mAb DV2D2 IgG4 against four DENV serotypes lysates.
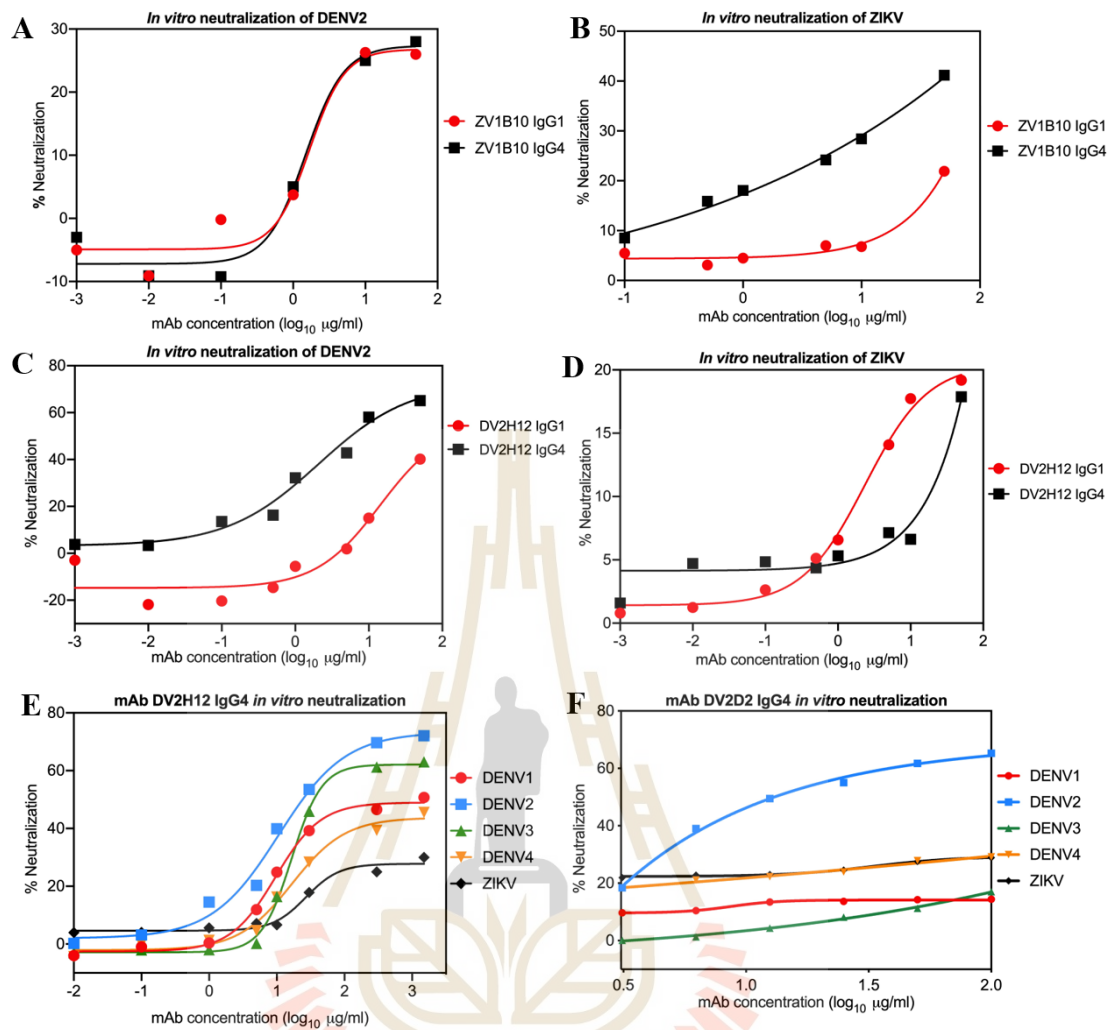
Figure 4.15 In vitro neutralization of mAb IgG1 and IgG4 against DENV serotype 1-4 and ZIKV. Neutralization efficiency of mAb ZV1B10 IgG1 and 4 against DENV 2 (A) and ZIKV (B) infection in U937+DC-SIGN cells. Neutralization activity of mAb DV2H12 IgG1 and IgG4 against DENV2 (C) and ZIKV (D). The cross-neutralization activity of mAbs DV2H12 (E) and DV2D2 IgG4 (F) were serially diluted and incubated with DENV1-4 and ZIKV before infected to the U937+DC-SIGN cells. Results are shown as the percentage of viral reduction.
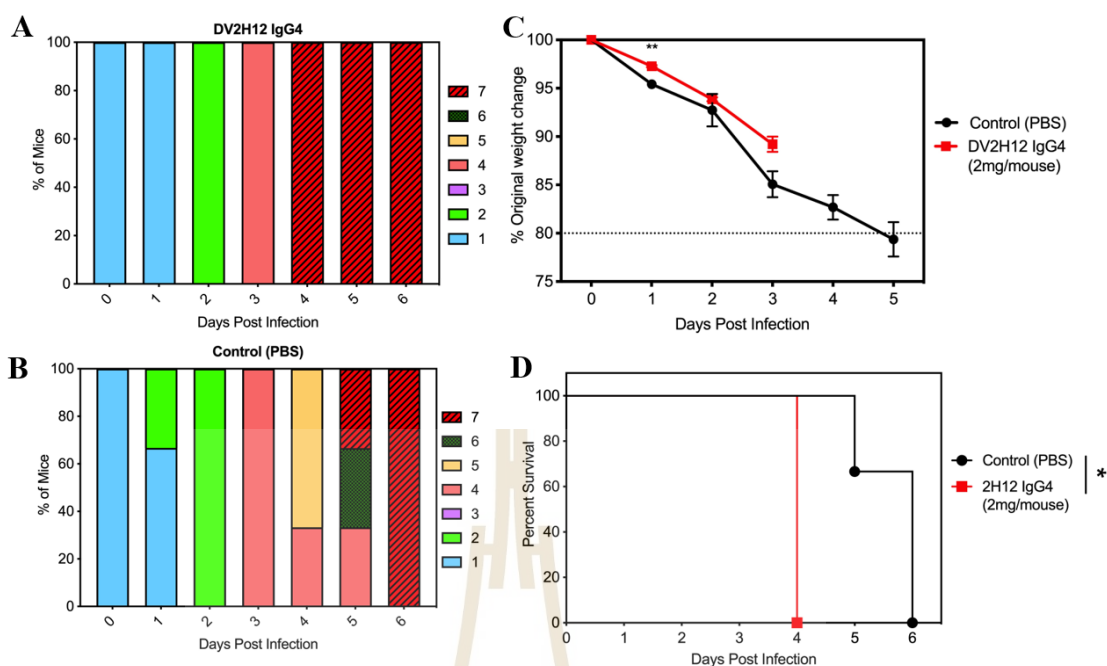
Figure 4.16 Prophylactic efficacy of human mAb DV2H12 IgG4 against DENV 2 infection in AG129 mice. Five weeks-old mice (N = 3) were administered 2 mg of mAb DV2H12 IgG4 or PBS (N = 3) followed by intravenous inoculation with 5×10^5 PFU of mouse-adapted DENV2 S221. PBS was administered as a negative control. Clinical scores of mice treated with mAb DV2H12 (A) or without mAb (B). Survival rate (D) and weight change (C) were determined in each group. Error bars represent standard error of the mean. Kaplan–Meier survival analysis with the Log-rank test was performed ($*p < 0.05$, $**p < 0.005$).
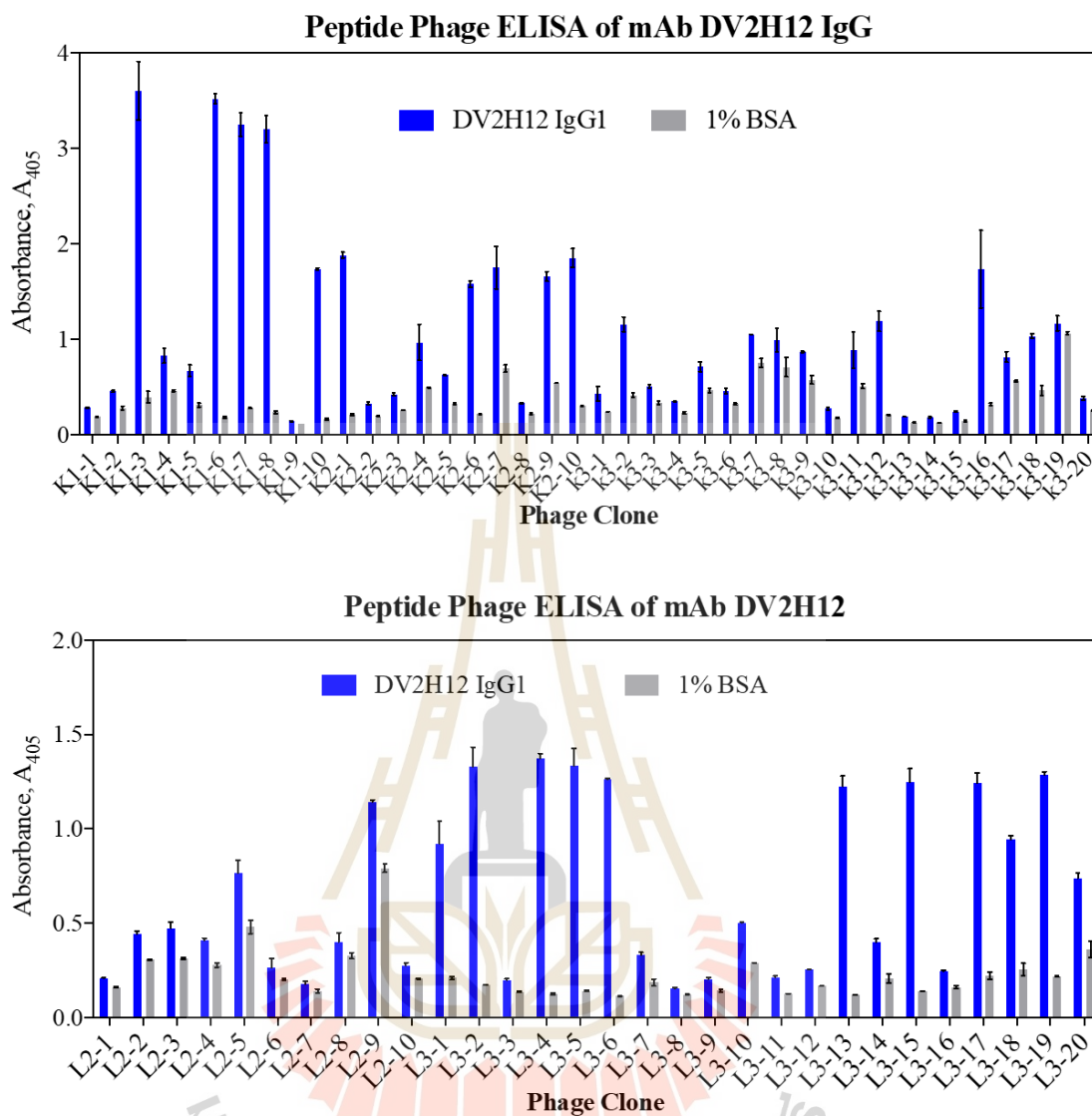
Figure 4.17 Selection for specific phage clones bound to mAb DV2H12. Twenty-two phage clones reacted strongly with DV2H12. After the third round of bio-panning, 22 phage clones from 70 selected phage clones showed significant reactivity to mAb DV2H12 but not to 1% BSA. Data are expressed as means of duplicated experiments. The error bars represent SD.

A
```
P5      ----------------DAHQWSVWGHHN----------------  12
P1      --------------GQEVWTVWGGEQ----------------  12
P3      ----------------GQQLWTVWGGEQ--------------  12
DV2prM  --------STSTWVTYGTWTTTGEHRREKRSVALVPHV------  30
P4      --------------PMHGSWTTMGWV----------------  12
P2      -----------------GCWTMWGPCERE-------------  12
P6      --------------------------RELVELANSWYR------  12
```

B
```
ZVprM    CNTTSTWVVYGTCHHKKGEARRSRRAVTLPSHSTRK-  36
DV4prM   CNLTSAWVMYGTCTQS-GERRREKRSVALTPHSGMGL  36
DV1prM   CNATDTWVTYGTCSQT-GEHRREKRSVALAPHVGLGL  36
DV3prM   CNLTSTWVTYGTCNQA-GEHRRDKRSVALAPHVGMGL  36
DV2prM   CNSTSTWVTYGTWTTT-GEHRREKRSVALVPHVGMGL  36
```

Figure 4.18 Alignment of amino acid of prM proteins of DENV1-4 and ZIKV with selected phage-displayed peptide. (A) The consensus sequence was compared with the primary amino acid sequence of the prM protein of DENV2. (B) The alignment of prM protein sequence from DENV1-4 and ZIKV.

Table 4.1 Primers for the construction of human scFv phage display library.

Primer	Sequence
V$_H$5'Sfi	1. 5' GCGGCCCAGCCGGCC**ATGGCCCAGGTGCAGCTGGTGCAGTCTGG** 3' 2. 5' GCGGCCCAGCCGGCC**ATGGCCGAGGTACAGCTGCAGCAGTCAGG** 3' 3. 5' GCGGCCCAGCCGGCC**ATGGCCCAGGTCAACTTAAGGGAGTCTGG** 3' 4. 5' GCGGCCCAGCCGGCC**ATGGCCGAGGTGCAGCTGGTGGAGTCTGG** 3' 5. 5' GCGGCCCAGCCGGCC**ATGGCCCAGGTGCAGCTGCAGGAGTCGGG** 3' 6. 5' GCGGCCCAGCCGGCC**ATGGCCGAGGTGCAGCTGTTGCAGTCTGC** 3'
V$_H$3'Linker	1. 5' ACCAGAGCCGCCGCCGCCGCTACCACCACCACC**TGAGGAGACGGTGACCAGGGTGCC** 3' 2. 5' ACCAGAGCCGCCGCCGCCGCTACCACCACCACC**TGAGGAGACGGTGACCGTGGTCCC** 3' 3. 5' ACCAGAGCCGCCGCCGCCGCTACCACCACCACC**TGAAGAGACGGTGACCATTGTCCC** 3' 4. 5' ACCAGAGCCGCCGCCGCCGCTACCACCACCACC**TGAGGAGACGGTGACCAGGGTTCC** 3'
V$_\lambda$5'Linker	1. 5' AGCGGCGGCGGCGGCTCTGGTGGTGGTGGATCC**AATTTTATGCTGACTCAGCCCCA** 3' 2. 5' AGCGGCGGCGGCGGCTCTG**GT**GGTGGTGGATCC**CAGTCTGTGTTGACGCAGCCGCC** 3' 3. 5' AGCGGCGGCGGCGGCTCTG**GT**GGTGGTGGATCC**CAGTCTGCCCTGACTCAGCCTGC** 3' 4. 5' AGCGGCGGCGGCGGCTCTG**GT**GGTGGTGGATCC**TCCTATGTGCTGACTCAGCCACC** 3' 5. 5' AGCGGCGGCGGCGGCTCTG**GT**GGTGGTGGATCC**TCTTCTGAGCTGACTCAGGACCC** 3' 6. 5' AGCGGCGGCGGCGGCTC**TGGTGG**TGGTGGATCC**CACGTTATACTGACTCAACCGCC** 3' 7. 5' AGCGGCGGCGGCGGCTC**TGGTGG**TGGTGGATCCC**CAGGCTGTGCTCACTCAGCCGTC** 3'
V$_\lambda$3'NotI	1. 5' CAGTCATTCTCGACTTGC**GGCCGC**ACCTAAAACGGTGAGCTGGGTCCC 3' 2. 5' CTCGACTTGCGGCCGCA**CCTAGGA**CGGTGACCTTGGTCCC 3' 3. 5' CTCGACTTGCGGCCGCA**CCTAGGA**CGGTCAGCTTGGTCCC 3'
V$_\kappa$5'Linker	1. 5' AGCGGCGGCGGCGGC**TC**TGGTGGT**GGT**GGATCC**GACATCCAGATGACCCAGTCTCC** 3' 2. 5' AGCGGCGGCGGCGGC**TC**TGGTGGT**GGT**GGATCC**GAAATTGTGCTGACTCAGTCTCC** 3' 3. 5' AGCGGCGGCGGCGG**GCTC**TGGTGGTGGT**GGATCC**GATGTTGTGATGACTCAGTCTCC** 3' 4. 5' AGCGGCGGCGGCGG**GCTC**TGGTGGTGG**GT**GGATCC**GAAATTGTGTTGACGCAGTCTCC** 3' 5. 5' AGCGGCGGCGGCGG**GCG**GCTCTGGTGGTGGTG**GA**TCC**GACATCGTGATGACCCAGTCTCC** 3' 6. 5' AGCGGCGGCGGCGG**GCG**GCTCTGGTGGTGGTG**GA**TCC**GAAACGACACTCACGCAGTCTCC** 3'
V$_\kappa$5'NotI	1. 5' CAGTCATTC**TCGA**CTTGCGGCCGC**ACGTTTGA**TTTCCAGCTTGGTCCC 3' 2. 5' CAGTCATTC**TCGA**CTTGCGGCCGC**ACGTTTAA**TCTCCAGTCGTGTCCC 3' 3. 5' CAGTCATT**CTCGA**CTTGC**GGCCGC**ACGTTTGA**TC**TCCAGCTTGGTCCC 3' 4. 5' CTCGAC**TT**GCGGCCGC**ACGTTTGA**TATCCACTT**TGGTCCC 3' 5. 5' CTCGA**C**TTGC**GGCCGC**ACGTTTGA**TCTCCACCTTGGTCCC 3'
Pull-Through-F	5' CCTTT**C**TATGC**GGCCC**AGCCGGCCATGGCC 3'
Pull-Through-R	5' CAGTC**ATT**CTCGACTTGC**GGCC**GCACG 3'

*Bold font indicates sequence complementary to the V-gene segments.

Table 4.2 Analysis of V-gene germline family

ScFv CLONE	V-GENE GERMLINE	GERMLINE IDENTITY (%)	VH-CDR3	V-GENE GERMLINE	GERMLINE IDENTITY (%)	VL-CDR3
	V_H			V_L		
1	IGHV4-61*07	81.28	ARAARPDNARKWGWLDP	IGLV1-44*01	94.74	AAWDDSLNGVV
2	IGHV3-7*01	94.44	ARGNSAAD	IGKV1-33*01	92.47	NHYSNWPRPMYT
3	IGHV4-61*06	92.49	VRYDQWLKLVRP	IGLV6-57*02	99.31	QSYDSTSMV
4	IGHV3-23*04	93.06	AKQGAASTVADPERIPLNV	IGKV2-28*01	98.98	MQPLQTPGT
5	IGHV1-8*01	97.92	ARGAPRGLVRGVITHYYYYGMDV	IGKV3-20*01	97.13	QQYGSSPKVT
6	IGHV4-31*03	100.00	ARGAWDFWSGYYTAFDY	IGKV1-16*02	89.96	QQYNFYPIT
7	IGHV1-24*01	90.62	ATGAVNNWFDP	IGLV5-45*03	95.75	MIWHSSAWV
8	IGHV4-61*01	94.85	ANLDISSTYNFNY	IGLV2-8*01	96.18	SAHGGSSKFYV
9	IGHV5-51*01	92.36	ARPPYPTSAVVGLGAFDL	IGLV6-57*01	92.78	QSFDNTNFYV
10	IGHV1-18*04	89.93	VRAARGTGGDY	IGKV2-30*01	97.28	MQGTYWPYT
11	IGHV6-1*01	99.66	ARVVVATGNNWFDP	IGKV3-20*01	92.20	QQYAASPLT
12	IGHV5-51*01	90.62	ARRQKVSQGGLNWGPGGGFDV	IGLV6-57*02	100.00	QSYDSSNVV
13	IGHV3-33*01	87.15	ARDWVRGGHYYGMDV	IGKV1-17*01	96.42	LQHNSYPYT
14	IGHV3-30*04	90.62	ASPGSTVTTFFD	IGKV1-39*01	96.42	QQSYGSPFG
15	IGHV3-74*02	94.44	TTVFEMWG	IGKV1-39*01	92.83	QQSYSIPRT
16	IGHV2-26*01	98.63	ARESSGWYYYYYGMDV	IGLV6-57*01	95.88	QSYDSSNHG
17	IGHV1-69*09	99.65	ALISSGYDGDWFDP	IGLV2-14*02	97.57	SSYTTTTV
18	IGHV3-23*04	99.65	AKSAARNFDY	IGLV2-23*01	92.78	AHMQVGHM
19	IGHV3-33*01	91.32	ARDHMMTFGGVIVPDAYEV	IGKV3-20*01	98.58	QQYGSS
20	IGHV3-11*01	85.42	ARIGRIEGSYNYYAMDV	IGKV3-11*01	88.17	QQRSDWLT
21	IGHV3-23*03	88.89	ARGSVGTTPDTGDP	IGLV5-45*02	98.69	MIWHSSAWV
22	IGHV6-1*01	82.49	AKGGIGTTVSLFHS	IGKV3-15*01	92.11	QQYNNWPPLT

Table 4.3 Result of affinity selections with different targets

Antigens	Round of panning	Number of clone after 1st round	Number of scFv producing clones	Number of different scFv producing clones
DENV2	1	6×10^2	17	9
ZIKV	3	4×10^3	25	5

Table 4.4 Genetic analysis of the variable region of selected scFv antibodies

SCFV CLONE	FREQUENCY (CLONE)	V-GENE GERMLINE	GERMLINE IDENTITY (%)	D GENE	J GENE	VH-CDR3	V-GENE GERMLINE	GERMLINE IDENTITY (%)	J GENE	VL-CDR3
DENV2		V_H					V_L			
DV2H12	5	IGHV3-66*01	98.95	D2-2*01	J5*02	ARERFCSSTSCYAGGNWFDP	IGLV6-57*02	100	J2*01	QSYDSSTVV
DV2E11	2	IGHV3-23*01	98.26	D3-22*01	J3*02	AKGWGYYDSSGPSGAFDI	IGLV1-47*02	98.60	J3*02	AAWDDSLSGWV
DV2D2	2	IGHV1-69*09	98.96	D1-26*01	J3*02	ASNSGSYGGHDAFDI	IGLV3-21*01	92.83	J1*01	QVWDSITDHYV
DV2B3	2	IGHV1-69*01	95.14	D3-10*01	J4*02	ATYYYGSGSSPFDY	IGLV3-19*01	98.92	J3*02	NSRDSSINQWV
DV2A3	1	IGHV1-69*01	99.31	D6-24*01	J4*02	ATTGYSSSHPYYFDY	IGLV3-21*01	98.21	J2*01	QVWDSRSDHVV
DV2E2	1	IGHV5-10*01	93.40	D1-14*01	J3*01	ARLGSSRINGMDV	IGLV6-57*02	92.78	J2*01	QSYDSTNEAAV
DV2B1	1	IGHV1-69*04	98.61	D4-17*01	J4*02	AREDGYYSFDY	IGKV3-11*01	98.92	J5*01	QQRSNWQIT
DV2A2	1	IGHV3-66*01	99.30	D6-13*01	J4*02	ASVSSSWGDLDY	IGKV3-20*01	99.65	J1*01	QQYGSSPRT
DV2D12	1	IGHV1-69*01	98.26	D3-10*01	J5*02	ARGSMVRGPINSLFDP	IGKV3-20*01	100	J4*01	QQYGSSLLT
ZIKV		V_H					V_L			
ZV1B7	12	IGHV3-23*01	88.89	D7-27*01	J4*02	AKDQRPRSLTRGPAFNYSFDL	IGLV2-14*02	97.57	J1*01	SSYTTTTV
ZV1H5	3	IGHV6-1*01	98.65	D3-10*01	J6*02	ARGGSGSYPYYYYYGMDV	IGLV6-57*02	97.25	J3*02	QSYDSSNQGV
ZV1B10	3	IGHV3-23*04	95.83	D2-21*01	J3*01	AKEGMPNGAFDV	IGLV3-10*01	87.81	J2*01	YSTDMTENERV
ZV1F8	1	IGHV3-64D*06	99.31	D5-18*01	J4*03	VKGGYSPEDY	IGLV3-21*02	92.47	J1*01	QVGDTHSDQYV
ZV1C11	1	IGHV1-69*01	97.92	D2-15*01	J6*02	ASGVQEAGYCSGGSCYRMDV	IGLV6-57*02	96.22	J2*01	QSYDGDNVV

Table 4.5 Primers for construction of IgG vector

Primer	Clone	Sequence
IgG-HC-F	DV2H12	5'-CCTGGTATTCTTTCGCAGGTGCAGCTGGTGCAGTCTGG-3'
	DV2D2	5'-CCTGGTATTCTTTCGGAGGTGCAGCTGGTGGAGTCTGG-3'
	ZV1B10	5'-CCTGGTATTCTTTCGGaGGTGCAGCTGGTGGAGTCTG-3'
IgG1-HC-R	DV2H12	5'-GATGGGCCCTTGGTGCTAGCTGAGGAGACGGTGACCAGGGTGCCCT-3'
	ZV1B10	5'-GATGGGCCCTTGGTGCTAGcTGAAGAGACGGTGACCATTGTCCC-3'
IgG4-HC-R	DV2H12	5'-GATGGGCCCCTTGGTGCTAGCTGAGGAGACGGTGACCAGGGTGCCCT-3'
	DV2D2	5'-GATGGGCCCCTTGGTGCTAGCCAAGGGACAATGGTCACCGTCTCTTC-3'
	ZV1B10	5'-GATGGGGCCCCTTGGTGCTAGCTGAAGAGACGGTGACCATTGTCCC-3'
IgG-LC-F	DV2H12	5'-ATAATGTCCAGAGGCAATTTTATGCTGACTCAGCCCCACTC-3'
	DV2D2	5'-ATAATGTCCAGAGGCTCCTATGTGCTGACTCAGCCACCCTC-3'
	ZV1B10	5'-ATAATGTCCAGAGGCTCCTATGTGCTGACTCAGCCACCCT-3'
IgG-LC-R	DV2H12	5'-CAGCCTTGGGCTGACCAAGGACGGTCAGCTTGGTCCCTCC-3'
	DV2D2	5'-CAGCCTTGGGCTGACCaAgAACGGTGAGCTGGGTCCCAGGTC-3'
	ZV1B10	5'-CAGCCTTGGGCTGACCaAgGACGGTCAGCTTGGTCCCTCC-3'

Table 4.6 Production yield of antibody expression

Ab Name	Species	Isotype	Expression volume (mL)	Concentration (µg/mL)	Yield (mg)	Endotoxin Results
DV2H12	human	IgG1-Lambda	100	2,640	10.56	<0.389 EU/mg
DV2H12	human	IgG4-Lambda	100	5,230	15.69	<0.191 EU/mg
DV2D2	human	IgG4-Lambda	50	980	10.50	<0.191 EU/mg
ZV1B10	human	IgG1-Lambda	100	2,595	18.17	<0.010 EU/mg
ZV1B10	human	IgG4-Lambda	100	2,140	12.80	<0.100 EU/mg

Table 4.7 Clinical score for mice study.

SCORE	DESCRIPTION	APPEARANCE	MOBILITY	ATTITUDE
1	Healthy	Smooth Coat. Bright Eyes.	Active, Scurrying, Burrowing	Alert
2	Slightly Ruffled	Slightly Ruffled coat (usually only around head and neck)	Active, Scurrying, Burrowing	Alert
3	Ruffled	Ruffled Coat throughout body. A "wet" appearance.	Active, Scurrying, Burrowing	Alert
4	Sick	Very Ruffled coat. Slightly closed, inset eyes.	Walking, but no scurrying.	Mildly Lethargic
5	Very Sick	Very Ruffled Coat. Closed, inset eyes.	Slow to no movement. Will return to upright position if put on its side.	Extremely Lethargic
6	Euthanize	Very ruffled Coat. Closed, inset eyes. Moribund requiring humane euthanasia.	No movement or Uncontrollable, spastic movements. Will NOT return to upright position if put on its side.	Completely Unaware or in Noticeable Distress
7	Deceased	---	---	---

Table 4.8 Nucleotide and peptide sequence of epitope mapping

Clone	Nucleotide sequence	Protein sequence
K1_6	GGGCAGGAGGTGTGGACGGTGTGGGGGGGGGAGCAG	GQEVWTVWGGEQ
K2_1	GGGCAGGAGGTGTGGACGGTGTGGGGGGGGGAGCAG	GQEVWTVWGGEQ
K2_7	GGGCAGGAGGTGTGGACGGTGTGGGGGGGGGAGCAG	GQEVWTVWGGEQ
K2_10	GGGCAGGAGGTGTGGACGGTGTGGGGGGGGGAGCAG	GQEVWTVWGGEQ
L3_4	GGGCAGGAGGTGTGGACGGTGTGGGGGGGGGAGCAG	GQEVWTVWGGEQ
L3_5	GGGCAGGAGGTGTGGACGGTGTGGGGGGGGGAGCAG	GQEVWTVWGGEQ
L3_6	GGGCAGGAGGTGTGGACGGTGTGGGGGGGGGAGCAG	GQEVWTVWGGEQ
L3_13	GGGCAGGAGGTGTGGACGGTGTGGGGGGGGGAGCAG	GQEVWTVWGGEQ
L3_15	GGGCAGGAGGTGTGGACGGTGTGGGGGGGGGAGCAG	GQEVWTVWGGEQ
K2_6	GGGCAGCAGCTGTGGACGGTGTGGGGGGGGGAGCAG	GQQLWTVWGGEQ
K1_7	GGGTGTTGGACGATGTGGGGTCCTTGTGAGCGGGAG	GCWTMWGPCERE
K2_9	GGGTGTTGGACGATGTGGGGTCCTTGTGAGCGGGAG	GCWTMWGPCERE
L3_2	GGGTGTTGGACGATGTGGGGTCCTTGTGAGCGGGAG	GCWTMWGPCERE
L3_17	GGGTGTTGGACGATGTGGGGTCCTTGTGAGCGGGAG	GCWTMWGPCERE
L3_19	GGGTGTTGGACGATGTGGGGTCCTTGTGAGCGGGAG	GCWTMWGPCERE
K1_8	CGGGAGCTTGTGGAGCTGGCGAATTCTTGGTATCGG	RELVELANSWYR
K3_12	CGGGAGCTTGTGGAGCTGGCGAATTCTTGGTATCGG	RELVELANSWYR
K1_3	CCTTTGCGTGATTATGGTTTTAAGATGTGGGCTGTT	PLRDYGFKMWAV
K3_18	CCTTTGCGTGATTATGGTTTTAAGATGTGGGCTGTT	PLRDYGFKMWAV
K3_2	CTGTTGGAGCTGGCGGGTAGTCATTATCAGAGGAAG	LLELAGSHYQRK
L3_1	CCTATGCATGGGAGTTGGACTACTATGGGGTGGGTT	PMHGSWTTMGWV
L3_18	GATGCTCATCAGTGGTCTGTGTGGGGTCATCATAAT	DAHQWSVWGHHN

Table 4.9 Amino acid sequences of linear peptide

Peptide	Frequency (No. of clones)	Peptide sequence
P 1	9	-GQEV**WTV WG**GEQ--
P 2	5	---GC**WT**M**WG**PCERE
P 3	1	-GQQL**WTV WG**GEQ--
P 4	1	PMHGS**WT**TM**G**WV---
P 5	1	-DAHQ**W**SV**WG**HHN--
Consensus		**WT/S-W/MG**

*Phage-displayed consensus amino acids are shown in bold.

4.7 References

Avnir, Y., Watson, C. T., Glanville, J., Peterson, E. C., Tallarico, A. S., Bennett, A. S.,Marasco, W. A. (2016). IGHV1-69 polymorphism modulates anti-influenza antibody repertoires, correlates with IGHV utilization shifts and varies by ethnicity. **Scientific Reports**, 6(1), 20842.

Bhatt, S., Gething, P. W., Brady, O. J., Messina, J. P., Farlow, A. W., Moyes, C. L., Hay, S. I. (2013). The global distribution and burden of dengue. **Nature**, 496(7446), 504-507.

Bhaumik, S. K., Priyamvada, L., Kauffman, R. C., Lai, L., Natrajan, M. S., Cho, A., Wrammert, J. (2018). Pre-existing dengue immunity drives a DENV-biased plasmablast response in ZIKV-infected patient. **Viruses**, 11(1), 19.

Bruhns, P., Iannascoli, B., England, P., Mancardi, D. A., Fernandez, N., Jorieux, S., & Daëron, M. (2009). Specificity and affinity of human Fcγ receptors and their polymorphic variants for human IgG subclasses. **Blood**, 113(16), 3716-3725.

Dejnirattisai, W., Jumnainsong, A., Onsirisakul, N., Fitton, P., Vasanawathana, S., Limpitikul, W., Screaton, G. (2010). Cross-reacting antibodies enhance dengue virus infection in humans. **Science**, 328(5979), 745-748.

Dejnirattisai, W., Wongwiwat, W., Supasa, S., Zhang, X., Dai, X., Rouvinski, A., Screaton, G. R. (2015b). A new class of highly potent, broadly neutralizing antibodies isolated from viremic patients infected with dengue virus. **Nature Immunology**, 16(2), 170-177.

Elong Ngono, A., Young, M. P., Bunz, M., Xu, Z., Hattakam, S., Vizcarra, E., Shresta, S. (2019). CD4+ T cells promote humoral immunity and viral control during Zika virus infection. **PLoS Pathogens**, 15(1), e1007474.

Fatima, A., Wang, H., Kang, K., Xia, L., Wang, Y., Ye, W. Wang, X. (2014). Development of VHH antibodies against dengue virus type 2 NS1 and comparison with monoclonal antibodies for use in immunological diagnosis. **PloS one**, 9(4), e95263.

Gao, F., Lin, X., He, L., Wang, R., Wang, H., Shi, X., Yu, L. (2019). Development of a potent and protective germline-like antibody lineage against Zika virus in a convalescent human. **bioRxiv**, 661918.

Hu, D., Zhu, Z., Li, S., Deng, Y., Wu, Y., Zhang, N., Ying, T. (2019). A broadly neutralizing germline-like human monoclonal antibody against dengue virus envelope domain III. **PLoS Pathogens**, 15(6), e1007836.

Jensen, S. M., Nguyen, C. T., & Jewett, J. C. (2016). A gradient-free method for the purification of infective dengue virus for protein-level investigations. **Journal of Virological Methods**, 235, 125-130.

Kyle, J. L., & Harris, E. (2008). Global Spread and Persistence of Dengue. **Annual Review of Microbiology**, 62(1), 71-92.

Li, L., Meng, W., Horton, M., DiStefano, D. R., Thoryk, E. A., Pfaff, J. M., Zhang, N. (2019). Potent neutralizing antibodies elicited by dengue vaccine in rhesus macaque target diverse epitopes. **PLoS Pathogens**, 15(6), e1007716-e1007716.

Lingwood, D., McTamney, P. M., Yassine, H. M., Whittle, J. R. R., Guo, X., Boyington, J. C., Nabel, G. J. (2012). Structural and genetic basis for development of broadly neutralizing influenza antibodies. **Nature**, 489(7417), 566-570.

Luo, Y.-Y., Feng, J.-J., Zhou, J.-M., Yu, Z.-Z., Fang, D.-Y., Yan, H.-J., Jiang, L.-F. (2013). Identification of a novel infection-enhancing epitope on dengue prM

using a dengue cross-reacting monoclonal antibody. **BMC microbiology**, 13, 194-194.

Pansri, P., Jaruseranee, N., Rangnoi, K., Kristensen, P., & Yamabhai, M. (2009). A compact phage display human scFv library for selection of antibodies to a wide variety of antigens. **BMC biotechnology**, 9, 6-6.

Priyamvada, L., Quicke, K. M., Hudson, W. H., Onlamoon, N., Sewatanon, J., Edupuganti, S., Wrammert, J. (2016). Human antibody responses after dengue virus infection are highly cross-reactive to Zika virus. **Proceedings of the National Academy of Sciences of the United States of America**, 113(28), 7852-7857.

Rey, F. A., Stiasny, K., Vaney, M.-C., Dellarole, M., & Heinz, F. X. (2018). The bright and the dark side of human antibody responses to flaviviruses: lessons for vaccine design. **EMBO reports**, 19(2), 206-224.

Saokaew, N., Poungpair, O., Panya, A., Tarasuk, M., Sawasdee, N., Limjindaporn, T., Yenchitsomanus, P. (2014). Human monoclonal single-chain antibodies specific to dengue virus envelope protein. **Letters in Applied Microbiology**, 58(3), 270-277.

Sapparapu, G., Fernandez, E., Kose, N., Bin, C., Fox, J. M., Bombardi, R. G., Crowe, J. E. (2016). Neutralizing human antibodies prevent Zika virus replication and fetal disease in mice. **Nature**, 540(7633), 443-447.

Smith, S. A., Nivarthi, U. K., de Alwis, R., Kose, N., Sapparapu, G., Bombardi, R., Crowe, J. E. (2016). Dengue virus prM-specific human monoclonal antibodies with virus replication-enhancing properties recognize a single immunodominant antigenic site. **Journal of Virology**, 90(2), 780.

Wirawan, M., Fibriansah, G., Marzinek, J. K., Lim, X. X., Ng, T.-S., Sim, A. Y. L., Lok, S.-M. (2019). Mechanism of enhanced immature dengue virus attachment to endosomal membrane induced by prM antibody. **Structure,** 27(2), 253-267.e258.

Wu, Y., Li, S., Du, L., Wang, C., Zou, P., Hong, B., Ying, T. (2017). Neutralization of Zika virus by germline-like human monoclonal antibodies targeting cryptic epitopes on envelope domain III. **Emerging Microbes & Infections**, 6(1), 1-11.

Zybert, I. A., van der Ende-Metselaar, H., Wilschut, J., & Smit, J. M. (2008). Functional importance of dengue virus maturation: infectious properties of immature virions. **Journal of General Virology**, 89(12), 3047-3051.
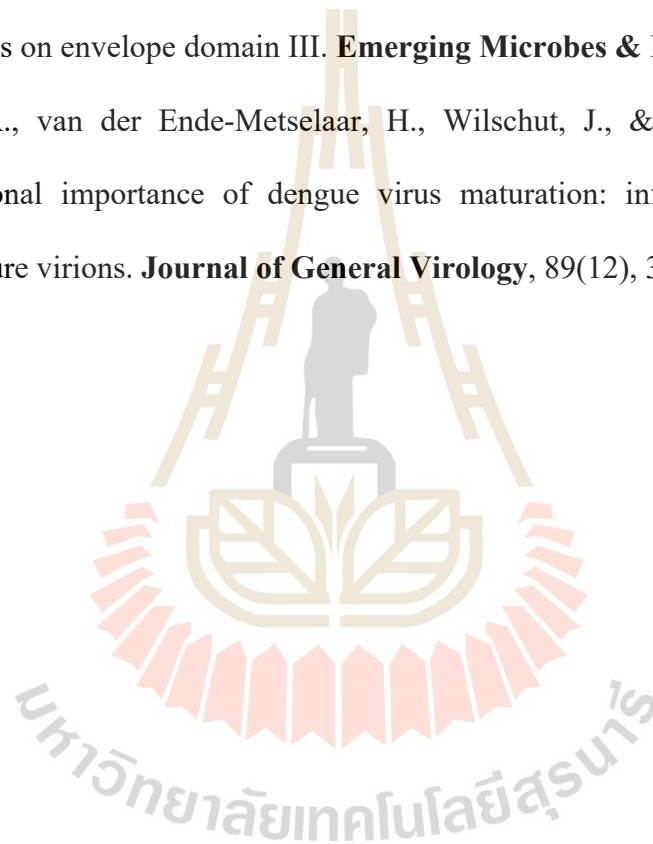
CHAPTER V

CD4+ T CELLS PROMOTE HUMORAL IMMUNITY AND VIRAL CONTROL DURING ZIKA VIRUS INFECTION

5.1 Abstract

Several Zika virus (ZIKV) vaccines designed to elicit protective antibody (Ab) responses are currently under rapid development, but the underlying mechanisms that control the magnitude and quality of the Ab response remain unclear. Here, we investigated the CD4+ T cell response to primary intravenous and intravaginal infection with ZIKV. Using the *LysMCre+If nar1$^{fl/fl}$* (myeloid type I IFN receptor-deficient) C57BL/6 mouse models, we identified six I-A^b-restricted ZIKV epitopes that stimulated CD4+ T cells with a predominantly cytotoxic Th1 phenotype in mice primed with ZIKV. Intravenous and intravaginal infection with ZIKV effectively induced follicular helper and regulatory CD4+ T cells. Treatment of mice with a CD4+ T cell-depleting Ab reduced the plasma cell, germinal center B cell, and IgG responses to ZIKV without affecting the CD8+ T cell response. CD4+ T cells were required to protect mice from a lethal dose of ZIKV after infection intravaginally, but not intravenously. However, adoptive transfer and peptide immunization experiments showed a role for memory CD4+ T cells in ZIKV clearance in mice challenged intravenously. These results demonstrate that CD4+ T cells are required mainly for the generation of a ZIKV-specific humoral response but not for an efficient CD8+ T cell

response. Thus, CD4$^+$ T cells could be important mediators of protection against ZIKV, depending on the infection or vaccination context.

5.2 Introduction

Research on the immune response to infection with Zika virus (ZIKV), a member of the *Flaviviridae* family that includes dengue virus (DENV), yellow fever virus (YFV), and West Nile virus (WNV), has intensified since the most recent outbreak in 2015 in Brazil. Many flavivirus infections are transmitted through the bite of infected mosquitoes. However, ZIKV shows some critical features in its transmission routes and clinical outcomes. ZIKV can be transmit- ted via sexual contact (D'Ortenzio et al., 2016), persists for weeks in the reproductive tract (Ma et al., 2016; Tang et al., 2016), and undergoes vertical transmission from mother to fetus (Miner et al., 2016; Yockey et al., 2016). ZIKV infection of pregnant women has been associated with an increased incidence of congenital disorders in fetuses, including microcephaly (Rasmussen, Jamieson, Honein, & Petersen, 2016), whereas ZIKV infection of adults is linked to the neurological disorder Guillain-Barré syndrome (Cao-Lormeau et al., 2016). Given the range of clinical symptoms, there is a pressing need to understand how different transmission routes affect the immune response to ZIKV infection.

Accumulating evidence suggests that both cellular and humoral responses are required for effective control of ZIKV (Ngono & Shresta, 2018). Infection with ZIKV induces the production of neutralizing antibodies (Abs), as evidenced by a study of two independent patient cohorts from Brazil and Mexico, where ZIKV is endemic (Robbiani et al., 2017). In rhesus macaques, primary ZIKV infection induces

neutralizing Abs that may be important for control of viral replication (Dudley et al., 2016), and the production of neutralizing Abs correlates with protection against secondary ZIKV infection (Aliota et al., 2016). Several groups have demonstrated in mouse models that protection against ZIKV can be conferred by a variety of monoclonal Abs, including DENV/ZIKV-cross-reactive Abs, and by vaccine-induced Ab responses (Dowd et al., 2016; Larocca et al., 2016; Stettler et al., 2016). Compared with the humoral response, relatively little is known about the cellular immune response to ZIKV, especially CD4$^+$ T cell responses. We and others recently identified an important role for CD8$^+$ T cells in controlling ZIKV infection using H-2^b mouse models (Elong Ngono et al., 2017; Huang et al., 2017). In H-2^b mice, CD8$^+$ T cells targeted peptides from all ZIKV proteins (three structural proteins [Capsid, Pre-membrane, Envelope] and seven nonstructural proteins [NS1, NS2A, NS2B, NS3, NS4A, NS4B, NS5]), with a preference for the structural proteins (Elong Ngono et al., 2017). In addition, DENV/ZIKV cross-reactive CD8$^+$ T cells played an important role in protecting against ZIKV in peptide vaccination and sequential DENV-ZIKV infection settings in various mice, including HLA transgenic and pregnant animals (Wen, Elong Ngono, et al., 2017; Wen, Tang, et al., 2017).

Studies of mouse models of flaviviral infection, including WNV (Brien, Uhrlaub, & Nikolich-Zugich, 2008), DENV (Yauch et al., 2010), and YFV 17D (Liu & Chambers, 2001), have suggested that CD4$^+$ T cells, particularly Th1 subsets, contribute to protection against infection. Accordingly, Pardy and colleagues revealed that CD4$^+$ T cells responding to ZIKV infection in wildtype mice were also predominantly of a Th1 phenotype, although the response to isolated ZIKV peptides was not investigated in this study (Pardy et al., 2017). In another report, Winkler and

colleagues detected proliferation of CD4$^+$ T cells in response to ZIKV infection of wildtype mice (Winkler et al., 2017). However, the role of CD4$^+$ T cells in generating efficient anti-ZIKV humoral and cellular responses and in mediating protection remains unclear, as does the extent to which CD4$^+$ T cell subsets, such as follicular helper T (T$_{FH}$) cells and regulatory T (T$_{reg}$) cells, are involved in the response. Because a variety of ZIKV vaccine candidates are under accelerated development, it is important to understand the precise contribution of CD4$^+$ T cells to protection against ZIKV and to determine whether ZIKV vaccine designs should optimize CD4$^+$ T cell responses.

In this study, we investigated the role of CD4$^+$ T cells in the response to primary ZIKV infection via systemic (intravenous) and sexually transmitted (intravaginal) routes using *LysMCre$^+$Ifnar1$^{fl/fl}$* and *Ifnar1$^{-/-}$* C57BL/6 mice, as we described previously for investigation of the CD8$^+$ T cell response to ZIKV. We evaluated the immune response via the two infection routes with respect to: the immunodominant H-2-restricted ZIKV epitopes, the quality and kinetics of activation of CD4$^+$ T cell subsets, the requirement for CD4$^+$ T cells in inducing ZIKV-specific Ab and CD8$^+$ T cell responses, and the impact on viral clearance. We found that the CD4$^+$ T cell response to primary infection was predominantly Th1 and was directed against a narrow range of immunodominant ZIKV epitopes in E, NS3, NS4B, and NS5 proteins. Notably, CD4$^+$ T cells contributed to the ZIKV-specific plasma cell, germinal center (GC) B cell, and IgG responses after both intravenous and intravaginal infection. However, CD4$^+$ T cells were required for local control of viral infection in the lower female reproductive tract and for protection against lethal intravaginal ZIKV infection. Additionally, memory CD4$^+$ T cells contributed to viral

clearance in mice after primary, but not secondary, intravenous ZIKV infection. Our data suggest that efficient ZIKV vaccines should promote CD4$^+$ T cell activation.

5.3 Material & Methods

5.3.1 Ethics statement

All experiments were performed in strict accordance with recommendations set forth in the National Institutes of Health Guide for the Care and Use of Laboratory Animals and approved by the Institutional Animal Care and Use Committee at the La Jolla Institute for Allergy and Immunology (protocol number APO28-SS1-0615 and AP00001029). Both ZIKV strains (MR766 and FSS13025) were obtained from the World Reference Center for Emerging Viruses and Arboviruses with Institutional Review Board approval. All samples were anonymized.

5.3.2 Mouse experiments

LysMCre$^+$Ifnar1$^{fl/fl}$ and *Ifnar1$^{-/-}$* mice were bred under pathogen-free conditions at La Jolla Institute for Allergy & Immunology. Sample sizes were based on similar studies (Elong Ngono et al., 2017). None of the experiments were randomized or blinded.

5.3.3 Virus culture and titration

Asian lineage strain FSS13025 was isolated from a 3-year-old boy in Cambodia in 2010 (Heang et al., 2012), and African lineage strain MR766 was isolated from a sentinel rhesus monkey in Uganda in 1947 (Dick, 1952). Both viruses were cultured in C6/36 Aedes albopictus mosquito cells (American Type Culture Collection [ATCC]; Manassas, Virginia). Viral supernatants were collected 7–10 days after infection, clarified by centrifugation, and concentrated by ultracentrifugation.

Viral titers were measured using a baby hamster kidney (BHK)-21 (ATCC) cell-based focus-forming assay (FFA). In brief, BHK-21 cells were plated at 2×10^5 cells per well in a 24-well plate and incubated overnight in complete MEM-α medium (containing 10% fetal bovine serum [FBS], 1% penicillin/ streptomycin, and 1% HEPES) at 37℃ in a 5% CO_2 atmosphere. Cells were infected with serial dilutions of virus for 1.5 h with gentle shaking every 15 min. The medium was then aspirated and replaced with fresh complete MEM-α medium supplemented with 1% carboxymethyl cellulose (Sigma), and the cells were cultured for 2 days. Cells were then fixed with 4% formalin (Fisher), permeabilized with 1% Triton X-100 (Sigma) and blocked by addition of 10% FBS in phosphate-buffered saline (PBS). ZIKV was detected by incubation of cells with 4G2, a pan-flavivirus E protein-specific monoclonal Ab (BioXcell) for 1.5 h. Cells were washed and incubated for 1.5 h with horseradish peroxidase (HRP)-conjugated goat anti- mouse IgG (Sigma). Finally, foci were detected by incubation with True Blue substrate (KPL) and counted manually. Viral titers were expressed as log FFU/g tissue or log FFU/ml serum. Next-generation sequencing of viral stocks confirmed the absence of competing pathogens.

5.3.4 Peptide prediction and synthesis

ZIKV MR766 and FSS13025 sequences were obtained from the NCBI protein database. MHC class II peptide binding affinity predictions were performed using the Immune Epitope Database (www.iedb.org) website tools using the "IEDB-recommended" method selection, as previously described (Kim et al., 2012). Predicted binding affinities were obtained for all non-redundant 15-mer peptides that bound H-2 I-Ab, and the peptide list was sorted by increasing consensus percentile rank and restricted to the top 1%. Peptides were synthesized by Synthetic Biomolecules as

crude material (1 mg scale) and validated by mass spectrometry. Peptides for in vitro stimulation followed by flow cytometric analyses were synthesized and purified by reverse-phase high performance liquid chromatography to 95% purity. Peptides were dissolved in DMSO for use.

5.3.5 Mouse infection

LysMCre[+]*Ifnar1*^{fl/fl} and *Ifnar1*^{−/−} mice (5- to 6-week-old males and females for RO and intra- footpad infection; 8- to 9-week-old females for IVag infection) were infected with ZIKV FSS13025 or MR766 at 10^1, 10^2, 10^3, 10^4, or 10^5 FFU RO, 10^5 or 10^6 FFU IVag, and 105 FFU via intrafootpad route in 10% FBS/PBS. Three days prior to IVag infection, mice were injected subcutaneously with 2 mg of progesterone (Millipore Sigma) in 100 μl of 5% ethanol, 5% Kolliphor, and 90% H_2O to induce a diestrus-like phase, which was confirmed as previously described (Tang et al., 2016).

5.3.6 CD8^{+} and CD4^{+} T cell depletion

T cell depletion Abs (CD8^{+} T cell-depleting clone 2.43 or CD4^{+} T cell-depleting clone GK1.5) were purchased from BioXCell and administered on days −3 and −1 pre-infection and every 2 days post-infection for the duration of the experiment. For long-term (30 day) depletion, mice were treated on days −3 and −1 and weekly thereafter until the end of the experiment. A rat IgG2 isotype control Ab (clone LTF-2) served as the control and was administered on days −3 and −1 pre-infection only.

5.3.7 Adoptive T cell transfer

CD4^{+} T cells were isolated from donor mice 34 days after infection with 104 FFU of ZIKV FSS13025. Spleens were harvested, and CD4+ T cells were positively selected using a CD4 T Cell Isolation Kit (Miltenyi Biotec). A total of 1 ×

10^7 or 1.5×10^7 purified CD4$^+$ T cells were then injected RO into the recipient mice 1 day prior to ZIKV infection. CD4$^+$ T cells purified from naïve *LysMCre$^+$Ifnar1$^{fl/fl}$* mouse spleens were harvested and injected into recipient mice as controls.

5.3.8 Tissue collection

For preparation of serum samples, mice were sacrificed by CO_2 inhalation and blood was collected by cardiac puncture. For vaginal washes, the vaginal canal was rinsed 3–5 times with 40 µl PBS and the washes were combined. Mice were then perfused with PBS and the desired organs were collected. For tissue FFA, organs were transferred to pre-weighed tubes contain- ing complete MEM-α medium and a metal bead, and the tubes were then stored at $-80\,℃$ until analyzed. For qRT-PCR, organs were stored in RNAlater (Invitrogen) at $4\,℃$ until analyzed.

5.3.9 Quantification of virus in tissues

For the FFA, pre-weighed tubes containing frozen organs were thawed, homogenized (Tissue-lyser II; Qiagen), and centrifuged. The supernatant was serially diluted, added to BHK-21 cells, and the titers were determined as described above. Titers were expressed as the log FFU/g of tissue. For qRT-PCR, RNA was isolated from tissues using an RNeasy Mini Kit (Qiagen) or from serum or vaginal washes using a Viral RNA Isolation Kit (Qiagen). qRT-PCR was per- formed using a qScript One-Step qRT-PCR Kit (Quanta, Bioscience) with a CFX96 TouchTM real-time PCR detection system (Bio-Rad CFX Manager 3.1). ZIKV-specific primers have been previously described. Cycling conditions were: $45\,℃$ for 15 min, $95\,℃$ for 15 min, followed by 50 cycles of $95\,℃$ for 15 s and $60\,℃$ for 15 s, and a final extension of $72\,℃$ for 30 min. Viral RNA concentration was calculated using a standard curve composed

of five 100-fold serial dilutions of in vitro-transcribed RNA from ZIKV strain FSS13025.

5.3.10 ZIKV-binding IgG/IgM ELISA

ELISA plates (96-well, Costar) were coated with ZIKV E protein (1 µg/ml, ZIKVSU-ENV, Native Antigen) in coating buffer (0.1 M NaHCO$_3$) overnight at 4℃ and then blocked for 1 h at room temperature (RT) with 5% Blocker Casein in PBS (Thermo Fisher Scientific). Mouse serum samples were diluted three-fold (from 1:30 to 1:65,610) in 1% bovine serum albumin (BSA)/PBS, added to the coated wells, and incubated for 1.5 h at RT. Wells were then washed with wash buffer (0.05% Tween 20 [Promega] in PBS), and HRP-conjugated goat anti-mouse IgG Fc or goat anti-mouse IgM (1:5000 in 1% BSA/PBS) was added to each well for 1.5 h at RT. TMB chromogen solution (eBioscience) was added to the wells, the reaction was stopped by addition of sulfuric acid, and the absorbance at 450 nm was read on a Spectramax M2E microplate reader (Molecular Devices). The ZIKV-specific Ab endpoint titers were calculated as the reciprocal of the highest serum dilution that gave a reading twice the cutoff absorbance based on the negative control (BSA/PBS).

5.3.11 Serum neutralization assay

Sera from naïve and ZIKV-immune mice were inactivated by incubation for 30 min at 56℃ and then serially diluted and added to 96-well round-bottom plates. Some sera were incubated for 30 min with dithiothreitol (0.01 M, Sigma) prior to infection to inactivate IgM. A sufficient amount of ZIKV FSS13025 causing 7-15% of infection in U937 DC-SIGN, was added to the sera and incubated for 1 h at 37℃ (titration of virus is determined for each batch of cells). U937 cells expressing dendritic cell-specific intracellular adhesion molecule-3-grabbing non-integrin (U937

DC-SIGN, ATCC) were then added at 1 x 105 cells/well and the plates were incubated for 2 h at 37℃ with rocking every 15 min. Cells and ZIKV FSS13025 incubated in the absence of serum served as the positive control. Plates were then centrifuged, the supernatants were aspirated, fresh RPMI medium supplemented with 10% FBS was added, and the cells were incubated for 16 h at 37℃. Finally, cells were harvested, stained with PE-conjugated anti-CD209 (DC-SIGN, clone DNC246), incubated with Cytofix/Cytoperm solution (BD Biosciences), and stained intracellularly with Alexa Fluor 647-conjugated 4G2 (to ZIKV E pro- tein). The cells were analyzed on an LSRII flow cytometer (BD Biosciences) and the percentage of infected cells was determined using FlowJo 10.4.2 software (Tree Star, Ashland, OR). The percentage serum inhibition was calculated as 100 − (% infected cells in the presence of serum) / (% infected cells in the absence of serum) x 100.

5.3.12 Intracellular cytokine staining (ICS) assay

Splenocytes were plated into 96-well round-bottom plates at 1×10^6 cells/well in complete RPMI 1640 medium (containing 10% FBS, 1% penicillin/streptomycin, and 1% HEPES (all from Gibco) and stimulated with 1 μg of the indicated ZIKV peptides. After 1 h at 37℃, brefeldin A (1000X, BioLegend) was added at a 1:1000 dilution and the cells were incubated for an additional 5 h. Cells incubated with RPMI medium or with RPMI medium + PMA/ionomycin (500X) served as negative and positive controls, respectively. After incubation, the splenocytes were stained with efluor 455 (UV) viability dye, (Invitrogen) and fluorophore-conjugated Abs against mouse CD3e (clone 145-2C11, Tonbo), CD8α (clone 53–6.7, BioLegend), CD4 (clone GK1.5, Invitrogen), CD44 (clone IM7, BioLegend), CD62L (MFL-14, BioLegend) CD25 (clone PC61, BioLegend), Biotin-

CD185 (clone SPRCL5, Invitrogen), CD279 (clone 29F.1A12, Bio- Legend), CD19 (clone ebio1D3, eBioscience), CD11a (clone M17/4, eBioscience), CD45.1 (clone A20, eBioscience), CD49d(clone R1-2, eBioscience), IgD (clone 11-26C.2a, BD Phar- mingen), CD138 (clone 281.2, BioLegend) and streptavidin-conjugated BV421 (BD Pharmin- gen), all at 1:200 dilution. The cells were then fixed and permeabilized with Cytofix/Cytoperm (BD Bioscience) (or Fixation/Permeabilization Concentrate [eBioscience] for analysis of Treg cells) and stained with fluorophore-conjugated Abs against mouse IFNγ (clone XMG1.2, Tonbo), TNF (clone MP6-XT22, eBioscience), IL-10 (clone JES5-16E3, BioLegend), IL-2 (clone JES6-5H4, BioLegend), IL-17A (clone eBio17B7, eBioscience), IL-4 (clone 11B11, Bio- Legend), IL-5 (clone TRFK5, Invitrogen), granzyme B (clone NGZB, eBioscience), Bcl-6 (clone K112-91, BD Pharmingen), and/or FOXP3 (clone FJK-16S, eBioscience). Data were collected on an LSR II (BD Bioscience) and analyzed using FlowJo software.

5.3.13 Peptide immunization

Five-week-old *LysMCre*$^+$*Ifnar1*$^{fl/fl}$ and *Ifnar1*$^{-/-}$ mice were injected subcutaneously with 100 μg each of six immunodominant peptides ($E_{346-360}$, $E_{644-658}$, $NS3_{1740-1754}$, $NS4B_{2480-2494}$, $NS5_{2604-2618}$, $NS5_{2738-2752}$) in complete Freund's adjuvant. Two weeks later, the mice were boosted by injection of the same peptides in incomplete Freund's adjuvant. Fourteen days later, the mice were infected retro-orbitally with 10^5 FFU ZIKV. Three days post-infection, organs were collected and infectious ZIKV particles were quantified using FFA.

5.3.14 In vivo cytotoxicity assay

To prepare target cells, splenocytes were harvested from naïve donor mice (C57BL6, CD45.1) and incubated for 3 h at 37℃ with a pool of H2-IA -

restricted peptides ($E_{346-360}$, $E_{644-658}$, $NS3_{1740-1754}$, $NS4B_{2480-2494}$, $NS5_{2604-2618}$, $NS5_{2738-2752}$) or DMSO. Cells were then washed and labeled with CSFE (Invitrogen) in PBS/0.1% BSA for 10 min at 37℃. To distinguish between target cells, cells incubated with DMSO and ZIKV peptides were labeled with 100 nM CSFE (low) and 1 μM CSFE (high), respectively. Cells were then washed and 5×10^6 each of CSFE-low and CSFE-high target cells were mixed and injected RO into recipient LysMCre+Ifnar1fl/fl mice that had been infected retro-orbitally with 104 FFU ZIKV FSS13025, 10^4 FFU ZIKV MR766, or vehicle (10% FBS/PBS; mock-infected). Twelve hours later, splenocytes were har- vested from the recipient mice and the number of CSFE-labeled cells was quantified by flow cytometry. The specific percentage killing was calculated as follows: 100 − ([percentage specific (CSFE-high) target cells present in infected mice]/[percentage non-specific (CSFE-low) target cells present in infected mice]/[percentage specific (CSFE-high) target cells present in mock- infected mice]/[percentage non-specific (CSFE-low) target cells present in mock-infected mice] x 100).

5.3.15 Clinical scoring of disease

Mice were weighed on the day of infection and then weighed and scored for disease daily post- infection. Clinical features were based on a 7-point scale: 1, healthy; 2, slightly ruffled coat around head and neck; 3, ruffled coat over the entire body; 4, severely ruffled coat and slightly closed eyes; 5, sick with closed eyes and slow movement (mice were euthanized); 6, no movement and slow breathing; 7 dead. Weight loss was calculated by comparison with the weight on the day of infection.

5.3.16 Statistical analyses

All data were analyzed with Prism software, version 7.0 (GraphPad Software). Results are expressed as the mean ± standard errors. A non-parametric Mann–Whitney test was used to compare differences between two groups, and the Wilcoxon test was used to compare two parameters from the same group. One-way or two-way ANOVA or a Kruskal–Wallis test was used to compare more than two groups. $P < 0.05$ was considered significant.

5.4 Results

5.4.1 Predominant Th1 response to primary ZIKV infection via the intravenous route in *LysMCre$^+$Ifnar1$^{fl/fl}$* mice

We have previously employed the *LysMCre$^+$Ifnar1$^{fl/fl}$* C57BL/6 mouse model to study the response of CD8$^+$ T cells to ZIKV infection. To validate the model for investigation of CD4$^+$ T cells, 5-week-old *LysMCre$^+$Ifnar1$^{fl/fl}$* mice were intravenously (retro-orbitally, RO) infected with ZIKV strains MR766 or FSS13025 or were mock-infected with vehicle (10% FBS/ PBS). Splenocytes were prepared 7 days later and analyzed for activated (CD44$^+$) or antigen- experienced (CD49d$^+$CD11a$^+$) CD4$^+$ T cells by flow cytometry. We found that cells from ZIKV-infected mice contained significantly more (2-fold) activated and antigen-experienced CD4$^+$ T cells compared with cells from mock-infected mice (Fig 5.1A and 5.1B). We also noted a striking increase in the number of CD4$^+$ T cells with cytotoxic potential (granzyme B$^+$) in the spleens of ZIKV-infected mice (Fig 5.1C), which is consistent with the known contribution of cytotoxic effector CD4$^+$ T cells in anti-flaviviral

control. These results confirmed the suitability of *LysMCre$^+$Ifnar1$^{fl/fl}$* mice to study the CD4$^+$ T cell response to ZIKV infection.

To identify potential CD4$^+$ T cell epitopes in the ZIKV proteome, we screened the Immune Epitope Data Base for predicted class II (H-2 I-Ab)-binding epitopes and selected 49 peptides (the top 1% of candidates) for further testing *in vitro* (Table 5.1). Splenocytes were harvested from ZIKV- or mock-infected *LysMCre$^+$Ifnar1$^{fl/fl}$* on day 7 post-infection and stimulated with the individual peptides. Flow cytometric intracellular staining (ICS) assays were then performed to determine the frequency of CD44$^+$CD4$^+$ T cells producing Th1 (IFNγ, TNF, IL-2), Th2 (IL-4, IL-5), or Th17 (IL-17A) cytokines. A strong Th1 response, as indicated by the production of IFNγ (with or without TNF) and IL-2, was induced by both the African and Asian ZIKV strain (Fig 1D–1F). Six immunodominant epitopes derived from the structural E protein (E$_{346-360}$, E$_{644-658}$) and nonstructural NS3 (NS3$_{1740-1754}$), NS4B (NS4B$_{2480-2494}$), and NS5 (NS5$_{2604-2618}$, NS5$_{2738-2752}$) proteins stimulated a particularly vigorous response by both ZIKVMR766- and FSS13025-primed CD4$^+$ T cells (Fig 5.1D–5.1G). However, none of the immunodominant epitopes stimulated the production of Th2 or Th17 cytokines, confirming the primacy of the Th1 response.

We confirmed that the granzyme B$^+$CD44$^+$CD4$^+$ T cells detected in vitro were bona fide cytolytic cells by performing an in vivo cytotoxicity assay. Naïve C57BL/6 splenocytes (CD45.1) were incubated with medium alone or pulsed with a mixture of the six immunodominant ZIKV epitopes and then labeled with a low (control target cells) or high (antigen-specific target cells) concentration of CSFE. The target cells were mixed and injected into mock- or ZIKV-infected mice, and splenocytes were harvested after 12 h and examined by flow cytometry to quantify

low- and high-CSFE cells. As shown in Fig 5.1H, we detected approximately 70% specific killing of ZIKV epitope-pulsed target cells by both MR766- and FSS13025-primed mice. Taken together, these results indicate that Asian and African ZIKV strains both induce a robust expansion of cytokine secreting and cytotoxic Th1 effector CD4$^+$ T cells in *LysMCre$^+$Ifnar1$^{fl/fl}$* mice.

5.4.2 Expansion of follicular helper CD4$^+$ T cells and reduction of regulatory CD4$^+$ T cells during primary ZIKV infection

To further dissect the CD4$^+$ T cell response to ZIKV, we investigated two subsets that regulate Ab and cytolytic responses. T$_{FH}$ cells are the major cell subset that provides help to B cells and promotes antiviral Ab production [33], while T$_{reg}$ cells play crucial roles in limiting the immune response during infection to avoid extensive tissue damage [34]. We analyzed the CD44$^+$CD4$^+$ T cells for expression of the T$_{FH}$ surface markers CXCR5 and PD-1 or the T$_{reg}$ markers CD25 and FoxP3. We observed a significant expansion of T$_{FH}$ cells that peaked on day 7 post-infection (~5-fold increase) and remained elevated thereafter for the duration of the experiment (Fig 5.2A and 5.2B). In contrast, we detected a significant (~2-fold) reduction in the frequency of CD44$^+$CD4$^+$ CD25$^+$FoxP3$^+$ T$_{reg}$ cells in day 7 splenocytes from ZIKV-infected compared with mock-infected mice (Fig 5.2C). Interestingly, this reduction was pre- ceded by a marked and transient increase in the frequency of T$_{reg}$ cells early in the response (day 3; Fig 5.2D). This decrease in splenic T$_{reg}$ cells is consistent with the findings of a recent study of ZIKV infection in wildtype mice and with our earlier study in Ifnar1-deficient mice infected with DENV (Yauch et al., 2010).

IL-10 is a key CD4$^+$ T cell-secreted immunoregulatory cytokine that controls viral immunity by inhibiting proinflammatory responses and preventing tissue

damage. Therefore, we also examined their frequency in ZIKV-infected mice. Unexpectedly, we saw a significant expansion of IL-10-producing $CD44^+CD4^+$ splenocytes from day 7 ZIKV- infected compared with mock-infected mice (Fig 5.2E), which contrasts with the pattern of T_{reg} cell retraction on day 7. The expression of IFNγ by $IL-10^+CD44^+CD4^+$ T cells indicated that a substantial proportion of the IL-10-producing cells were Th1 effector cells with a regulatory phenotype, rather than T_{reg} cells. Collectively, these results demonstrate that, at the peak of the T cell response, ZIKV infection induces expansion of Ab-promoting T_{FH} cells and IL-10-producing $CD4^+$ T cells but suppresses the population of T_{reg} cells.

5.4.3 Requirement for $CD4^+$ T cells for induction of virus-specific IgG, but not for the $CD8^+$ T cell response or viral control, after intravenous infection with ZIKV

T_{FH} cells play important roles in generating mature B cells and supporting long-lived Ab-producing plasma cells (Crotty, 2014). Since ZIKV infection leads to a rapid expansion in the frequency of T_{FH} cells, we next investigated the requirement for $CD4^+$ T cells in generating ZIKV-specific Abs during primary infection. *LysMCre$^+$Ifnar1$^{fl/fl}$* mice were treated with isotype control or anti-CD4 Ab, and serum samples were taken on day 7 post-infection for analysis of IgM and IgG reactivity to ZIKV E protein by ELISA. As an estimate of anti-ZIKV E Ab concentrations, we determined the endpoint titer (defined as the reciprocal of the highest serum dilution to give a reading twice the cutoff absorbance). Although the ZIKV E-specific IgM titer was the same in sera from control Ab- and anti-CD4-treated mice, depletion of $CD4^+$ T cells significantly reduced the ZIKV E-specific IgG endpoint titer compared with the control sera (Fig 5.3A and 5.3B), suggesting that $CD4^+$ T cell help is required for

the development of the IgG, but not IgM, response to ZIKV. Surprisingly, we also found that CD4$^+$ T cells were not required for generation of ZIKV-specific neutralizing Abs (Fig 3C). Chemical inactivation of IgM reduced the neutralizing capacity of serum samples from anti-CD4-treated mice, indicating that this isotype was largely responsible for the neutralizing activity at day 7 after infection (Fig 5.3C). To verify these findings, we also analyzed the Ab response at 10 days post-infection. Although we again observed that CD4$^+$ T cells were not required to generate ZIKV-specific IgM Abs, there was a marked reduction in neutralizing activity in the sera from anti-CD4 Ab-treated compared with control mice, consistent with production of IgG neutralizing Abs at this later time point during the primary infection. These data therefore show that CD4$^+$ T cells are not required for generation of the neutralizing Ab response at the peak of the T cell response at day 7 post-infection; however, they do not exclude the possible involvement of CD4$^+$ T cells at later times. Indeed, analysis of splenocytes on day 7 post-infection revealed a significant reduction in the frequencies of plasma and GC B cells in CD4$^+$ T cell-depleted mice compared with control mice (Fig 5.3D and 5.3E), supporting the potential role of CD4$^+$ T cells in virus-specific IgG production at later time points after infection.

We next asked whether CD4$^+$ T cells are required for the primary CD8$^+$ T cell response to ZIKV infection, as we have previously demonstrated a critical role for CD8$^+$ T cells in protecting against primary ZIKV infection. Splenocytes from control and anti-CD4 Ab-treated mice were isolated on day 7 post-ZIKV infection, stimulated in vitro with three immunodominant class I-restricted CD8 epitopes (PrM$_{169-177}$, E$_{297-305}$, or NS5$_{2783-2792}$), and analyzed for the frequencies of CD8$^+$ T cells producing IFNγ alone or and IFNγ and TNF. We observed no difference in the frequency of either

CD8$^+$ T cell subset between splenocytes from control and CD4$^+$ T cell-depleted mice (Fig 5.3F) or in the absolute number of total CD8+ T cells, high low effector memory (CD44 CD62L) CD8 T cells, or IFNγ- or IFNγ TNF -producing CD8+ T cells. Thus, the primary CD8$^+$ T cell response to ZIKV does not require CD4$^+$ T cell help.

To investigate the impact of CD4$^+$ T cell depletion on viral clearance, *LysMCre$^+$Ifnar1$^{fl/fl}$* mice were treated with control or anti-CD4 Ab prior to intravenous infection with 10^5 or 10^3 FFU of ZIKV FSS13025. Seven days later, infectious ZIKV particles in the serum, brain, and testes were quantified using a cell-based focus-forming assay. Although the serum and brain were devoid of infectious particles in the majority of animals at this time point, ZIKV particles were detectable in the testes at levels not significantly different between the CD4$^+$ T cell -sufficient and -depleted animals (Fig 5.3G and 5.3H).

To better mimic viral transmission via a mosquito bite in this animal model, we also evaluated the role of CD4$^+$ T cells in the anti-ZIKV response of mice infected via the intrafootpad route. Here, too, we found as shown for the intravenous route that depletion of CD4$^+$ T cells reduced the magnitude of the ZIKV-specific IgG, plasma cell, and GC B cell responses and there were no difference between control and CD4$^+$ T cell-depleted mice in the CD8$^+$ T cell response or in viral titers in serum, brain, and testes. Overall, these results suggest that, although CD4$^+$ T cells are required for the differentiation of plasma and GC B cells and for the production of virus-specific IgG, they are not involved in viral clearance during primary ZIKV infection via either the intravenous (RO) or intrafootpad routes, which contrasts with the role of CD8$^+$ T cells.

5.4.4 CD4+T cell-mediated regulation of the antiviral Ab response, control of local viral burden, and protection from lethality following intravaginal infection with ZIKV

Our results thus far reveal a mixed role for CD4+ T cells in promoting Ab and viral clearance to ZIKV infection via the RO route. To determine whether this was also the case for the primary response to IVag infection, we performed a similar analysis using progesterone pretreated *LysMCre+Ifnar1fl/fl* mice that were infused with a control or depleting anti-CD4 Ab before IVag ZIKV infection. Analysis of serum on day 10 post-infection revealed that, in contrast to the findings with mice infected RO, depletion of CD4+ T cells significantly reduced the titers of ZIKV-specific IgM and IgG as well as the anti-ZIKV neutralizing Ab activity compared with control mice (Fig 5.4A–5.4C). We observed a reduction in the frequency of splenic plasma cells and GC B cells (Fig 5.4D and 5.4E) in CD4-depleted mice but saw no effect on the CD8+ T cell response, as reflected by the frequency of IFNγ^- and IFNγ^+ TNF-producing cells after in vitro stimulation of splenocytes with E$_{297-305}$ ZIKV epitope (Fig 5.4F), on day 7 post-infection.

To assess the requirement for CD4+ T cells for viral clearance after IVag infection, we quantified infectious ZIKV particles in serum, vaginal washes, and the FRT on day 10 post-IVag infection of control or anti-CD4 Ab-treated *LysMCre+Ifnar1fl/fl* mice. Although the viral bur- den in serum and FRT was unaffected by CD4+ T cell depletion, ZIKV RNA levels were significantly higher in the vaginal washes of anti-CD4-treated compared with isotype control Ab- treated mice (Fig 5.4G). To determine whether viral clearance from vaginal washes was medi- ated by CD4+ T cells alone, CD8+ T cells were depleted by injection of anti-

CD8 Ab on days −3 and −1 before IVag infection with ZIKV, and serum and vaginal washes were analyzed for ZIKV RNA levels at 10 days post-infection. We detected no difference in viral RNA levels between anti-CD8 Ab and isotype control Ab-treated mice in either sample (Fig 5.4H), indicating that CD8$^+$ T cells are likely not involved in control of viral burden following IVag infection. However, animals lacking CD8$^+$ T cells showed an enhanced CD4$^+$ T cell response, with increased IFNγ$^-$ and IFNγ$^+$ TNF-producing cell frequencies and numbers in the spleen and increased frequencies in the iliac lymph nodes, suggesting that the CD4$^+$ T cell response to ZIKV compensates for the absence of CD8$^+$ T cells by increasing the abundance of Th1 cells.

To confirm and extend this result showing CD4$^+$ T cell contribution to protection against IVag ZIKV infection in *LysMCre$^+$Ifnar1$^{fl/fl}$* mice, we depleted CD4$^+$ T cells in *Ifnar1$^{-/-}$* mice on days −3 and −1 before IVag infection with a lethal dose of ZIKV. Only 22% of CD4-depleted mice survived to day 15 post-infection compared with 78% of control Ab-treated mice, and the CD4$^+$ T cell-depleted animals showed greater body weight loss and more severe clinical disease scores than the control animals. Collectively, the results of the experiments with *LysMCre$^+$Ifnar1$^{fl/fl}$* and *Ifnar1$^{-/-}$* mice infected via the IVag route indicate that CD4$^+$ T cells are required to mount an efficient Ab response, to control the local viral burden, and to reduce clinical signs and mortality following IVag infection.

5.5 Discussion

The role of CD4$^+$ T cells in the regulation of anti-ZIKV adaptive immunity has yet to be defined. In this study, we explored the CD4$^+$ T cell response to primary RO

and IVag infection with ZIKV using *LysMCre+Ifnar1fl/fl* mice, in which the type I IFN receptor is absent from myeloid cells but present on T and B cells. We previously used these mice to study the $CD8^+$ T cell response to RO ZIKV infection (Elong Ngono et al., 2017) and to establish a model of sexually transmitted ZIKV infection. In the present study, we demonstrate that RO and IVag ZIKV infection both induce robust antigen-specific Th1, T_{FH}, plasma cell, GC B cell, IgM, and IgG responses, and that $CD4^+$ T cells contribute to the generation of Ab responses, but not $CD8^+$ T cell responses, and to the control of viral infection. Thus, provision of help for Ab responses may be a dominant feature of the protective role of $CD4^+$ T cells during primary ZIKV infection.

Using the *LysMCre+Ifnar1fl/fl* C57BL/6 mouse model, we first mapped the $CD4^+$ T cell response to ZIKV proteins and identified immunodominant epitopes from structural and nonstructural proteins. Similar to our findings here, previous work has shown that the human $CD4^+$ T cell response to ZIKV is targeted against epitopes in both structural and nonstructural proteins, with the most immunodominant epitopes being located in ZIKV E, NS1, and NS5 (Badolato-Correa et al., 2018; Lai et al., 2018; Ricciardi et al., 2017). In our study, the strongest response following ZIKV infection via both RO and IVag routes was to the $E_{644-658}$ epitope, which is located in domain III (EDIII) of the ZIKV E protein. EDIII is exposed on the virion surface and is one of the main targets of neutralizing Ab responses to flaviviruses (Priyamvada et al., 2016; Richner et al., 2017; Wahala & Silva, 2011). Indeed, several groups have identified highly neutralizing ZIKV EDIII-specific Abs (Hasan et al., 2017; Robbiani et al., 2017; Stettler et al., 2016; Wang, Yan, & Gao, 2017). The fact that the most

immunodominant ZIKV epitope for CD4$^+$ T cells is in EDIII could suggest that robust T cell help drives the production of EDIII-reactive and neutralizing Abs.

Although recent work has shown that ZIKV infection induces activation and expansion of CD4$^+$ T cells with a Th1 phenotype (Pardy et al., 2017; Winkler et al., 2017), those studies did not analyze the antigen specificity of the response. Here, we confirmed the earlier findings that Th1 CD4$^+$ T cells with cytotoxic activity are the major cell type elicited during the primary ZIKV response. We also found that the percentage and absolute number of T$_{reg}$ cells were both reduced at the peak of the T cell response to ZIKV infection via RO and IVag routes. A similar effect on Treg cells was observed in mouse models of systemic ZIKV (Winkler et al., 2017) and DENV infection. We also detected an expansion of T$_{reg}$ cells at an early time point, day 3, after ZIKV infection. Winkler and colleagues examined the kinetics of the CD4$^+$FoxP3$^+$ cell response in C57BL/6 mice infected with ZIKV intraperitoneally (Winkler et al., 2017); however, these authors detected a reduction, not an expansion, of CD4$^+$FoxP3$^+$ cells on day 3. This apparent discrepancy may have been due to a difference in analytical gating strategy. Whereas we analyzed the CD4$^+$CD44$^+$FoxP3$^+$CD25$^+$ T cell subset, Winkler et al. examined the larger pool of CD4$^+$FoxP3$^+$ cells, which may have limited their capacity to detect subtle changes in minor subpopulations (Winkler et al., 2017). We demonstrated that ZIKV infection via the RO and IVag routes generates IL-10-producing Th1 cells, which also possess regulatory activity but are distinct from the CD25$^+$FoxP3$^+$ subset that develops in the thymus (Jankovic, Kugler, & Sher, 2010). In future, studies examining the relationship between these T cell subsets in regulating the balance between promoting antiviral

immunity and restraining inflammatory processes during ZIKV infection will be critical for deciphering the mechanisms of adaptive immune protection against ZIKV.

Our study demonstrates that RO or IVag infection with ZIKV induces TFH cells, which are required for GC development and function (Crotty, 2014; Victora & Nussenzweig, 2012). The finding that CD4^{+} T cells are necessary for the generation of plasma and GC B cell responses, in addition to the production of ZIKV-specific IgG after infection via either the RO, intrafootpad or IVag routes, suggests that T_{FH} cells could control B cell maturation and Ab production in response to ZIKV infection. Depletion of CD4^{+} T cells impaired the generation of neutralizing Abs during the peak of the T cell response following IVag, but not intravenous, ZIKV infection, which is probably due to the different times at which the T cell response peaks post-infection via the two routes. Similarly, production of ZIKV-specific IgM was disrupted in the absence of CD4^{+} T cells mainly after IVag but not RO infection. Moreover, the neutralizing Ab response at the peak of the T cell response to RO infection was mainly due to IgM, which is consistent with the response to WNV (Sitati & Diamond, 2006). These observations suggest that the T_{FH} and, possibly, Th1 responses (which can regulate the magnitude and quality of T_{FH} responses (Liang et al., 2017; Pardi et al., 2018)) differentially regulate the anti- ZIKV Ab response during systemic versus mucosal infection.

Scott and colleagues recently reported the effects of prior cellular and humoral immunity on subsequent IVag ZIKV exposure in mice (Scott et al., 2018). In particular, they showed that CD4^{+} T cells were required for the production of ZIKV-specific IgG, but not for viral clearance during either primary or secondary infection (Scott et al., 2018). Similarly, another study observed that CD4^{+} T cells were not

necessary to control secondary subcutaneous ZIKV infection of mice (Turner et al., 2017). In our study, we showed using peptide vaccination and adoptive cell transfer approaches that memory $CD4^+$ T cells contributed to viral clearance from multiple tissues during systemic challenge, but they were not required to protect against lethal challenge. Two potential explanations for the discrepancies between these studies and ours are the use of different mouse models (strain and age) and different ZIKV challenge doses. However, consistent with the finding by Scott and colleagues (Scott et al., 2018), we found that $CD4^+$ T cells were required for generation of plasma cell, GC B cell, and Ab responses upon infection via both systemic and mucosal routes, suggesting that the anti-ZIKV $CD4^+$ T cell response plays a dominant role in driving Ab production, irrespective of the infection route.

In our study, we used peptide vaccination and adoptive transfer experiments to demonstrate that ZIKV-specific memory $CD4^+$ T cells can promote viral clearance during RO ZIKV infection. However, this was only true for adoptive transfer before challenge with a low dose of virus. Based on our previous study demonstrating a critical role for $CD8^+$ T cells in controlling RO ZIKV infection, we speculate that high-dose viral challenge more effectively activates multiple innate immune and $CD8^+$ T cell responses than does low-dose challenge. In the present study, $CD4^+$ T cells play a dominant role in promoting humoral immunity to ZIKV after infection via both systemic and genital mucosal routes, and $CD4^+$ T cells, but not $CD8^+$ T cells, contribute to local control of ZIKV infection in the vagina and protect against lethal disease following IVag ZIKV challenge. Thus, the viral challenge dose and the route of exposure may differentially dictate the quantity and quality of induced T_{FH} cells.

In conclusion, our data provide evidence for qualitatively different protective roles of CD4$^+$ T cells in ZIKV infection via the RO and IVag routes. Since we previously reported that CD4$^+$ T cells play a limited role in protecting pregnant mice against primary infection via the RO route (Regla-Nava et al., 2018), our results here highlight the importance of exploring whether CD4$^+$ T cells are protective when infection occurs intravaginally during pregnancy. The majority of current work on ZIKV vaccines is focused on eliciting a neutralizing Ab response. However, based on our data suggesting that T$_{FH}$ and antigen specific Th1 cells may regulate the magnitude and quality of the anti-ZIKV Ab response, it may be prudent to design ZIKV vaccines that induce robust CD4$^+$ T cell responses in addition to Abs. This study provides the foundation for further dissection of the H-2^b restricted CD4 T cell response to ZIKV in various mouse models, including pregnant mice infected via systemic and mucosal routes in both natural infection and vaccination con- texts. Such studies should help to identify the precise features of the anti-ZIKV CD4$^+$ T cell response that can be manipulated to generate ZIKV vaccines that are safe and effective against infection in multiple contexts, including pregnancy and sexual transmission.
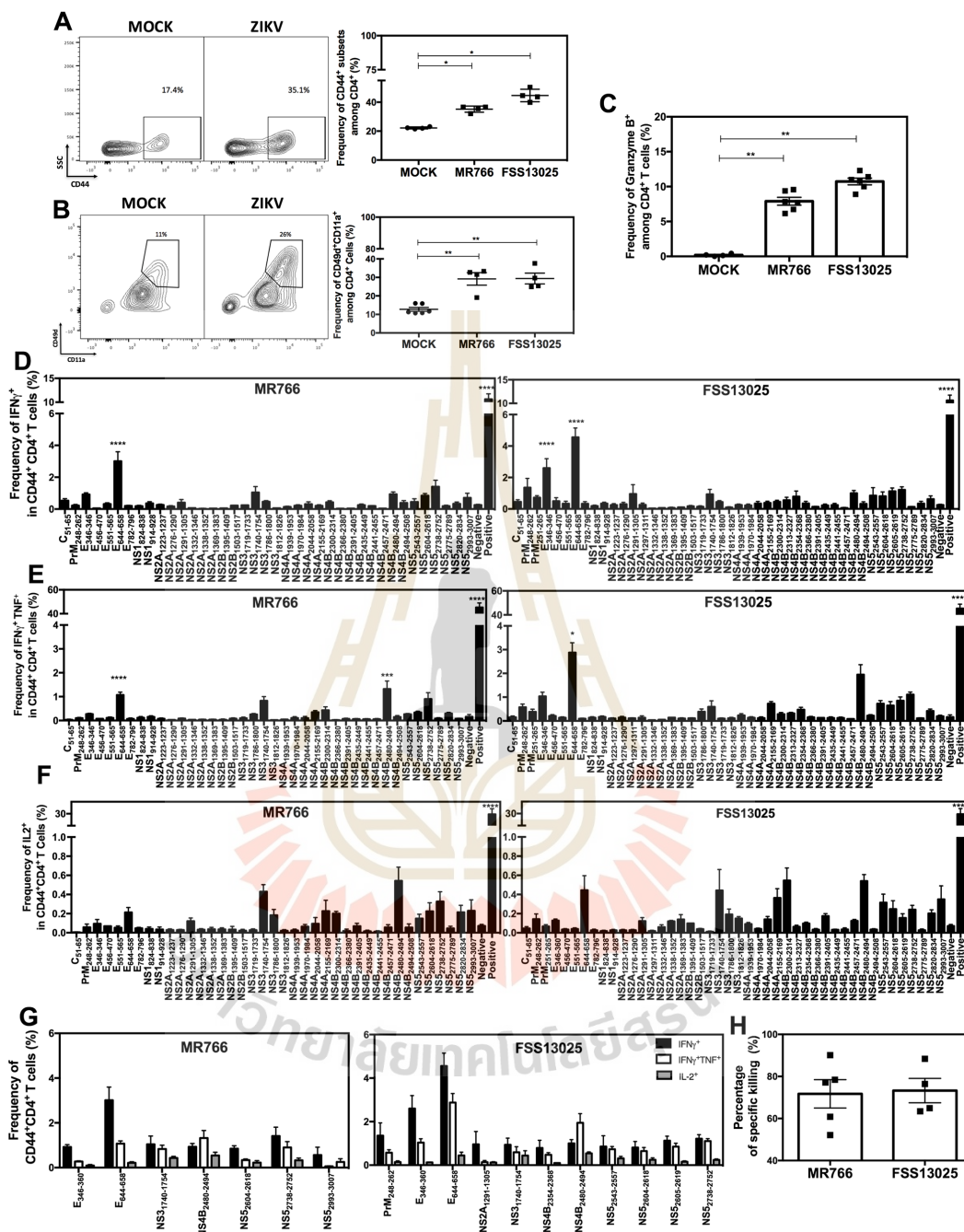
5.6 Figures and Tables

Figure 5.1   Mapping of the CD4+ T cell response in the *LysMCre+IFNAR^fl/fl* mouse model of primary ZIKV infection. Five-week-old *LysMCre+Ifnar1^fl/fl* C57BL/6 mice were infected retro-orbitally with 10^4

FFU of ZIKV strain MR766 or FSS13025 in 10% FBS/PBS or were mock-infected (10% FBS/PBS alone). Data are the mean ± SEM of n = 4–6 mice/group. (A–C) Splenocytes were removed on day 7 post-infection and analyzed for the percentage of (A) $CD44^+CD4^+$ T cells, (B) $CD49d^+CD11a^+$ T cells, and (C) granzyme B^+CD4^+ T cells. (D–F) Splenocytes were removed on day 7 post-infection and stimulated with the indicated ZIKV-derived peptides and brefeldin A. The percentage $CD44^+CD4^+$ T cells producing (D) IFNγ, (E) IFNγ and TNF, and (F) IL-2 was measured by ICS. Cells stimulated with DMSO or PMA/ionomycin served as negative and positive controls, respectively. (G) Summary of the data shown in (D–F). (H) In vivo killing of ZIKV peptide-pulsed target cells. $LysMCre^+Ifnar1^{fl/fl}$ mice were retro-orbitally mock-infected (n = 4) or infected with 10^4 FFU ZIKV MR766 (n = 5) and FSS13025 (n = 4) for 7 days, and then injected retro-orbitally with naïve C57BL/6 splenocytes (n = 4) pulsed with a pool of ZIKV peptides ($E_{346-360}$, $E_{644-658}$, $NS3_{1740-1754}$, $NS4B_{2480-2494}$, $NS5_{2604-2618}$, $NS5_{2738-2752}$) or treated with DMSO. After 12 h, the splenocytes were harvested from recipient mice, analyzed by flow cytometry, and the percentage ZIKV-specific cytotoxicity was calculated. *$P < 0.05$, **$P < 0.01$ by the Mann–Whitney U test. The production of cytokines after stimulation with each peptide was compared to the negative control (DMSO) using one-way ANOVA **** $P < 0.0001$. Data are representative of two independent experiments.
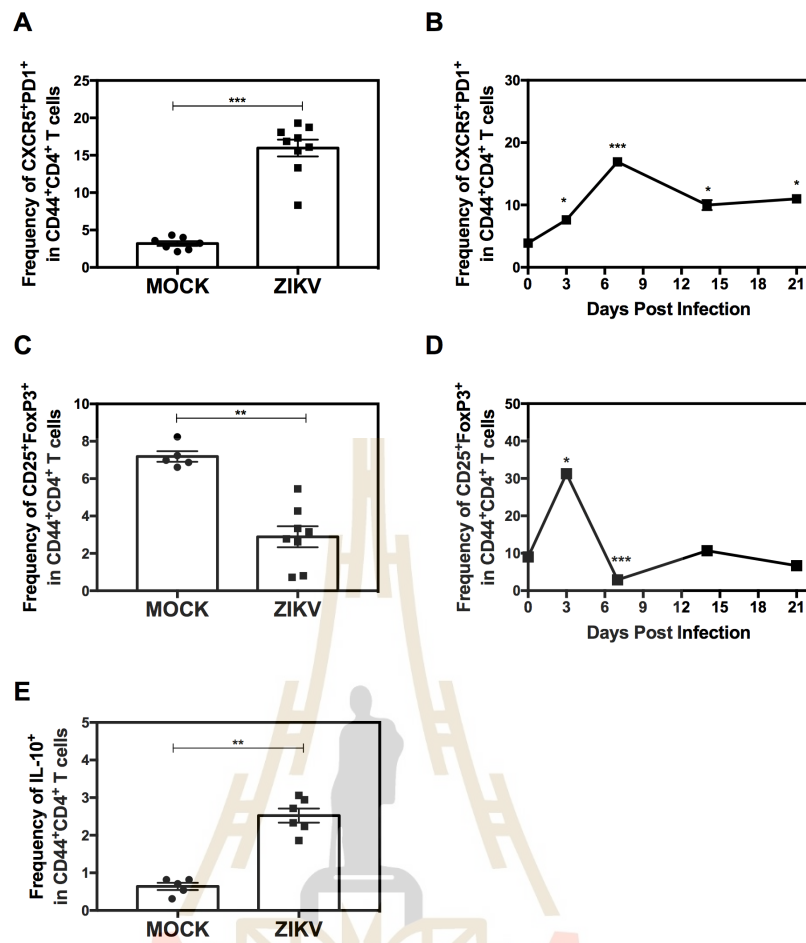
Figure 5.2 **Kinetics of the follicular helper and regulatory CD4^{+} T cell responses in the *LysMCre^{+}Ifnar1^{fl/fl}* mouse model of primary ZIKV infection.** Five-week-old *LysMCre^{+}Ifnar1^{fl/fl}* C57BL/6 mice were infected retro-orbitally with 104 FFU of ZIKV strain FSS13025 or were mock-infected. Data are the mean ± SEM of n = 7 (A), n = 4 (B), n = 5 (C), n = 4 (D), n = 5 (E) mock-infected and n = 9 (A), n = 4–6 (B), n = 8 (C), n = 4–6 (D), n = 6 (E) ZIKV-infected mice. **$P < 0.01$, ***$P < 0.001$, by the Mann–Whitney U test. For the kinetic analysis, each time point was compared to day 0 using the Mann–Whitney U test, *$P < 0.05$, ***$P < 0.001$. Data are representative of two independent experiments.
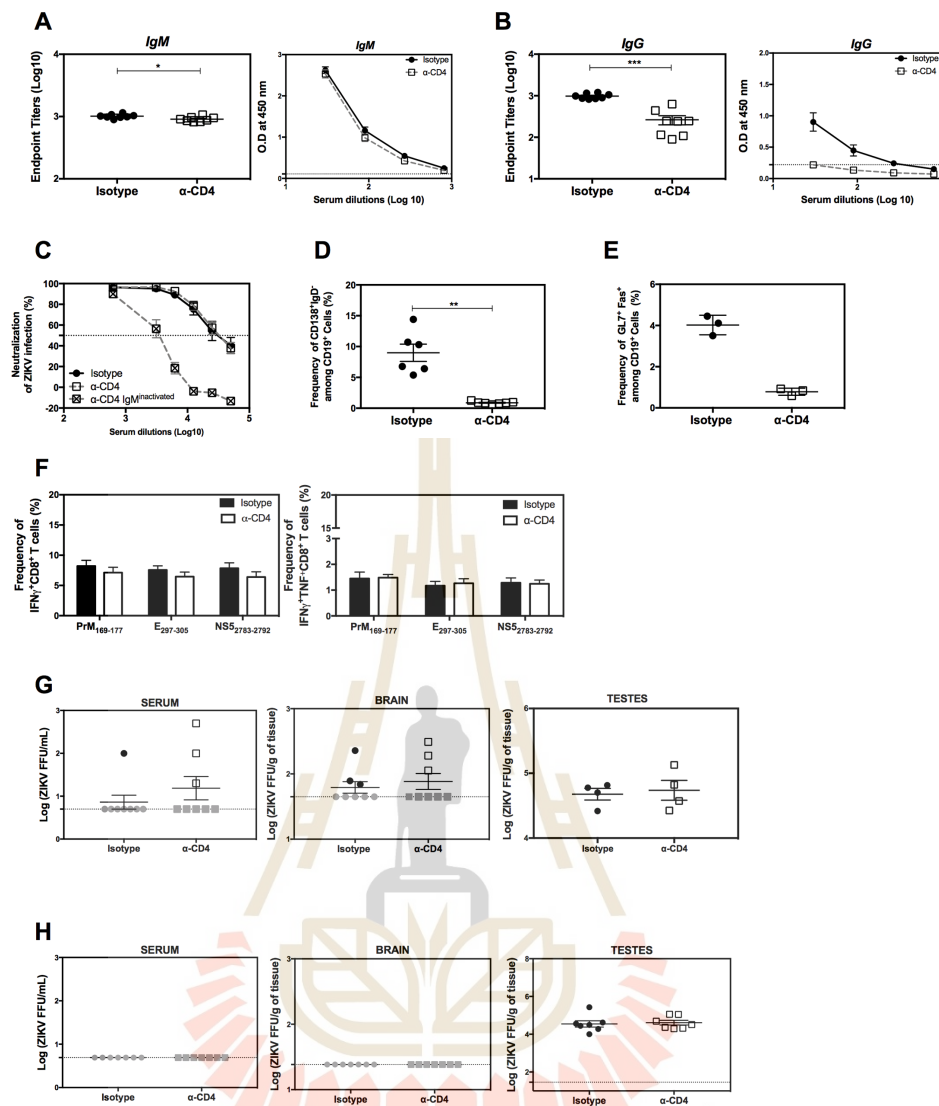
Figure 5.3 **Contribution of CD4+ T cells to Ab and CD8+ T cell responses and to viral control during primary ZIKV infection in LysMCre+Ifnar1fl/fl mice.** *LysMCre⁺Ifnar1^{fl/fl}* C57BL/6 mice were treated with a depleting anti-CD4 Ab (n = 8) or isotype control Ab (n = 8) on days −3 and −1 prior to and every 2 days after retro-orbital infection with 10^5 FFU of ZIKV FSS13025. (A–C) Sera were collected on day 7 post-infection to measure anti-ZIKV IgM.
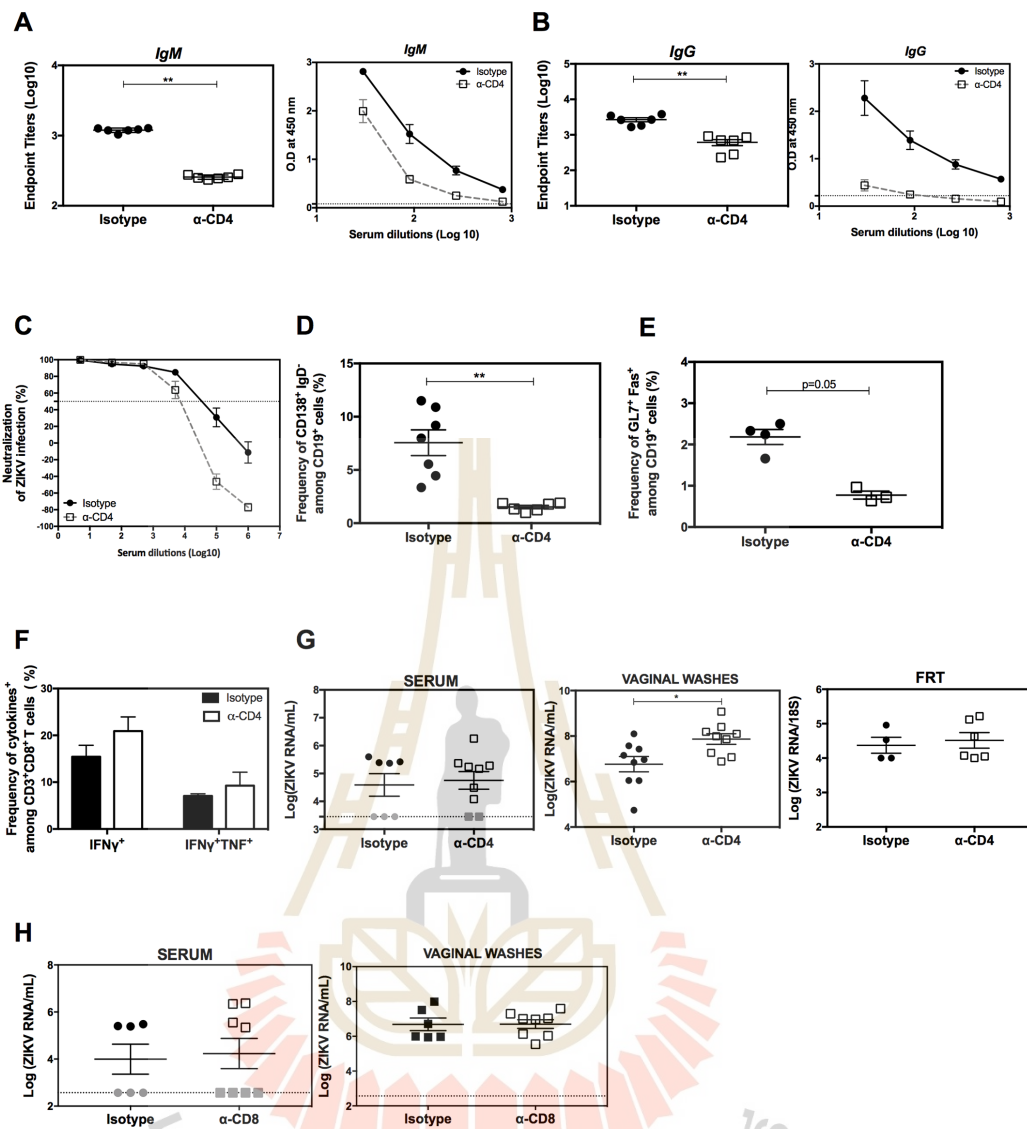
Figure 5.4 Contribution of CD4⁺ T cells to antibody production, CD8⁺ T cell response, and local viral control during primary intravaginal ZIKV infection of *LysMCre⁺Ifnar1ᶠˡ/ᶠˡ* mice. Female *LysMCre⁺Ifnar1ᶠˡ/ᶠˡ* C57BL/6 mice were treated with a depleting anti-CD4 Ab (n = 7) or isotype control Ab (n = 6) on days −3 and −1 prior to intravaginal infection with 105 FFU of ZIKV FSS13025. Mice were also treated with progesterone on day −3. (A–C) Sera were collected on day 10 post-infection to measure anti-ZIKV IgM (A) and IgG (B) titers by ZIKV E-

specific ELISA and neutralizing activity (C) using a U937 DC-SIGN cell-based flow cytometric assay. (D and E) Splenocytes were collected on day 10 post-infection and analyzed by flow cytometry for the percentage plasma cells (CD138+IgD−) (D) or germinal center B cells (GL7+Fas+) (E). *$P < 0.05$, **$P < 0.01$ by the Mann–Whitney U test.
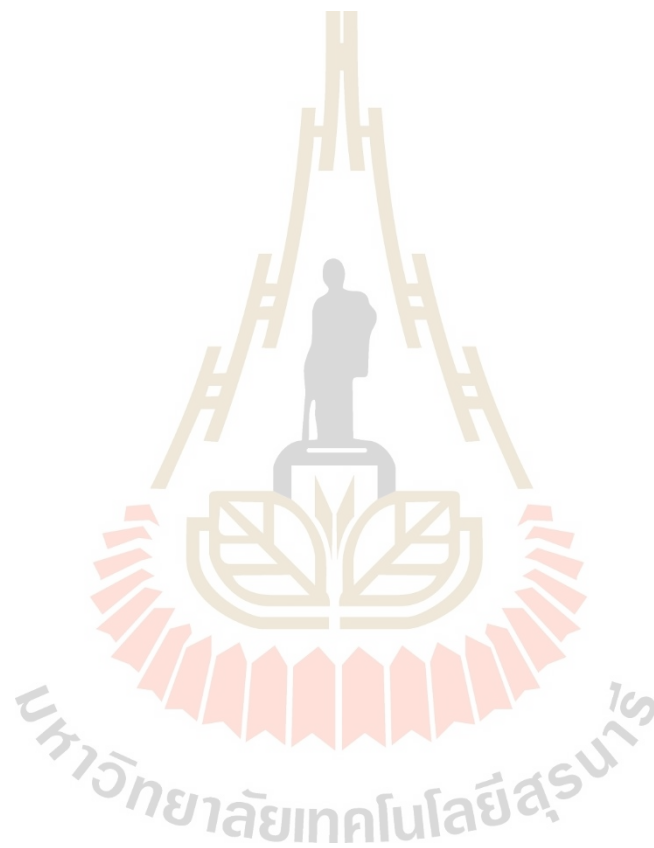
5.7 References

Aliota, M. T., Dudley, D. M., Newman, C. M., Mohr, E. L., Gellerup, D. D., Breitbach, M. E., . . . O'Connor, D. H. (2016). Heterologous protection against asian zika virus challenge in Rhesus Macaques. **PLoS Neglected Tropical Diseases**, 10(12), e0005168.

Badolato-Correa, J., Sanchez-Arcila, J. C., Alves de Souza, T. M., Santos Barbosa, L., Conrado Guerra Nunes, P., da Rocha Queiroz Lima, M., . . . de-Oliveira-Pinto, L. M. (2018). Human T cell responses to dengue and Zika virus infection compared to dengue/Zika coinfection. **Immunity Inflammation Disease**, 6(2), 194-206.

Brien, J. D., Uhrlaub, J. L., & Nikolich-Zugich, J. (2008). West Nile virus-specific CD4 T cells exhibit direct antiviral cytokine secretion and cytotoxicity and are sufficient for antiviral protection. **Journal of Immunology**, 181(12), 8568-8575.

Cao-Lormeau, V. M., Blake, A., Mons, S., Lastere, S., Roche, C., Vanhomwegen, J., Ghawche, F. (2016). Guillain-Barre syndrome outbreak associated with Zika virus infection in French Polynesia: a case-control study. **Lancet**, 387(10027), 1531-1539.

Crotty, S. (2014). T follicular helper cell differentiation, function, and roles in disease. **Immunity**, 41(4), 529-542.

D'Ortenzio, E., Matheron, S., Yazdanpanah, Y., de Lamballerie, X., Hubert, B., Piorkowski, G., Leparc-Goffart, I. (2016). Evidence of Sexual Transmission of Zika Virus. **New England Journal of Medicine**, 374(22), 2195-2198.

Dick, G. W. (1952). Zika virus. II. Pathogenicity and physical properties. **Transaction of the Royal Society Tropical Medicine and Hygiene**, 46(5), 521-534.

Dowd, K. A., Ko, S. Y., Morabito, K. M., Yang, E. S., Pelc, R. S., DeMaso, C. R., . . . Graham, B. S. (2016). Rapid development of a DNA vaccine for Zika virus. **Science**, 354(6309), 237-240.

Dudley, D. M., Aliota, M. T., Mohr, E. L., Weiler, A. M., Lehrer-Brey, G., Weisgrau, K. L., O'Connor, D. H. (2016). A rhesus macaque model of Asian-lineage Zika virus infection. **Nature Communication**, 7, 12204.

Elong Ngono, A., Vizcarra, E. A., Tang, W. W., Sheets, N., Joo, Y., Kim, K., . . . Shresta, S. (2017). Mapping and role of the CD8(+) T cell response during primary Zika virus infection in mice. **Cell host & microbe**, 21(1), 35-46.

Hasan, S. S., Miller, A., Sapparapu, G., Fernandez, E., Klose, T., Long, F., Rossmann, M. G. (2017). A human antibody against Zika virus crosslinks the E protein to prevent infection. **Nature Communications**, 8, 14722.

Heang, V., Yasuda, C. Y., Sovann, L., Haddow, A. D., Travassos da Rosa, A. P., Tesh, R. B., & Kasper, M. R. (2012). Zika virus infection, Cambodia, 2010. **Emerging Infectious Disease**, 18(2), 349-351.

Huang, H., Li, S., Zhang, Y., Han, X., Jia, B., Liu, H., Zhang, F. (2017). CD8$^+$T cell immune response in immunocompetent mice during Zika virus infection. **Journal of Virology**, 91(22).

Jankovic, D., Kugler, D. G., & Sher, A. (2010). IL-10 production by CD4$^+$ effector T cells: a mechanism for self-regulation. **Mucosal Immunology**, 3(3), 239-246.

Kim, Y., Ponomarenko, J., Zhu, Z., Tamang, D., Wang, P., Greenbaum, J., . . . Peters, B. (2012). Immune epitope database analysis resource. **Nucleic Acids Research**, 40(Web Server issue), W525-530.

Lai, L., Rouphael, N., Xu, Y., Natrajan, M. S., Beck, A., Hart, M., . . . Mulligan, M. J. (2018). Innate, T-, and B-cell responses in acute human zika patients. **Clinical of Infectious Disease**, 66(1), 1-10.

Larocca, R. A., Abbink, P., Peron, J. P., Zanotto, P. M., Iampietro, M. J., Badamchi-Zadeh, A., . . . Barouch, D. H. (2016). Vaccine protection against Zika virus from Brazil. **Nature**, 536(7617), 474-478.

Liang, F., Lindgren, G., Sandgren, K. J., Thompson, E. A., Francica, J. R., Seubert, A., . . . Lore, K. (2017). Vaccine priming is restricted to draining lymph nodes and controlled by adjuvant-mediated antigen uptake. **Science Translational Medicine**, 9(393).

Liu, T., & Chambers, T. J. (2001). Yellow fever virus encephalitis: properties of the brain-associated T-cell response during virus clearance in normal and gamma interferon-deficient mice and requirement for CD4$^+$ lymphocytes. **Journal of Virology**, 75(5), 2107-2118.

Ma, W., Li, S., Ma, S., Jia, L., Zhang, F., Zhang, Y., . . . Gao, G. F. (2016). Zika virus causes testis damage and leads to male infertility in mice. **Cell**, 167(6), 1511-1524.e1510.

Miner, J. J., Cao, B., Govero, J., Smith, A. M., Fernandez, E., Cabrera, O. H., . . . Diamond, M. S. (2016). Zika virus infection during pregnancy in mice causes placental damage and fetal demise. **Cell**, 165(5), 1081-1091.

Ngono, A. E., & Shresta, S. (2018). Immune response to dengue and Zika. **Annual review of immunology**, 36, 279-308.

Pardi, N., Hogan, M. J., Naradikian, M. S., Parkhouse, K., Cain, D. W., Jones, L., Weissman, D. (2018). Nucleoside-modified mRNA vaccines induce potent T follicular helper and germinal center B cell responses. **Journal of Experimental Medicine**, 215(6), 1571-1588.

Pardy, R. D., Rajah, M. M., Condotta, S. A., Taylor, N. G., Sagan, S. M., & Richer, M. J. (2017). Analysis of the T cell response to zika virus and identification of a novel CD8^{+} T cell epitope in immunocompetent mice. **PLoS Pathogens**, 13(2), e1006184.

Priyamvada, L., Quicke, K. M., Hudson, W. H., Onlamoon, N., Sewatanon, J., Edupuganti, S., Wrammert, J. (2016). Human antibody responses after dengue virus infection are highly cross-reactive to Zika virus. **Proceedings of the National Academy of Sciences of the United States of America**, 113(28), 7852-7857.

Rasmussen, S. A., Jamieson, D. J., Honein, M. A., & Petersen, L. R. (2016). Zika virus and birth defects reviewing the evidence for causality. **The New England Journal of Medicine**, 374(20), 1981-1987.

Regla-Nava, J. A., Elong Ngono, A., Viramontes, K. M., Huynh, A. T., Wang, Y. T., Nguyen, A. T., Shresta, S. (2018). Cross-reactive dengue virus-specific CD8+ T cells protect against Zika virus during pregnancy. **Nature Communications**, 9(1), 3042.

Ricciardi, M. J., Magnani, D. M., Grifoni, A., Kwon, Y. C., Gutman, M. J., Grubaugh, N. D., Watkins, D. I. (2017). Ontogeny of the B- and T-cell response in a

primary Zika virus infection of a dengue-naive individual during the 2016 outbreak in Miami, FL. **PLoS Neglected Tropical Diseases**, 11(12), e0006000.

Richner, J. M., Jagger, B. W., Shan, C., Fontes, C. R., Dowd, K. A., Cao, B., . . . Diamond, M. S. (2017). Vaccine mediated protection against Zika virus-induced congenital disease. **Cell**, 170(2), 273-283.e212.

Robbiani, D. F., Bozzacco, L., Keeffe, J. R., Khouri, R., Olsen, P. C., Gazumyan, A., . . . Nussenzweig, M. C. (2017). Recurrent potent human neutralizing antibodies to Zika virus in Brazil and Mexico. **Cell**, 169(4), 597-609.e511.

Scott, J. M., Lebratti, T. J., Richner, J. M., Jiang, X., Fernandez, E., Zhao, H., . . . Shin, H. (2018). Cellular and humoral immunity protect against vaginal Zika virus infection in mice. **Journal of Virology**, 92(7).

Sitati, E. M., & Diamond, M. S. (2006). CD4+ T-cell responses are required for clearance of West Nile virus from the central nervous system. **Journal of Virology**, 80(24), 12060-12069.

Stettler, K., Beltramello, M., Espinosa, D. A., Graham, V., Cassotta, A., Bianchi, S., . . . Corti, D. (2016). Specificity, cross-reactivity, and function of antibodies elicited by Zika virus infection. **Science**, 353(6301), 823-826.

Tang, W. W., Young, M. P., Mamidi, A., Regla-Nava, J. A., Kim, K., & Shresta, S. (2016). A mouse model of Zika virus sexual transmission and vaginal viral replication. **Cell Press**, 17(12), 3091-3098.

Turner, L. H., Kinder, J. M., Wilburn, A., D'Mello, R. J., Braunlin, M. R., Jiang, T. T., . . . Way, S. S. (2017). Preconceptual Zika virus asymptomatic infection

protects against secondary prenatal infection. **PLoS Pathogens**, 13(11), e1006684.

Victora, G. D., & Nussenzweig, M. C. (2012). Germinal centers. **Annual review of immunology**, 30, 429-457.

Wahala, W. M., & Silva, A. M. (2011). The human antibody response to dengue virus infection. **Viruses**, 3(12), 2374-2395.

Wang, Q., Yan, J., & Gao, G. F. (2017). Monoclonal antibodies against Zika virus: therapeutics and their implications for vaccine design. **Journal of Virology**, 91(20).

Wen, J., Elong Ngono, A., Regla-Nava, J. A., Kim, K., Gorman, M. J., Diamond, M. S., & Shresta, S. (2017). Dengue virus-reactive CD8^{+} T cells mediate cross-protection against subsequent Zika virus challenge. **Nature Communications**, 8(1), 1459.

Wen, J., Tang, W. W., Sheets, N., Ellison, J., Sette, A., Kim, K., & Shresta, S. (2017). Identification of Zika virus epitopes reveals immunodominant and protective roles for dengue virus cross-reactive CD8^{+} T cells. **Nature Microbiology**, 2, 17036.

Winkler, C. W., Myers, L. M., Woods, T. A., Messer, R. J., Carmody, A. B., McNally, K. L., . . . Peterson, K. E. (2017). Adaptive immune responses to Zika virus are important for controlling virus infection and preventing infection in brain and testes. **Journal of Immunology**, 198(9), 3526-3535.

Yauch, L. E., Prestwood, T. R., May, M. M., Morar, M. M., Zellweger, R. M., Peters, B., . . . Shresta, S. (2010). CD4^{+} T cells are not required for the induction of

dengue virus-specific CD8$^+$ T cell or antibody responses but contribute to protection after vaccination. **Journal of Immunology**, 185(9), 5405-5416.

Yockey, L. J., Varela, L., Rakib, T., Khoury-Hanold, W., Fink, S. L., Stutz, B., Iwasaki, A. (2016). Vaginal exposure to Zika virus during pregnancy leads to fetal brain infection. **Cell**, 166(5), 1247-1256.e1244.
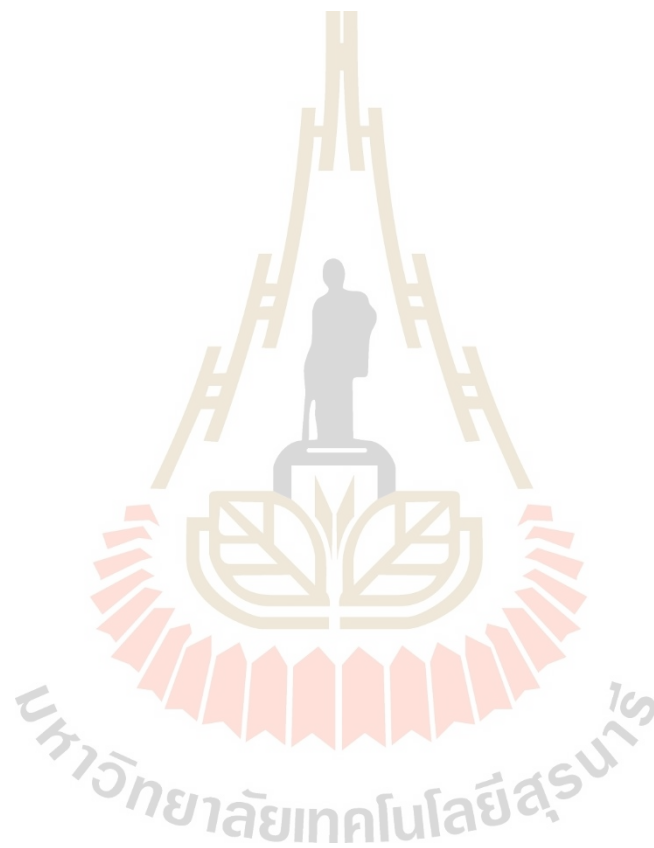
CHAPTER VI

CONCLUSIONS

In summary, the epidemiological study from 64 adults in Nakhon Ratchasima confirmed that ZIKV co-circulation in this region. Our results suggest that a large proportion of residents in a DENV-endemic region generate a strong and potentially protective immunity against ZIKV and DENV heterotypes. The successful construction of a high-quality human antibody library from 40 DENV immune adults can contribute to the expansion of the use of this technology. The library has proven useful for the selection of antibody fragments to the DENV target. The full-length human monoclonal antibody IgG1 and IgG4 were successfully constructed and used for study DENV infection in the mouse model. In view of the potentially large harvest of monoclonal antibodies for diagnostic and therapeutic purposes, high throughput antibody selections can be envisaged, especially considering the spread of automation technology the time and effort invested in antibody production by phage display technology is an important accomplishment.

APPENDIX

List of publications

Elong Ngono A, Young MP, Bunz M, Xu Z, Hattakam S, Vizcarra E, Regla-Nava JA, Tang WW, Yamabhai M, Wen J, Shresta S. (2019) CD4+ T cells promote humoral immunity and viral control during Zika virus infection. PLoS Pathogens. 2019 Jan 24;15(1):e1007474. doi: 10.1371/journal.ppat.1007474.

Hattakam S, Elong Ngono A, McCauley M, Shresta S, M Yamabhai. Repeated exposure to the dengue viruses elicits robust cross-neutralizing antibodies against Zika virus in residents of a dengue-endemic region of Thailand. (Manuscript preparation)
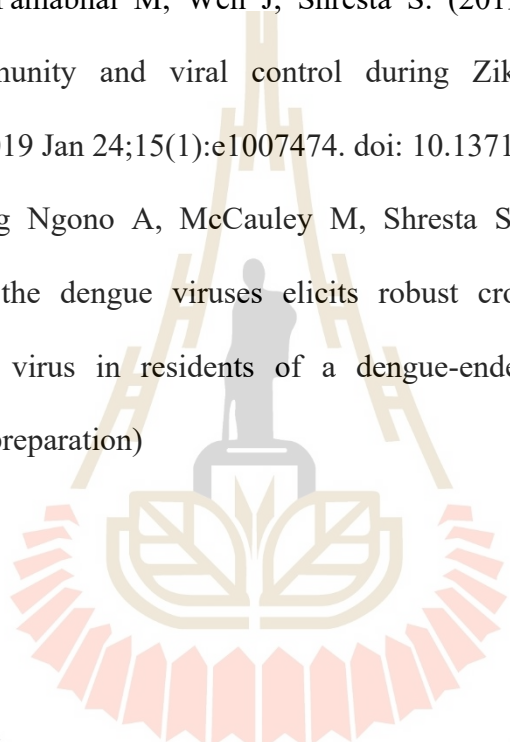
BIOGRAPHY

The author, Miss Sararat Hattakam, was born on July 12, 1987 in Nakhon Ratchasima. She graduated from Chulalongkorn University in 2010 with a bachelor's degree in sciences (Genetics). Later, she finished her master's degree in sciences (molecular genetics and genetic engineering) from Mahidol University, Bangkok, Thailand in 2013. She is continuing studying Ph.D. at the school of biotechnology, Suranaree University of Technology, Nakhon Ratchasima since 2013. She had been working as a visiting Ph.D. student to research in Shresta's lab from August 2017 to February 2019, at La Jolla Institute for Immunology, California, USA. She has been interested in genetic engineering, molecular biology technology, immunology and virology. Her research focus is on dengue and Zika virus and engineered antibody for therapeutic, diagnosis and T cell vaccine for dengue and zika infectious diseases. Her career goal is to invent the knowledge or something that has the benefit to humankind.